The Feasibility of Ceramic Studies for Development and Characterization of Bio-ceramic and Glass Based Dental Implants.

For Functional Restoration of Stomatognathic System and Regeneration of Supporting Bony Tissue

Dr. Abhijit Chakraborty

Medical and Research Publications

The Feasibility of Ceramic Studies for Development and Characterization of Bio-ceramic and Glass Based Dental Implants.

For Functional Restoration of Stomatognathic System and Regeneration of Supporting Bony Tissue.

Written by

Dr. Abhijit Chakraborty

Head Of The Department, Proffesor

The Feasibility of Ceramic Studies for Development and Characterization of Bio-ceramic and Glass Based Dental Implants.

For Functional Restoration of Stomatognathic System and Regeneration of Supporting Bony Tissue.

Medical and Research Publications

First printing, 2022.
ISBN:

Published by
Medical and Research Publications,
124SpencerRd,Stoke-on-TrentST42BE,
United Kingdom.

www.medicalandresearch.com
Email: info@medicalandresearch.com

ACKNOWLEDGEMENT

My journey in this field of scientific research work could not have been completed without active help, support and appreciation of several people. These people played an indispensable role, without thanking whom my thesis would remain incomplete. Late Dr. Debabrata Basu was a person who had started my journey in this new area of scientific research. He was a person who helped me to achieve not only scientific results, but I have also grown as a person under him. An untiring academician whom I hold in highest reverence.

My supervisor Dr. Ratna Ghosh, Associate Professor in the Dept. of Instrumenta- tion and Electronics Engineering, JU is a rock who has stabilized my pathway after the passing away of Late Dr. Debabrata Basu and led me in every corner to the final goal towards my achievements. She can be truly described as a philosopher and guide in my search in this field of doctoral thesis.

Sir, Dr. T. K. Pal, my H.O.D., P.G. guide and now my Ph.D. supervisor, my true teacher in the field of periodontology, is someone for whom words are insufficient to express the amount of respect and gratitude I owe him as my supervisor.

Dr. R. R. Pal, our revered Principal of GNIDSR, has always given me full support in my ongoing work.

Dr. Biswanath Kundu, scientist in a true sense, had the fortitude to help me out and drag me out of every difficult corner I was placed in my journey in this research. He was my true brother in the journey without whose support I could not have com- pleted this difficult pathway.

I should also mention specially Dr. Someswar Dutta, scientist, for his knowledge in the field of Biomaterials science which he shared unreservedly with me in my needs. There were several others of CGCRI, Kolkata to whom I owe my gratitude for their help in small and big things during my ongoing work.

Dr. Bhaswati Gowsami, Associate Professor in the Dept. of Instrumentation and Electronics Engineering, JU, a lady who tolerated and supported me in her Dept. during my ongoing work. She has been a continuous well wisher for preparing this thesis project with her ideas and encouragement.

I would like to thank Mr. Nishant Pathak for his mental support in the last phase of this project.

Dr. Samit Kumar Nandi, an Associate Professor of West Bengal University of Ani- mal and Fishery Sciences, Kolkata extended continuous help and sincere knowledge regarding animal testing and experimentation in for the total duration of this work. Dr. Tirthakar Debnath and his wife Urmi Debnath helped me in all small matters. Aratrika Ghose, a would be engineer, whose

help regarding my thesis was invaluable. Dr. Manoj Singh, Dr. Rabi Prakash, Dr. Sarbani Ghosh, Dr. Sheena Lala, Dr. Amit De and all other faculty members of my Dept. of Periodontics in GNIDSR have actively contributed in this process of my work completion.

Family, my wife Dr. Mousumi Chakraborty and son Mohojit Chakraborty are the most tolerant of the lot, who have borne with me all my problems and supported me all through these long years.

April, 2015 Abhijit Chakraborty

CONTENTS

3. **DESIGN OF BIO-CERAMIC AND GLASS BASED DENTAL IM- PLANTS**

- Human Jaw Bone: Quality and Type
- Typical Macro-Design of Dental Implant
- Dental Implant Body
- First Stage Cover Screw or Healing Screw
- Healing Abutment
- Hygiene Screw
- Abutment
- Prosthetic Abutments
- Proposed Design Simplification
- Implant Body Design
- Implant Body Crest Module
- Healing Screw Design
- Abutment Screw Design
- HAP Coating: Plasma spray method
- Phase analysis using XRD
- FTIR analysis for functional groups
- Coating Surface Morphology from SEM
- Bonding Strength
- Bioactive glass Coating: Conventional dip coating
- Phase analysis using XRD
- FTIR analysis for functional groups
- Coating Surface Morphology from SEM
- Bonding Strength
- Discussion

4. **IMPLANTATIONS IN RABBIT BONE TO STUDY TISSUE RE GENERATION**

- Implant Design for Rabbit Studies
- Comparative studies 1: HAP filler, Ti (smooth) and Ti (screw) Implants80
- Surgical Method
- Post-operative Evaluation
- Post-Euthanasia Evaluation
- SEM-EDAX
- Analysis of interfacial gap
- Histopathological Evaluation
- Push Out Tests
- Interpretation of Results
- Comparative studies 2: HAP and bioactive glass coated implants

- Surgical Method and Post-operative Evaluations
- SEM-EDAX
- Analysis of Interfacial Gap
- Histopathological Evaluation
- Push Out Tests
- Interpretation of Results
- Discussions

5. **IMPLANTATIONS IN CANINE JAW BONE TO STUDY FUNC TIONAL RESTORATION**

- In-Vivo Study
- Implant Design for Dog Jaw Bones
- Surgical Procedure
- Clinical Observations
- Resonance Frequency Analysis (RFA)
- RFA Observations
- Interpretation of Results
- Discussions

6. **HUMAN CLINICAL TRIALS**

- Human Subject Selection
- Implantation Site Selection
- Patient Evaluation
- Radiographic analysis
- Tissue regeneration using HAP Filler
- Case Study
- Results of Multi-Patient Trials
- Dental Implantation
- Pre-operative Tasks
- Surgical Procedure
- Armamentarium
- Post-operative Procedures
- Case Study
- Evaluation of Patients with Dental Implants
- Clinical Observations
- Radiographic Analysis
- Proposed Evaluation of Patient Satisfaction
- Discussions

7. **CONCLUSION**

- Scope for Future Work

8. **References**

Introduction

The goal of present-day dentistry is to rehabilitate the functional stomatognathic system, in particular the jaw bones, of a patient to a normal contour, function, comfort, and aesthetics regardless of the atrophy, injury or disease of the functional system [129]. The stomatognathic system referred here is composed of the teeth, the jaws, the masticatory muscles, the tongue, the lips, the surrounding tissues, and the nerves that control these structures [194]. In several cases, the disruption of this functional system is due to the loss of teeth or injury to it or due to diseased teeth. In such cases, a dental implant is often used by the dental surgeon as a permanent replacement for the root(s) of a tooth (teeth) in the patient jaw [100].

Dental implantology is the branch of dentistry which deals with the innovation, science, arts and clinical application of dental implants. Like any tooth root, a dental implant is secured in the jawbone and is not visible once it is surgically placed. They are used to secure crowns, bridgework, or dentures by a variety of means. Hence, the design of dental implants has to address multiple issues dealing with the implant structure and components, aesthetics of the complete denture, implant-bone interfacial dynamics which must ensure tissue regeneration, long term retention of the implant and finally, the functional restoration of the patient jaw.

It is well known that the long-term success of surgical implants is often restricted by their surface properties [59]. This problem can be overcome to a large extent by coating the implant surfaces with suitable natural or artificial biomaterials. These have been traditionally used in different parts of the human body to replace a lost or diseased biological structure and to restore its form and function [162, 213, 153]. Artificial biomaterials are increasingly being used in dental implantations also to help in restoring the function of otherwise functionally compromised structures [59]. A particularly effective class of such biomaterials are the bioactive ceramics, or bioceramics. This is a term coined to include many new materials and products being formed from variations on ceramics such as synthetic hydroxyapatite (HAP) and other calcium phosphates [103], bioactive glasses [75] as well as glass-ceramic composites [92].

It has been widely accepted that the most important applications of these bioceramics is in the healing of bone defects, which can arise due to trauma, congenital defects or disease [87].

This thesis deals with the design of a simple yet effective dental implant and investigates the use of two indigenously developed bioceramic materials as coatings on the designed implant and as fillers for bony tissue regeneration in the region to be implanted. One variant each of the two main classes of such materials, namely HAP and bioactive glass, have been considered in this thesis for the purpose. In order to appreciate the various aspects of the present work, it is worthwhile to review the state of art in dental implant design as well as issues concerning dental implantation, which include related procedures as well as in-vivo trials that have to be conducted prior to use of a particular dental implant variety in patients on a large scale.

(6) Literature Survey

The development of modern dental implants started in 1930. In 1952, a cylindrical implant, made of titanium, was first placed in the rabbit thigh bone by Brandmark et al. [161]. They found that the Ti implants were fused to the surrounding bone, thus reporting the first observation of osseointegration using an implant. Presently, implants provide some of the most successful treatments used in medicine and their survival rates are known to exceed 95% in most of the published long term (6, 10 or 13 years) studies [70, 66, 53]. However, the number of failures is still relevant and limiting these failures remains one of the goals in today's implant research.

Although titanium and its alloys mainly Ti6Al4V have an excellent reputation for corrosion resistance and biocompatibility, yet the long-term performance of these alloys has raised some concerns [140]. A probable cause for this is that several titanium-based alloys have a high coefficient of friction, which can lead to formation of wear debris. This results in inflammatory reaction, causing pain and loosening of implants due to osteolysis [108]. It has also been established that the inability of an implant surface to integrate with the adjacent bone and other tissues due to micromotions results in implant loosening. In such cases, a fibrous tissue is formed between the bone and the implant, if the implant is not well integrated with the bone [202]. On the other hand, the influence of physical properties such as surface topography and roughness on osseointegration have translated to shorter healing times from implant placement to restoration [32]. Materials with an appropriate surface are thus essential for the implant to integrate well with the adjacent bone.

Preliminary in vivo tests on the surface of titanium implant that was modified by micro arc oxidation treatment showed improvement in osseointegration, as compared to the untreated surface. The improved osseointegration was attributed to rough, porous oxide layer in which Ca and P ions were incorporated. Alkaline phosphate (ALP) activity was found to increase with increase in oxide layer thickness and increase in Ca and P ions in the layer [107]. In fact, calcium phosphate materials have been used since the 1920s in many medical and dental applications due to their biocompatibility and the nontoxicity of their chemical components [47, 76, 101, 74]. Applications of these bio ceramics include repair of periodontal defects, augmentation of alveolar bone, sinus lifts, tooth replacement, and repair of large bone defects caused by tumours [84, 128, 103, 52, 30, 200, 176]. They are also used as scaffolds in tissue engineering for bone or dentin regeneration [176, 68, 81, 11, 111]. Calcium phosphates are also used in the form of injectable cements [44, 18], or as coatings on titanium and titanium alloy implants to combine the bioactivity of the calcium phosphates and the strength of the metal [57, 15].

In recent times also, research work related to implant design, implant coating using numerous biomaterials, as well as more efficient surgical techniques is being undertaken worldwide to achieve the suitable bone implant interface, which will ensure the prolonged survival of dental implants [181, 188].

Aspects of Implant Design

As soon as the implant is fixed into a body, a number of biological reactions occurs in various stages [59]. Initially, there is an adsorption of water molecules and proteins and then, one of the following processes take place:

1. Formation of new bone cells on the implant surface, bone cells proliferation and differentiation leading to osseointegration. When this sequence of events occurs, then the implant is said to be well accepted by the body in which it is inserted. In fact, higher the degree of osseointegration, higher is the mechanical stability and so, the probability of implant loosening becomes smaller.

2. Micromotions of the implant leading to the formation of a soft fibrous tissue around the implant, instead of a hard bony interface. This growth of fibrous tissue is undesirable since it impedes the osseointegration and hence, the long term acceptance of the implant by the body.

3. Inflammatory response by the human body, which causes it to reject the im- plant. Thus, the clinical goal of implant surgery is stated to be osseointegration, which is the process of bone healing and the formation of new bone. It has been reported that osseointegration is affected by many factors, which include the implant design, the implant surface treatment, material biocompatibility, the bone quality or host bed, the surgical technique, the loading conditions and the postoperative care [9, 31].

More specifically, the bone forming processes that will occur depend upon the surface properties of the implant such as surface topography, surface roughness, surface chemistry, and mainly the surface energy which changes with all the aforementioned factors affecting the osseointegration [219].

So, the first step in dental implant engineering is to take into account the relation- ship between osseointegration and the mechanical features of the implant. Implant design features are one of the most fundamental elements that have an effect on implant primary stability and the ability of the implant to sustain loading during or after osseointegration. Implant design can be divided into the two major categories: microdesign and macrodesign. While microdesign constitutes the implant materials, surface morphology and surface coating; the macrodesign includes the implant body shape as well as the implant threads and thread design [5, 60, 62].

Dental implants have different shapes, simple or complex geometries, various length and diameters and they can be inserted in different positions, but they have the same objective, which is to remain incorporated in the patient's bone by physiological bone regeneration actions [28]. Different varieties of the basic form of the implant design have been proposed by various researchers, of which the ones approved by both the FDA and the American Dental Association belong to the endosteal implant and the subperiosteal implant categories [149]. These two types of implants have the following features.

• Endosteal implants: These are surgically implanted directly into the jawbone. Once the surrounding gum tissue has healed, a second surgery is needed to connect a post to the original implant. Finally, an artificial tooth (or teeth) is attached to the post-individually, or grouped on a bridge or denture.

• Subperiosteal implants: These consist of a metal frame that is fitted onto the jawbone just below the gum tissue. As the gums heal, the frame becomes fixed to the jawbone. Posts, which are attached to the frame, protrude through the gums. As with endosteal implants, artificial teeth are then mounted to the posts.

Of these, the subperiosteal implants, which are generally used in severely resorbed areas, are dwindling in use. Recently, a case of maxillary subperiosteal implantitis that caused sinusitis has also been reported in literature [192], which increases the concerns regarding its use. In the present study, the implant design considered is that of an endosteal implant.

Implant material

Biocompatibility, which is indicative of the reaction of the human body to the ma- terial in contact with it, is the feature which determines the retention or rejection of the dental implant in the human jaw [212]. The two main factors that influence the biocompatibility of a material are the host response induced by the material and the degradation of the material in the highly corrosive body environment. An ideal bone implant material is that which has a biocompatible chemical composition that avoids adverse tissue reaction and also has excellent corrosion resistance in the phys- iologic milieu, acceptable strength, a high resistance to fatigue and/or wear and a low modulus of elasticity similar to that of bone to minimise bone resorption around the implant [172, 112, 205].

The materials currently used for surgical implants include 316L stainless steel (316LSS), cobalt chromium (Co-Cr) alloys and titanium (Ti) and its alloys. Ele- ments such as nickel (Ni), chromium (Cr) and cobalt (Co) are found to be released from the stainless steel and cobalt-chromium alloys due to the corrosion in the body environment [148]. The toxic effects of metals namely Ni, Co and Cr, released from prosthetic implants have been reviewed by Wapner [206]. In addition, both 316L SS and Cr-Co alloys possess much higher modulus than bone, leading to insufficient stress transfer to bone, leading to bone resorption and loosening of implant after some years of implantation [195].

In contrast, titanium is found to be well tolerated and nearly an inert material in the human body environment. Moreover, in an optimal situation, titanium is capable of osseointegration with bone [145]. Titanium also forms a very stable passive layer of TiO2 on its surface and provides superior biocompatibility. Even if the passive layer is damaged, the layer is immediately rebuilt [59]. Amongst the materials available for implant applications, the natural selection of titanium-based materials for implantation is thus due to the combination of its outstanding characteristics such as high strength, low density (high specific strength), high immunity to corrosion, complete inertness to body environment, enhanced biocompatibility, low modulus and high capacity to join with bone and other tissues [144]. Commercially pure Ti and Ti-6Al-4V ELI (Ti6Al4V, Extra Low interstitial) are most commonly used titanium materials for implant applications. In the present study, all implants used in in-vivo studies are made of the titanium alloy Ti6Al4V.

Implant body shape

In the design of implants, determining the implant body shape is another important factor. Of the various shapes tested, cylindrical implants were the first to be used [161] and are till date the most widely accepted [130]. In subsequent studies by various researchers, tapered cylindrical implants have been shown to produce more compressive force than uniformly cylindrical implants, which have more shear forces [106]. Studies have also shown that cylindrical implants have a higher implant failure rate than tapered implants, which can be ascribed to the predominance of defect in- ducing shear forces, as opposed to the bone forming compressive forces, in cylindrical implants [130]. Consequently, the present study uses a smooth, but tapered, cylindrical blank of Ti6Al4V for the proposed threaded implant design.

Implant thread design

It has been shown that while cylindrical (tapered or non-tapered) smooth implants are dependent on exact fit in order to be stable within the bone, the geometrical constraints imposed by threads on the implant surface have a positive impact on the initial stability [23, 214]. Threads are used to maximize initial contact, improve initial stability, enlarge implant surface area, and favor the dissipation of interfacial stress.

In several comprehensive reviews [5, 60, 62], it has been observed that the thread design, which involves issues like thread geometry, face angle, thread pitch, thread depth (height), thickness (width) and thread helix angle, affect the primary stability as well as the osseointegration of the implant in different clinical conditions. It must be noted that once the primary stability is ensured, only then does stabilization of the implant occur with subsequent osseointegration of the threaded surface with the bone [12].

Thread configuration is an important objective in the biomechanical optimization of dental implants [164, 61, 21, 201, 209]. Thread configurations presently represented in the commercially available dental implant designs include V-shaped thread (Nobel Biocare, 3I, Paragon, Lifecore), thin thread (IMTEC Sendax MDI), reverse buttress thread (Steri-Oss), and square thread (BioHorizons) [35, 17]. The original Branemark screw had a V-shaped threaded pattern [6, 19]. In an initial study, implants with V-shaped and buttress threads have been shown to generate forces that may lead to defect formation [14]. However, subsequent studies have shown that the V-shape and the broader square shape generate significantly less stress, as compared with the thin and narrower square thread, in cancellous bone. Presently, both the V-shape and the square shape thread configurations are most favored for dental implants, especially when dealing with cancellous bone [60, 62]. An interesting research [114] has further established that in terms of implant stability, the single-threaded implant design is most favored, followed by the double threaded, then the triple threaded implant designs.

A critical aspect of the thread shape is the face angle. The face angle is the angle between a face of a thread and a plane perpendicular to the long axis of the implant. In the implant literature, the most studied face angle is that of the apical face where most of the loading forces are dissipated. The face angle of the thread could change the direction of force at the bone implant interface [22]. In fact, since

the amount of the adversely affecting shear force generated by the different thread shapes increases as the thread face angle increases [5], the face angle must be decided with care.

Crest module area is typically the topmost smooth part of the implant, where the implant meets the soft tissue and changes from a virtually sterile environment to an open oral cavity. The threaded portion of the implant starts below this region. This is also the region where the implant abutment, which holds the final dentures or crown, is connected to the implant. Recent research shows that short term as well as long term implant failures are likely to occur due to the design of the neck of the implant [5].
Typically, in this area, the bone density is thicker due to the presence of primary cortical bone. So, the design of this region plays a major role in achieving implant primary stability and maintaining long term implant stability, since the forces are concentrated in this area when the implant is inserted and put into function [118, 124, 190]. Some studies suggest that the addition of threads or microthreads up to the crestal module of an implant might provide a potential positive contribution on bone-to to implant contact as well as on the preservation of marginal bone; nonetheless this remains to be determined [5].

Another aspect of the thread geometry affecting the distribution of stress forces around the implant is the thread pitch. Thread pitch refers to the distance from the center of the thread to the center of the next thread, measured parallel to the axis of a screw [45]. It may be calculated by dividing unit length by the number of threads [135]. In implants with equal length, the smaller the pitch, the more threads there are. Motoyoshi et al. [138] concluded that the maximum effective stress decreased as screw pitch decreased gradually. Kong et al. [93], on the other hand, considered 0.8mm as the optimal thread pitch for achieving primary stability and optimum stress production on cylindrical implants with V-shape threads and found that a shorter or a longer pitch had unfavorable stress generation. Furthermore, they also indicated that stresses are more sensitive to thread pitch in cancellous bone than in cortical bone.
In this thesis, the proposed design of the dental implant uses a Ti alloy based endosteal implant design with a tapered cylindrical form and V-shaped single threads. Various aspects like crest module design, thread design, face angle, implant length as well as the pitch of the bare Ti alloy implant have been addressed in this study, with the objective of ensuring the success of the final coated form of the implant.

Implant surface coating

A major objective of any implant design is to maximize the amount of bone-to- implant contact (BIC), which is expected to lead to rapid healing with safe functional integration of the implant into the jaw bone [8]. The BIC as well as the osseoin- tegration are both enhanced by suitably modulating the implant surface roughness [183]. This is so since the surface topography affects the osteogenesis at the implant surface, which consists of a series of coordinated events, including cell proliferation, transformation of osteoblasts and bone tissue formation [180]. Also, bone ingrowth into a porous threaded surface can cause strong interlocking of surrounding bone tissue with the implant, resulting in improved biomechanical compatibility and high resistance to fatigue loading [82, 171, 165].
Such a porous implant surface, which is bioactive and promotes osteogenesis, is obtained by coating the implant with suitable biomaterials [87]. Various techniques for coating the bare Ti alloy implants with suitable bioceram- ics are under investigation to achieve good adhesion and other required properties, without compromising the advantageous properties of titanium alloys [43, 20]. These bioceramics are primarily calcium phosphate based materials, which are similar to bone in composition and have the required bioactive and stress dissipative properties. The bioactivity of these materials is due to a positive interaction with living tissue, that includes differentiation of immature cells towards bone cells [74, 196]. These materials also have chemical bonding to the bone along the interface, thought to be triggered by the adsorption of bone growth mediating proteins at the biomaterials surface [74, 150]. Hence, a biochemically mediated strong bonding osteogenesis is expected [150, 16]. These materials are also capable of transmitting the bone forming compressive forces through the interface, referred to as the bony ingrowth. However, in the process, a part of the undesirable tensile and shear forces also get transmitted.

Focussing on the two classes of coating materials used in this study, it is known that surface coating of synthetic hydroxyapatite (HAP), a calcium phosphate com- pound that is similar to the bone, helps in early fixation into bone, promotes bone apposition to the surface and enhances the osteoconductivity, by providing the space and a substratum for the cellular and biochemical events to lead to bone formation [182, 58, 40, 41, 80]. The HAP coating thus improves prosthesis life in spite of a biomechanical mismatch [115, 116]. In case of bioactive glass coatings, the main discovery was that a particular composition of glass, later termed 45S5 and Bioglass, formed a bond with bone so strong that it could not be removed without breaking the bone [78]. The osteoinduction of the glass [122],

which stimulates the pluripoten- tial, mesenchymal-derived cells to produce a bone matrix, are thought to be due to the dissolution products of the glass, namely soluble silica and calcium ions [77, 80]. Recently, interest has increased in borate glasses and phosphate glasses, which is related more to their very rapid solubility rather than bioactivity [88, 4]. However, a disadvantage of Bioglass 45S5 and several other available bioactive glasses over other bioceramics is that they cannot be made into amorphous bioactive glass scaffolds, because they crystallize during sintering [87].

In the present study, the aspect of implant surface modifications by coating the designed implant using these two different varieties of bioceramic coatings have been considered in order to address the aspects of primary stability, biocompatibility, os- seointegration and subsequent stress dissipative ability of the implant. In order to appreciate the material characteristics required from a bioceramic used for coating the implant, a review of the two classes of bioceramics used, namely HAP and bioac- tive glass, is presented herewith in terms of the material developed and its relevant properties.

HAP coating

In recent times, HAP is one of the most common types of the calcium phosphate materials which are currently used in dental applications [8]. Hydroxyapatite has excellent biocompatibility and is able to promote osseointegration. As a result of excellent favorable bioactive and stress dissipative properties, it is widely preferred as the biomaterial of choice in dentistry. HAP has been used as coating in both orthopedic and dental implants [139, 25], restoration of edentulous atrophic ridges [159], intrabony periodontal pockets (a periodontal pocket in which the bottom is apical to the level of the adjacent alveolar bone) [123], and ridge augmentation prior to implant for metal prosthetics [109].

Furlong and Osborn first began clinical trials using the HAP-coated implants in 1985 [54] and reported that these coatings can successfully enhance clinical success. Thereafter, Okamoto et al. [147] reported that a significantly higher number of cells adhered to hydroxyapatite than to uncoated titanium. In various studies using HAP till date, less than 2% failure rate have been reported during a mean follow-up study of 10 years [33, 89, 57].

However, several factors may influence the performance of any hydroxyapatite coating such as coating thickness, chemical composition, crystallinity, phase purity, cohesive and adhesive strengths, and

resorption resistance. Adhesion strength of the coating to the implant surface appears to be a property that needs to be maximized to avoid cracking, shearing off, and chipping of the HAP coating during the placement of the implant. The ideal hydroxyapatite coating would be one with low porosity, strong cohesive strength, good adhesion to the substrate, a high degree of crystallinity, high chemical purity, and phase stability [199].

Apart from the essential material properties required for adherence of the HAP coating to the implant surface, the success or failure of HAP coated orthopaedic im- plants depends on the control and consequences of cell behaviour after implantation [163]. Thus, an essential step in bone tissue-implant interface studies is conducting in-vivo tests to study the formation of osteoblast cells, which play an important role in the osseointegration of the implant. Many studies have indicated that the dissolu- tion of well-crystallized hydroxyapatite in the human body after implantation is too low to achieve optimum results [98, 146, 48]. Some concerns have also been pointed out regarding the resorption, fracture, fatigue and macrobiological susceptibility of HAP coatings, yet the long term effect or mitigation of these issues remain to be ex- plored [89]. So, newer HAP materials need to tested for use as coatings on implants that can be used to achieve an optimum dissolution rate of bone graft materials. Hence, for any novel HAP coating material to be used successfully on an implant, both the material characterization and suitable animal in-vivo trials are essential prior to proceeding for human clinical trials.

Bioactive glass coating

In vivo studies have shown that bioactive glasses bond with bone more rapidly than other bioceramics [155, 75]. These materials are capable of direct bone to bone contact [186] and also have an osteo promoting effect on cells due to the formation of hydrated silica layer and hydroxyl carbonate apatite (HCA) on the glass surface that resembles the inorganic phase of bone [198]. Several studies have also established the long term stability of bioactive glass coated implants. In particular, a study in which the devices were inserted into fresh tooth extraction sites to repair tooth roots and to provide a stable ridge for dentures proved to be extremely stable, and a 5-year study established quantified improvements of these implants over HAP coated dental implants [187]. Thus, the bioactive glass is also established as a viable material for use as implant coatings.

However, despite these desirable biological characteristics, the use of bioactive glasses as a coating material for bone implants has been limited as compared to other calcium phosphates such as tricalcium phosphate (TCP) and synthetic HAP. This is due to the fact that such coatings show low adhesive properties in terms of the chemical bonding between the glass and titanium substrates. When glass coatings are applied on the implant material, the thermal expansion coefficient of the glass must match that of the metal to prevent the glass pulling away from the metal during processing [65]. This is a challenge for bioactive glasses, since the thermal expansion coefficient of the original Bioglass 45S5 composition as well as several other variants does not match that of titanium or similar metals [65]. An additional problem for these glasses is that they crystallize on sintering, which is a hindrance to a good coating. It has been reported that this problem has been overcome recently by understanding how the glass composition can be tailored to prevent crystallization [87].
New compositions of these bioactive glasses thus need to be tested for thermal coefficient matching with the underlying Ti alloy, non-crystallization on sintering and thereafter, for scaffold production in in-vivo tests.

Implant surface evaluation

As is evident from the study of the coating characteristics, prior to any in-vivo tests, one must first accurately determine the implant surface characteristics with regard to the chemical composition of the material and the surface topography in order to draw accurate conclusions regarding the effects of implant modification. These material characterizations should be performed both visually, using techniques like light microscopy and scanning electron microscopy, as well as numerically, using techniques like profilometry, contact angle, X-ray photoelectron spectroscopy or energy dispersive X-ray microscopy, thus including both qualitative and quantitative data [156].

The mechanical properties of these coating materials that need to be quanti- fied include hardness, tensile strength, modulus of elasticity and elongation. The hardness and tensile strength are essential to ensure that an implant will not fracture due to inadequate strength or mismatch in mechanical property between the bone and implant, referred to as biomechanical incompatibility; while the modulus of elasticity and elongation of the material replacing the bone are expected to have values equivalent to that of the bone. The fatigue strength of the material, which indicates the response of the

material to repeated cyclic loads or strains, also has to be measured, since this determines the long-term success of the implant, which is functionally subjected to cyclic loading after implantation [59].

In vivo dental implantation

The advances in biomaterials and techniques have contributed to increased appli- cation of dental implants in the restoration of partial and completely edentulous patients. Albrektsson et al. [9] reported that apart from the material based factors such as material biocompatibility, implant design and implant surface, several pro- cedural factors like host bed, surgical technique and loading conditions also affect implant osseointegration. The host bed in this case is the human jaw bone, which is composed of the outer cortical layer and the inner cancellous layer. Often, in these patients, the presence of soft and hard tissue defects create an anatomically less favorable foundation for ideal implant placement.
In such cases, reconstruction of the alveolar bone through a variety of regenerative surgical procedures is necessary prior to implant placement or simultaneously at the time of implant surgery to provide a restoration with a good long-term prognosis. Such regenerative procedures, which are used for socket preservation, sinus augmentation, and horizontal and vertical ridge augmentation [122], provide an underlying structure similar to that of the nat- ural human jaw. In the jaw, the dense haversian systems of cortical bone provide skeletal strength, while interposed between the cortices is a three-dimensional lattice network of trabeculae that acts as a reservoir for active bone metabolism. This bony architecture is naturally dynamic and undergoes continuous remodeling to repair and shape the bone to ensure renewal of form and function [122].

The principles of osteogenesis, osteoconduction, and osteoinduction, which are effective in the natural system, can be used to optimize therapeutic approaches to bone regeneration and functional restoration [80]. Osteogenesis has been described as the direct transfer of vital cells to the area that will regenerate new bone, osteo- conduction embraces the principle of providing the space and a substratum for the cellular and biochemical events progressing to bone formation, while osteoinduction embodies the principle of converting pluripotential, mesenchymal-derived cells along an osteoblast pathway with the subsequent formation of bone [122].

These requirements mandate the rigorous testing of any designed dental implant firstly in animal trials, followed by human clinical trials, in order to evaluate the pro- cedural factors affecting the osseointegration and ensure the bony tissue regeneration as well as functional restoration of the stomatognathic system in in-vivo conditions.

Regeneration of bony tissues

As mentioned earlier, the regeneration of bony tissues in case of dental implantations is primarily related to the osseointegration. But, in cases where there is lack of sufficient bone, augmentation and regeneration of the lost bone is often necessary, that will aim at preservation of the natural tissue contours in preparation for the proposed implant prosthesis [193]. In both cases, the concept of bone regeneration is to use a scaffold that would act as a three-dimensional (3-D) temporary template to guide bone repair. Ideally, the scaffold will stimulate the natural regenerative mechanisms of the human body to form new bone and also share the loading caused by the various stresses with the bone. Blood vessels must also penetrate if the new bone is to survive. Over time, the scaffold should degrade, leaving the bone to remodel naturally [87]. A detailed review of the effect of implant surface coatings using HAP and bioac- tive glass on osteogenesis and osseointegration in case of dental implantations has been presented in Section 1.2.4. In particular, it is well documented that titanium implants with bioceramic coatings, which provide a moderately roughened surface, have a superior influence on the bone response, in comparison with polished or smooth implant surfaces [211]. Histologically, comparing the osseous apposition in HAP coated implants and titanium implants has demonstrated the mineralization of bone directly on HAP surfaces with no fibrous tissue layer formation. However, a predominately fibrous tissue interface was observed on titanium implants, with only minimal areas of direct bone contact [197]. In addition, in an animal study, HAP coated implants showed an increased coronal bone growth that was not observed with titanium implants [56]. Other histometric studies in animal models have also exemplified that bone adapts in much less time to HAP coated implants than to titanium implants [67, 208].

Considering the choice of materials for ridge augmentation, calcium phosphate and calcium sulfate compounds are known to be attractive synthetic alternatives to autografts, which use bone from the patient’s body, because of their biocompatibility, handling characteristics, porosity, different rates of dissolution, chemical and physical resemblance to bone mineral, and potentially unlimited supply at a

modest cost [71, 85, 167, 174, 157]. In particular, successful ridge augmentations with HAP particulate material, with and without autogenous bone or plaster, has been reported in literature [51].

The quality of the tissue regeneration in dental implantation is characterized using common mechanical tests of tissues harvested from in vivo studies. These include torque removal tests for threaded implants, pullout tests and push-out tests for threaded and smooth cylindrical implants. These tests are used to evaluate the strength of the interaction between the bone and implant surface. High forces encountered during these tests indicate a good integration between the bone and implant surface or in the case of porous materials, a high degree of bone ingrowth into the pores of the implant [156].

In the present study, the bioceramic HAP has been used in the powder form for ridge augmentation in cases where it was required, while the HAP and bioglass coated Ti alloy implants have been used in dental implantations. Standard push out tests as well as histological tests have been used in animal (rabbit) in-vivo studies for the implant characterizations, along with other tests.

Functional restoration

When considering the various modalities of treatment for the prosthetic replacement of teeth following tooth loss, the end goal of therapy is to provide a functional restoration that is in harmony with the adjacent natural dentition [193]. Functional occlusal loading on an implant triggers the remodeling of the surrounding alveolar bone. A mild load induces a bone remodeling response and reactive woven bone production. However, an excessive load results in microfractures [72]. In cases where functional restoration is not ensured, the bone remodeling capacity is insufficient to keep pace with the microdamage and these defects accumulate and coalesce to form a bigger defect [160]. As a consequence, the defect formed gets filled with fibrous tissues and microorganisms [133]. Eventually, severe bone loss occurs, decreasing the bony support around the implant and increasing the risk of implant failure [21].

It is well known that a phase of traumatic osteolysis at the implant-bone interface is an essential step in the functional restoration of the jaw, which occurs in the period immediately after the surgical insertion of the dental implant [119]. Typically, the RFA value decreases during the first 2 weeks after

implant placement, and this change can be related to early bone healing such as biological change and marginal alveolar bone resorption [154]. However, in case of successful implantations, this is followed by osseointegration in the region and within a reasonable time, usually lasting 3 to 4 months, the implant is well accepted in the human jaw [125]. Resonance frequency analysis (RFA) is an accepted non-invasive technique used to monitor this whole process and determine the implant stability. RF studies have been used in rabbits, dogs as well as in human trials to obtain a measure of the changes in the hard issue formation around the implant in in-vivo situation [126, 127, 178, 154]. RFA based instruments are presently available commercially for monitoring the implant stability in situ. In the present study, implantation studies were conducted in dogs to ascertain the functional restorative ability of the designed implants using RFA technique, prior to testing them in human clinical trials.

Animal studies

In order to determine whether a newly developed implant material conforms to the various requirements of biocompatibility, mechanical stability and bioactivity, it must undergo rigorous testing both in vitro and in vivo. Results from in vitro studies can be difficult to extrapolate to the in vivo situation. For this reason, the use of animal models is often an essential step in the testing of dental implants prior to clinical use in humans [156].

For the evaluation of bone-implant interactions, some frequently used animal models are the dog, sheep, goat, pig and rabbit models [156, 191]. However, since both the anatomy and physiopathology of these animals are different from those of humans, it is difficult to evaluate new therapies in these models and extrapolate the results to the human situation [191]. So, the choice of the species should be done by taking into account the bone macrostructure and microstructure, bone composition and remodelling, with emphasis being placed on the similarity between the animal model and the human clinical situation in terms of the stated objective [156]. Even when such similarity can be established, it must be noted that extra care must be taken before choosing and using experimental animal models, particularly primates and canines, primarily due to ethical reasons [117, 177]. In view of these consider- ations, multiple model systems are likely to be required to establish various aspects of a study, prior to the human trials [73].

Rabbit Studies

The review of the typical animal models used for implant research showed that although the rabbit bone shows the least similarities to human bone, yet it is the most commonly used of all the species for osseointegration studies [126, 189, 156].

Rabbits have mainly been used for testing biomaterials or for treatment of peri- implantitis. However, transcortical drilled holes creating tibial or radial critical- sized femoral defects are traditionally the most commonly used models in rabbits [3, 86, 173], which are typically used for testing the bone healing [127].

Review reports show that rabbits are used in approximately 35% of musculoskele- tal research studies [143]. This is in part due to the ease of handling and their size. The rabbit is also convenient in that it reaches skeletal maturity shortly after sexual maturity at around 6 months of age [63]. But, in this case, the size of the implant which may be inserted is limited. So, although it is difficult to extrapolate results from studies performed in rabbits onto the likely human clinical response however, rabbits are commonly used for screening implant materials prior to testing in a larger animal model [156].

In the present study, studies in rabbit tibia using various types of the designed implant and HAP powder have been performed to screen the various materials in terms of their tissue regenerative abilities, prior to their use in further trials.

Dog studies

Of the various species used for in vivo studies, namely dog, sheep, goat, pigs and rabbits, the dog has the most similar bone structure to humans [156]. However, as noted in the review of experimental animal models [156], the use of large animals with ethical and social issues such as monkeys and dogs should be reserved for the last phase validation of new treatments, prior to use in human clinical practice. Among the large animal species, the dog is one of the more frequently used for musculoskeletal and dental research. Martini et al. [121] reports that between 1970 and 2001, 9% of orthopaedic studies utilised dogs as an animal model. In dental research, dogs have been frequently

used for modeling the regeneration of periodontal defects with biomaterials. RFA studies to ascertain dental implant stability have also been performed using the dog model [166, 178].

In the present case, implantation studies were conducted in dogs in the last phase prior to human clinical trials to ascertain the functional restorative ability of the designed implants using the non-invasive RFA technique.

Human clinical trials

The main function of the dental implant is to support the prosthesis after osseoin- tegration with the jaw bone to rehabilitate missing teeth and to maintain clinical success over time [207, 79]. This is a biological process and it needs a healing pe- riod of at least 3-4 months. As stated by Albrektsson [9], thorough assessment and treatment planning is imperative while conducting human clinical trials for dental implantation studies. The prerequisites for such studies involve the detailed eval- uation of the implantation site, like the assessment of available bone quality, bone height, clearance above vital structures, such as neurovascular bundles or air pas- sages/ sinus cavities, presence or absence of any ridge defects or edentulous ridge spans [131, 179].

As per the prevalent ADA guidelines, the dental surgeon must make the patient aware of the various available prosthetic options. This is to be rigorously followed by diagnostics including imaging modalities. Based on this, the overall treatment procedure, including the surgical protocol and restorative protocol, has to be planned in advance. Thereafter, subject to obtaining the patient's informed consent, the pre- surgical preparation of the patient is undertaken prior to the actual procedure. The actual implantation procedure is followed up by post-surgical instructions and peri-odical check ups to ensure the dental hygiene and proper care of the prosthesis [136]. In case of in-vivo clinical trials, both pre-operative and post-operative evaluations have to be done systematically to ascertain the pros and cons of the implantations. This forms the ultimate step for testing the designed implant preparatory to its clinical use.

Aim and Organization of the Thesis

The aim of this thesis is to design a simple yet effective dental implant and to in- vestigate the use of certain specific indigenously developed bio-active materials, as coatings on the designed implant and as fillers for hard tissue regeneration in the region to be implanted. This is expected to lead to the development of a novel, com- plete coated dental implant system, which will provide a human acceptable option, both functional and aesthetic. This indigenously developed system, being simpler in design, can be used to develop a commercial product which is available to the common man in developing or under-developed countries at an affordable price.

In view of these objectives, two particular bio-materials, one of which is a variant of the bio-ceramic hydroxyapatite, henceforth referred to as HAP, and the other is a variant of bio-active glass, henceforth referred to simply as bioactive glass, have been considered in Chapter 2 in order to evaluate their use in dental implantation applications. These materials have been synthetically prepared and characterized at the CSIR-Central Glass and Ceramic Research Institute (CSIR-CGCRI), Kolkata [97, 184, 39, 141] The preparation of these powder materials is reviewed in this Chap- ter for easy reference. Key findings, which are relevant to the use of these powders in dental implantations, have been identified from the available characterizations of these powders [97] and stated in this Chapter. Based on these findings, the feasibil- ity of using these ceramic and glass based powders in dental implantations has been interpreted in this work.

In Chapter 3, the focus is on the design of a cost-effective, yet functionally com- plete dental implant system for the human subject. A review of the bone quality and bone type classifications for the human jaw bone has been provided in this Chapter in order to appreciate the manifold implant design considerations. The macrodesign of an uncoated threaded Titanium (Ti) implant is proposed in this Chapter as an equally effective, yet simplified, alternative to one of the most common commercially available (threaded) implant systems.

The design details of the commercial implant system have been considered as the basis for analyzing how the proposed alterations in the implant macrodesign address both the functional and the aesthetic aspects of the dental implantation. Thereafter, in order to address the aspect of increasing the surface roughness of the proposed implant, the coating of suitable metallic sub- strates with HAP and bioactive

glass, along with their characterizations, as stated in detail in Dey et al. [39] and Soundrapandian [184] respectively, have been reviewed in this Chapter. As in Chapter 2, these findings, along with the proposed implant design alterations, have been used to systematically assess the long term success of the proposed coated dental implant systems in the human jaw.

The feasibility studies in the Chapters 2 and 3 form the basis for the next two Chapters, which contain details of some systematic in-vivo animal studies performed in order to study and validate the expectations from the proposed implant design, both uncoated and coated (with the HAP or bioactive glass powder, as the case may be). The use of the HAP powder as bio-active filler for hard tissue augmentation has also been investigated in one of the studies. Ethical Committee clearances have been obtained for all animal and human in-vivo trials.

In Chapter 4, studies were performed in-vivo in the metaphyseal region of the hind leg of rabbits to observe the tissue regeneration at the implant-bone interface after implantation. The region of the implantation necessitated the use of a single stage Ti implant, which was similar to the proposed implant design, yet was smaller in size. In order to satisfy the broad objective, the study was further subdivided into two sub-objectives. The first set of studies was performed to ascertain the bioactivity of the smooth variant, as well as the threaded form, of the uncoated Ti implant. The bio-ceramic HAP powder has been used in this study as a positive control. The second set of studies was done with all 4 variants of coated Ti implants, specifically HAP coated Ti (smooth or screw) implants as well as bioactive glass coated Ti (smooth or threaded) implants. Detailed clinical studies, SEM-EDAX characterizations, histopathological tests and push-out results have been performed in all cases, for both sets of studies. Thereafter, a detailed analysis of these studies has been done in order to evaluate the hard tissue regenerative ability of the proposed implant macro-design in the two cases, when kept uncoated or when coated (using any one of the two coating materials- HAP or bioactive glass). The use of the HAP powder as a positive control in the first study enabled the analysis of its possible use as a bone filler.

The feasibility of functional restoration of the human jaw bone using the proposed dental implant forms the focus of the animal study discussed in Chapter 5. This has been analyzed based on in-vivo implantation studies performed in the anterior aspect of dog mandibles and in edentulous portions of the canine jaw, since the canine bone quality as well as food habits are similar to that of humans. Both

uncoated and coated varieties of the proposed threaded Ti implants designed in the present work, as discussed in Chapter 3, have been used for the canine implantations. Mongrel dogs were used for the study and these were kept in natural habitats all through. The stability of the dental implants placed in the jaw bones of these dogs was monitored periodically using an indigenously developed resonance frequency analysis (RFA) based instrumentation system [26, 168] for a specific duration of time. The RFA results obtained over the specified duration were analyzed to interpret the bio-compatibility, and hence the functional restorative ability, of the implants in the canine jaw bones.

On the basis of the results obtained from these animal studies, several in-vivo hu- man implantations have been performed using the HAP and bioactive glass coated threaded Ti dental implants, which are discussed in Chapter 6. Prior to the den- tal implantation, it is necessary for the clinician to identify whether the particular human subject approaching the clinician is a suitable candidate for dental implanta- tion. The specific inclusion and exclusion criteria for patients, as well as the specific implantation site selection criteria used for the present trials is stated at the outset in this Chapter. The radiological techniques which have been used to assess the pre- operative need and post-operative success of the surgical procedures in the human subjects selected in this study have also been discussed, specially in terms of their clinical utility vis-a-vis their affordability by the intended population. In cases where the pre-operative assessment shows a deficiency of bone, ridge augmentation in the region to be implanted has to be done prior to the dental implantation. A detailed case study pertaining to the use of the HAP powder as filler for hard tissue augmen- tation has been discussed in this Chapter. Thereafter, the clinical and radiological results of multi-patient trials conducted using the HAP powder as bone filler have been analyzed to assess the success of this procedure in a large population. This is followed by an illustrative case study of the dental implantation procedure adopted in this study using the proposed coated dental implant system.

In the present work, implantations have been done on several patients using the HAP coated as well as the bioactive glass coated varieties of the proposed threaded Ti dental implant. Detailed post-operative objective patient evaluations of these procedures, based on long term clinical observations and radiographic studies, have been analyzed and compared for a conventional assessment of the success of the implantations. In addition to this, a novel quantitative evaluation of patient satisfaction has been proposed and imple- mented in the present study, which extends the ICMR guidelines available online at http://icmr.nic.in/ ethical guidelines.pdf. The interpretation of the corresponding

results obtained from the multi-patient trials and their comparison with the conven- tional, earlier mentioned, objective findings has been done in this study to ascertain the utility of the proposed evaluation in assessing the human acceptability of the proposed dental implant system.

Chapter 7 contains the conclusions and the scope for future work.

DENTAL IMPLANTS: MATERIALS

Nowadays, bone regenerative materials are often used for the augmentation of the natural bone. More specifically, various types of alloplastic materials are being widely used to regenerate the lost hard tissues or as bone filling materials for the purpose of conserving the natural dentition. The most acceptable class of alloplastic materials consists of the calcium-phosphate based osseous regenerative materials [130]. Two of the commonly used varieties of these materials are hydroxyapatite (HAP) and bioactive glass.

In the present work, particular preparations of HAP powder and bioactive glass powder have been used for tissue regeneration and dental implantation procedures, as discussed in subsequent chapters. The details of the powder preparation process and their characterization have been stated in this Chapter from the viewpoint of their usability primarily as coatings on dental implants and also as bone filling material. These powder materials were prepared and their detailed characterizations were done at the CSIR-Central Glass and Ceramic Research Institute (CSIR-CGCRI), Kolkata [97, 184, 39, 141]. The powder preparation methods for HAP and bioactive glass powders have been stated in Sections 2.1 and 2.3 respectively. Relevant and key findings stated in [97], that have been obtained from the powder characterizations and which are relevant to use of these powders in dental implantations, have been reported in Sections 2.2 and 2.4 respectively. Based on these, the feasibility of using these ceramic based powders in dental implantations have been stated in Section 2.5.

HAP powder preparation: Wet chemical method

Hydroxyapatite powders can be prepared by various methods like sol-gel, dry chem- ical and wet chemical methods. In this case, an unique wet chemical method has been used for the production of the powder, the scheme of which is shown in Figure 2.1.

In this method, the powder was synthesized at about 80◦C in an aqueous medium. The raw materials used for the purpose were A.R. grade calcium hydroxide [Ca(OH)2, Central Drug House, India] and ortho-phosphoric acid (H3PO4, Ranbaxy, India). Initial stoichiometry of the reactants were maintained around 1.67 to obtain a pure phase. The reactions were carried out in air atmosphere with a relative humidity of 90%. The pH of the reacting solutions were maintained at about 10-12 which were

controlled by the addition of ortho-phosphoric acid and monitored through a pH meter (Sension1, Hach, USA). The calculations were based on a 2l batch.

After completion of addition of H3PO4, the stirring was continued upto 1h with a fixed temperature of 80◦C and thereafter kept for 24h for precipitation. This step is called aging. The precipitate was further washed with DDW (double distilled water) and filtered through a vacuum filtration unit. The cake, thus obtained, was dried in an air oven (S.D. Industries and Equipments, India) for 24h again at 80◦C.

In order to obtain the HAP powder, the dried cake was ground to fine powder in agate-mortar and passed through 52 BSS to obtain a homogeneous particle having size range of < 296µm. This powder was fired at two different temperatures of 800◦C and 1250◦C. In both cases, the powders were kept for 2h at the corresponding firing temperature.

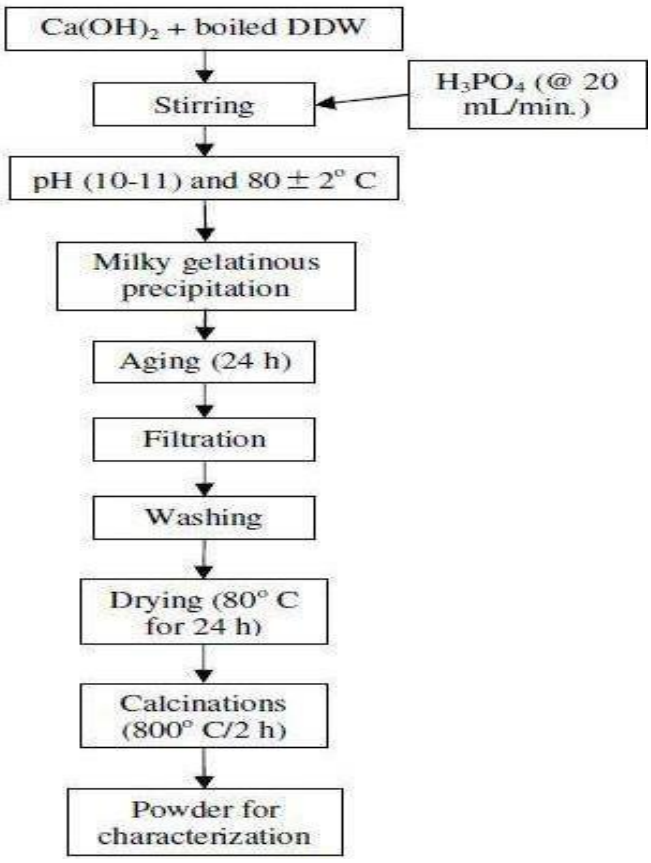

Figure 2.1: HAP Powder Preparation by Wet Chemical Method

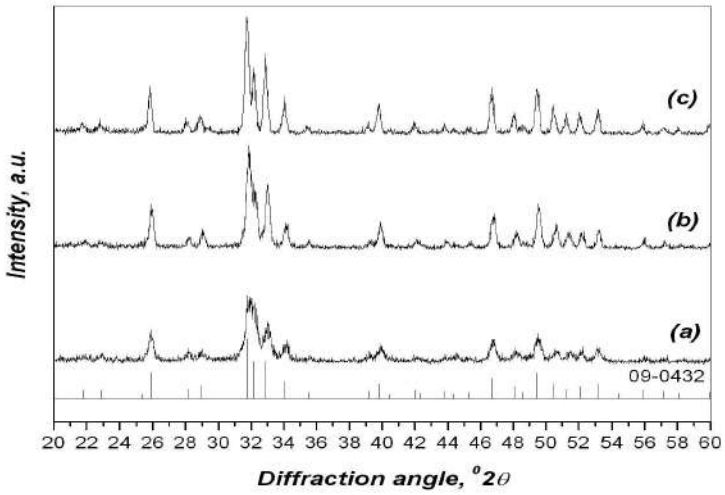

Figure 2.2: X ray diffraction of the HAP powder: (a) as-dried, (b) calcined at 800◦C and (c) sintered at 1250◦C

HAP Powder Characterization

The powder characterizations relevant to the present work are X-ray diffraction (XRD) analysis, field emission scanning electron microscopy (SEM), Fourier-transformed infra-red (FTIR) spectroscopy and differential thermal analysis/ thermo-gravimetric analysis (DTA/TGA) of the powders. The characterization methods as well as the observations for both the powders are stated hereafter.

X-Ray Diffraction (XRD)

The phase composition, extent of crystallization, crystallinity as well as the crystal- lite sizes of the powders calcined at different temperatures were analyzed by X ray diffraction (XRD) using a X'Pert Pro, Philips Analytical B.V., Netherlands powder diffractometer. Continuous data were collected over the 2θ range 20-60◦, using monochromatic Cu Kα1 radiation (operating conditions being 30 mA and 40 kV the wavelength of 1.5406 ˚A), with a step size of 0.017◦ and a count time of 10.34s. The diffraction patterns were compared with the database available in the Joint Commission on Powder Diffraction's Powder Diffraction Files, referred usually as JCPD's PDFs.

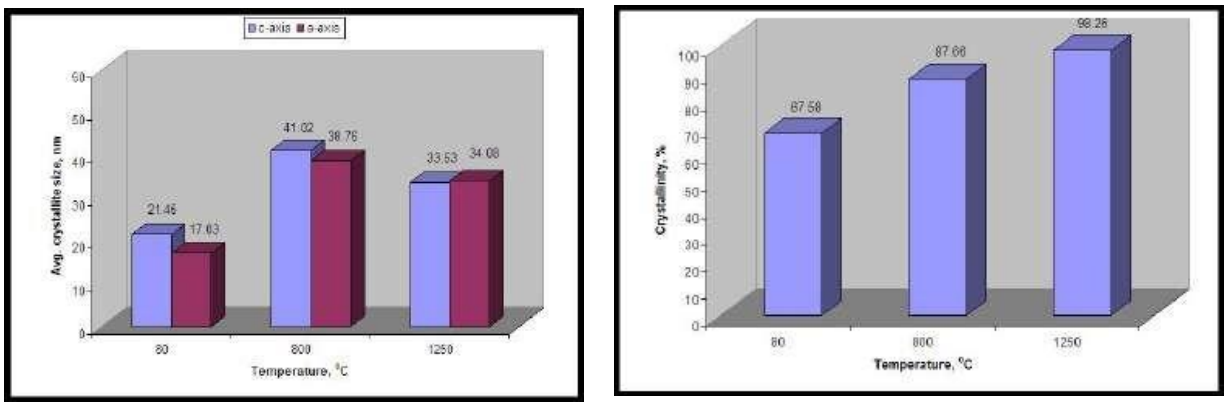

(a) (b)

Figure 2.3: Variation of average crystallite size and percent crystallinity (as calcu- lated from XRD) with variation of temperature of HAP powder.

X ray diffraction of powder synthesized by wet chemical method, calcined at two different temperatures, namely 800◦C and 1250◦C are given in Fig. 2.2. The powder was fired at 800◦C to optimize crystallinity, phase stability and powder morphol- ogy suitable for the final application. The other higher temperature of 1250◦C was selected to check the phase stability of the powder when fired to its sintering tem- perature. It is observed from Fig. 2.2 that the patterns are well matched with the JCPDS PDF no. 09-0432. All the standard peaks corresponding to different crys- talline planes and diffraction angles closely matched with the XRD pattern of the respective powders. This finding reveals that the powders are composed of single phase HAP and eliminate the presence of any other phase, even in minor quantity.

Crystallite size of the powder is another very important parameter which needs special attention because it influences the physical, chemical, biochemical and me- chanical properties of the dense and porous bodies prepared with it. XRD can be used to infer information about the crystallite size. In case of HAP crystal, (300)

plane which corresponds 32.902◦ 2θ and relative intensity (I/I0) ∼ 62% was used to calculate the crystallite size along the a-axis while (002) plane corresponding to 25.879◦ 2θ and I/I0 ∼ 33% was used to calculate the same parameter along the c-axis. The average crystallite sizes, that have been calculated along these axes for as-prepared and fired powders at different temperatures, are given in Fig. 2.3(a). It has been found that the average sizes increase along both the axes till the powders are calcined at 800◦C, but thereafter decrease as evident from the observations at 1250◦C. This is ascribed to the fact that in the second stage, the energy input was consumed both by sintering of the powder and for crystallite growth. The powder was characterized by XRD at these temperatures in order to show its stability of phase at these high temperatures and indeed, it was found that the phase which was formed initially was retained at these high temperatures.

Another important parameter which can be deduced from any XRD pattern of polycrystalline material is the degree of crystallinity (Xc) which gives an idea of the presence of amorphous content in the material, which in turn can affect different physical and mechanical properties. Xc corresponding to the fraction of crystalline phase present in the examined mass is evaluated by the relation: $Xc \approx 1 - \frac{V112/300}{I300}$

where I300 is the intensity of (3 0 0) reflection and V112/300 is the intensity of the hollow between (1 1 2) and (3 0 0) reflections, which completely disappears in non- crystalline samples [99]. The crystallinity increases from 67.6% to 98.3% when the powders are fired from 80◦ to 1250◦C, as seen in Fig. 2.3(b).

Scanning Electron Microscopy (SEM)

FESEM provides information about the morphology of the individual powder par- ticles and also helps to determine the particle size distribution. The HAP powder calcined at 800◦C has been observed for powder size, shape and morphology using Field Emission Scanning Electron Microscopy (FESEM) (Supra 35 VP, Carl Zeiss, Germany). For this, the powder particles were suspended in ethanol, mechanically shaken (GL 83, Toshniwal Flask shaker, India) for 30 min, immersed in ultrasonic bath for another 30 min and finally supernatant was collected and few drops of the same was spread on a watch glass before observation. The dried powder was then sputter-coated (Polaron, Quoram Technology, U. K.) with gold-palladium having a coating thickness ∼ 6nm to reduce charging and to improve the image quality prior to testing.

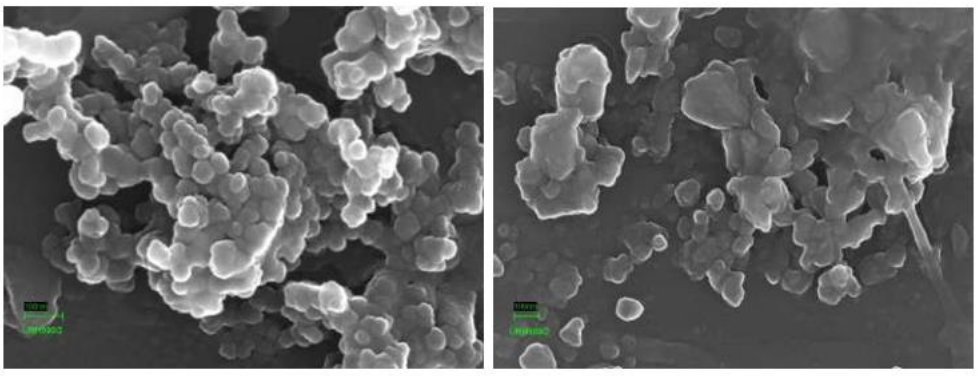

Figure 2.4: SEM microstructure of the HAP powders calcined at 800◦C

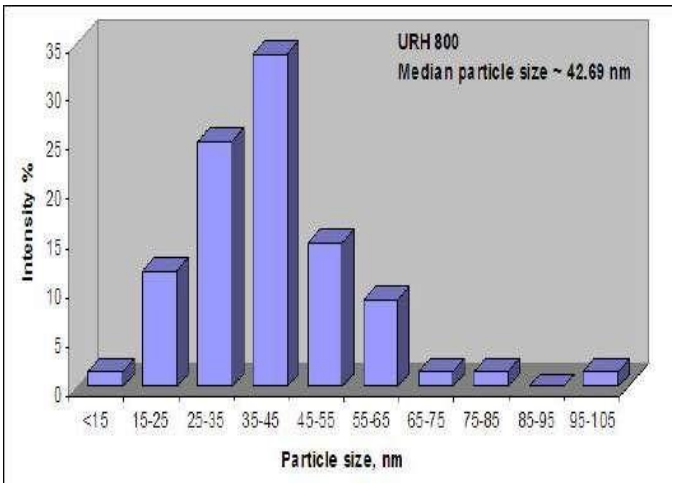

Figure 2.5: Particle size distribution of 800◦C calcined HAP powder

The FESEM micrographs are shown in Fig. 2.4. More or less spherical particle morphology could be observed with few agglomerated ones. Initial crystallinity of the powder has a role in this formation of agglomerate. Amorphous calcium phosphate in the as-dried powder facilitated material transfer across a continuous boundary phase. The average crystallite size of the 800◦C powder is calculated from the FESEM to be 41 and 39 nm along the c- and a-axis. The ratio of c/a is very close to 1, which indicates that the crystal should have an equiaxed shape. This is supported by the observations in the SEM microstructure.

Thereafter, the particle size distribution of this powder has been assessed from all the micrographs. Using the scale bar of each micrograph, the length and breadth of at least 250 particles have been calculated and the summarized results are presented through a histogram shown in Fig. 2.5. The median particle size is calculated to be ~ 43nm, as also observed from the histogram. This closely matches the findings from the XRD. The FESEM micrographs also show the presence of some amorphous content between the particles and the agglomerated state (Fig. 2.4b), which can be corroborated with the findings from the XRD of ~ 88% crystallinity or ~ 12% amorphous content.

Fourier Transformed Infra-Red (FTIR) Spectroscopic Analysis

Fourier transformed infra red (FTIR) spectroscopy is always used as a supportive tool for XRD, but sometimes it gives more information than XRD. FTIR spectrum has been employed to determine the chemical bonding in the functional groups present and stereochemistry of the powders calcined at different temperatures. The alkali halide disk technique was employed using ~ 2mg of respective powders in 200mg of powdered spectroscopic grade KBr (FTIR grade, Merck KGaA, Germany) which had been dried at 100◦C and allowed to cool in a vacuum desiccator to avoid absorption of moisture. The mid-IR spectra (4000 to 400 cm−1) were obtained with a double beam spectrophotometer (Spectrum 100, Perkin-Elmer, USA) which was purged of H2O vapour and CO2 by an air drier. The absorption bands of H2O vapour, CO2 and polystyrene film were used to calibrate the spectra in this region. The wavenumber accuracy of all sharp bands was 2 cm−1.

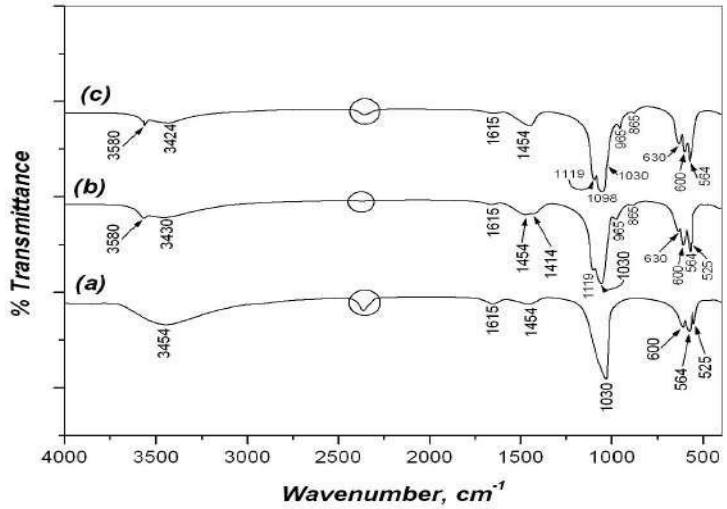

Figure 2.6: FTIR spectrum of the HAP powder: (a) as-dried, (b) calcined at 800◦C and (c) sintered at 1250◦C

IR spectra are caused by the different modes of vibrations and rotation of func- tional groups in a compound. The general principles which are useful in correlating the spectra with the molecular structure are: (a) each vibrational frequency or spec- tral band is related to a definite motion (e.g. stretching or bending) of the vibrating functional groups; (b) each functional group will produce a characteristic vibrational spectrum; (c) the vibrational frequency is dependent both on the masses of the atoms and the internal forces which maintain the configuration of the molecule (such as in- teratomic distances).

However, changes in the environment of the molecular groups may alter the equilibrium parameter of the molecular group (symmetry) and hence may cause the appearance of inactive vibrational modes and/or the removal or loss of degeneracies of others [49, 50]. More specifically, the IR analyses of the calcium phosphate powders give the fol- lowing information [102]: (a) identity, (b) purity, whether uni- or multiphasic, (c) presence of functional groups like HPO42−, CO32−, PO43−, P2O74−, organic com- ponent, etc., (d) environment of the functional groups -whether in free state or in crystal field, whether surface or lattice-bound, (e) effect of the incorporation of one element on the vibration frequency of other functional groups, (f) type of substitution, (g) crystallinity -whether well crystallized, poorly crystallized or amorphous as deduced from the resolution or loss of resolution of the vibrational bands. On the basis of this, the band assignments of HAP interpreted from the FTIR spectrum obtained at different temperatures could be summarized in Table 2.1.

The FTIR spectrum of as-dried as well as powders fired at different temperatures are plotted together and given in Fig. 2.6. Percentage transmittance has been hidden since all the graphs are plotted on the same y-axis. While XRD give similar patterns for several types of amorphous calcium phosphates, the FTIR spectra can show the functional group (e.g. carbonate or pyrophosphate) which contribute to the amorphous character of the Ca-P [104]. It is clear from Fig. 2.6 that the amorphous nature of the formed apatite crystal decreases with temperature. The lattice OH group at 3580 and 630 cm−1, which are characteristic of the HAP crystal, are observed at the higher temperatures while being absent in the as-dried sample [29, 210]. Hence, as in the case of the XRD, the FTIR also shows that there is no degradation of the HAP phase from as-dried state to sintered stage.

Wavenumber (cm^{-1})	Assignments
3700-3000	H-O-H, Water of crystallization or adsorbed water
3580	O-H group
1615	H-O-H, Water of crystallization or adsorbed water
1454,1414	C-O of CO_3 groups
1119,1098	P-O and P-OH, HPO_4 and PO_4 groups
1030	P-O in HPO_4 and PO_4 groups (stretching mode)
965	P-O in PO_4 group
865	P-OH stretching mode of HPO_4 groups
630	O-H of OH group
600,564	P-O in PO_4 groups (bending mode)
525	$HO-PO_3$ bending mode in HPO_4

Table 2.1: Band assignments of IR spectrum indicating vibrational frequencies of HAP

Differential Thermal Analysis (DTA)/ Thermo-Gravimetric Analysis (TGA)

Thermal decomposition of HAP powder results in oxyapatite [Ca10(PO4)6O] (OA), thereafter hydroxy-oxyapatite [Ca10(PO4)6O(OH)2−2x] (OHA) and finally calcium phosphates during sintering [55, 203, 218]. This decomposition exhibits some un- desirable influences on the physical, chemical, mechanical and especially biomedical properties of HAP based products [13, 55, 169]. The exact temperature of the mass changes, that occur when the sample dissociates and releases the reaction products to the atmosphere or reacts with the surrounding, can be identified using Simultaneous differential thermal analysis and thermogravimetric analysis (DTA-TGA) curves.

Simultaneous DTA and TGA analysis (DTA-TGA, Model STA 409, Netzsch GmbH, Selb, Germany) have been conducted till a temperature of 1300◦C with a faster heating rate (10◦C/min) to monitor the weight loss/gain and thermal be- haviour including phase transition (inversion/conversion) upto that high tempera ture. A stagnant air atmosphere has been employed for most of the experiments. The Al2O3 crucible, dried airflow at the rate of 100 cc/min and Al2O3 powder, as a reference sample, were used in the experiments. About 100mg of the powder has been used and filled loosely in the crucible for every measurement.

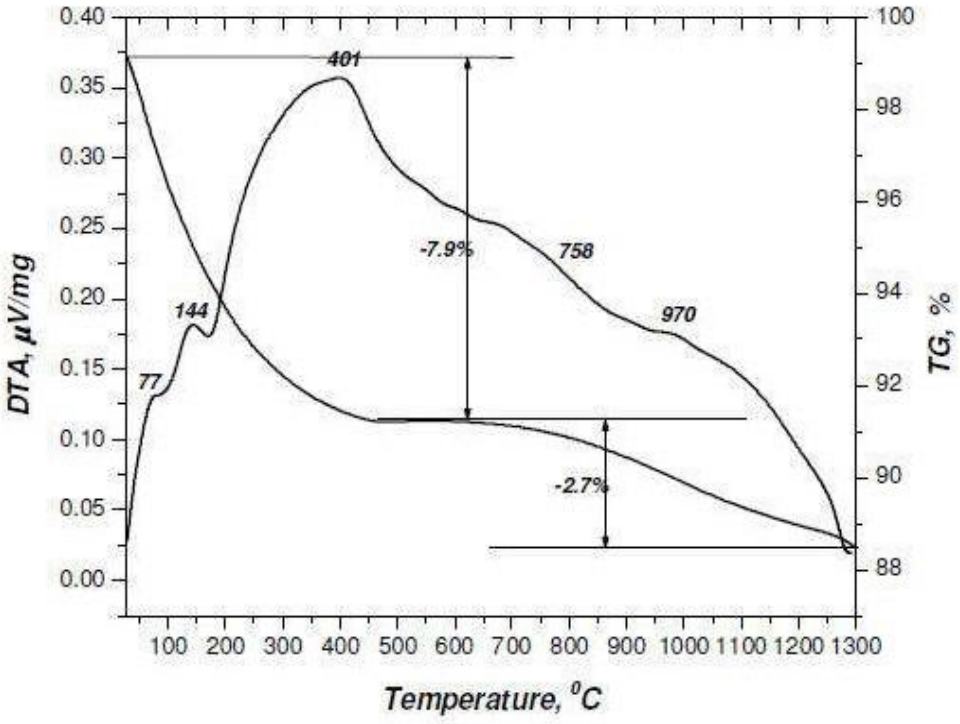

Figure 2.7: DTA-TGA plot of the HAP powders (from room temperature to 1300◦C)

DTA-TGA of the as prepared powder synthesized by URH method upto a tem- perature of 1300◦C is given in Fig. 2.7. Fast rate of heating was employed to identify the exact temperature of conversion/inversion. Endothermic reactions corresponding to the loss of adsorbed water and loss as structural water have been found in the temperature range of 140-450◦C with corresponding weight loss of ∼ 8%. A shallow broad exotherm is observed over the total temperature regime, which is indicative of crystallization in the initially formed amorphous HAP, as confirmed from the XRD.

There is no sharp exo-or endothermic peak after 800◦C. This indicates that beyond 800◦C, only crystal structural rearrangements occur without any decomposition re- action. Furthermore, beyond 700◦C, there is very slow incomplete dehydroxylation stage of decomposition of HAP powder till 1300◦C. Based on these study results, HAP powder calcined at 800◦C have been used in the present study for subsequent fabrication of granules. These were finally sintered at 1250◦C prior to subsequent use as filler material or as coatings on bare titanium dental implants.

Bioactive glass powder preparation

Bioactive glass was prepared through a conventional glass melting procedure. Ap- propriate amounts of reagents/ raw materials like silica (SiO2), calcium carbonate (CaCO3), dry soda ash (Na2CO3), decahydrated borax (Na2B4O7.10H2O), titania (TiO2), di-ammonium hydrogen ortho-phosphate (DAP) were mixed homogeneously in water. The batch composition of the glass is shown in Table 2.2, while Fig. 2.8 shows the schematic representation of the procedures followed to prepare the final glass composition. In a nutshell, the mixture was dried at 120◦C and subsequently melted in air at 1400◦C for 3h in a platinum-crucible.

SiO_2	$Na_2B_4O_7.10H_2O$	Na_2CO_3	$CaCO_3$	$(NH_4)_2HPO_4$	TiO_2
43-44	6-7	11-12	29-30	8-9	1-2

Table 2.2: Batch composition of the glass (wt %)

In order to obtain the bioactive glass in powder form, the melt was quenched in water to obtain flaky glass particles, which were dried and further ground for 48h in aqueous medium using zirconia balls in a planetary ball-mill.

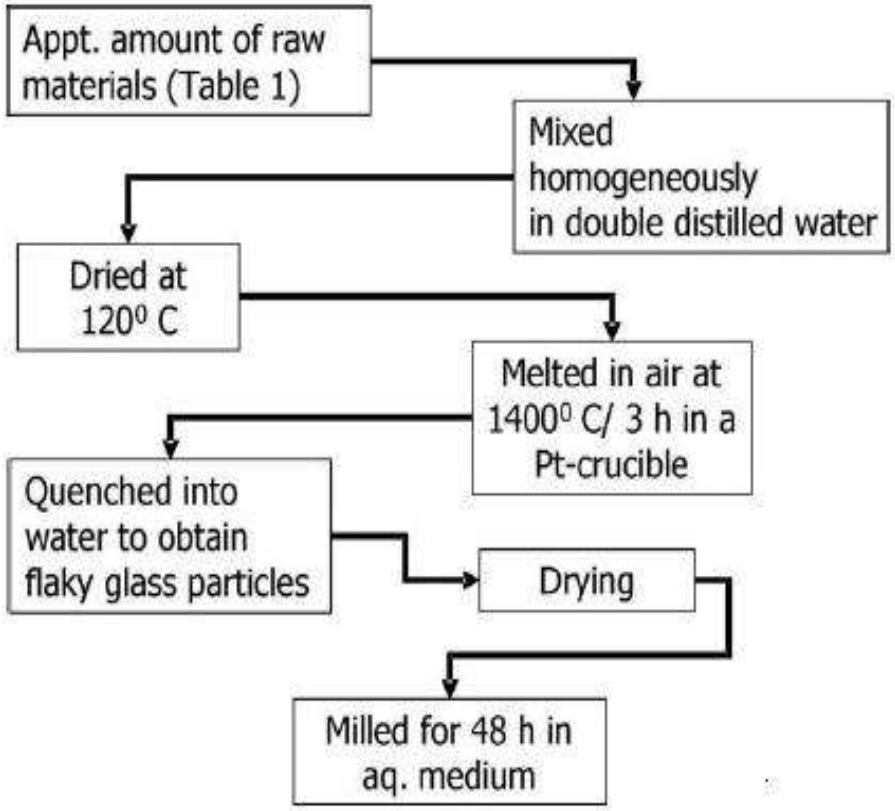

Figure 2.8: Bioactive glass Powder Preparation

Bioactive glass powder characterization

Thorough chemical analysis of the bioactive glass powder prepared at 1400◦C was performed to ascertain the final composition. Inductively coupled plasma-atomic emission spectral (ICP-AES) analysis was performed using Spectro flame Modula (Spectro Analytical Instruments, Germany) which yielded the final bioactive glass powder composition stated in Table 2.3.

Composition	SiO_2	CaO	P_2O_5	B_2O_3	Na_2O
% by wt	43.70	19.20	5.46	9.40	22.24

Table 2.3: Final composition of bioactive glass powder(wt %)

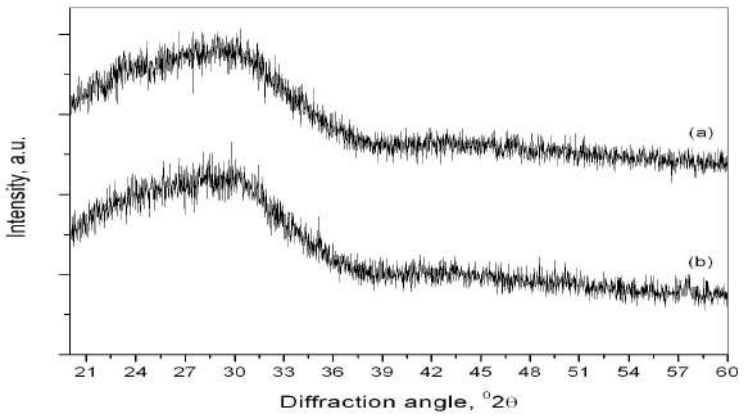

Figure 2.9: X-ray diffraction of bioactive glass powders prepared (a)at 1400◦C and (b) at 725◦C

X-Ray Diffraction (XRD)

XRD of bioactive glass powders, formed after rapid quenching from 1400◦C, was performed using the same equipment and same parameters as stated in Section 2.2.1 and is shown in Fig. 2.9. The XRD technique is used to assess the phase purity and crystallographic changes, if any. Bioactivity of bioactive glass depends on crystallo- graphic changes. Thus, it is necessary to study its nature of phase before intending to use it in in-vitro and in-vivo applications.

A crystallite comprises of a number of cells systemically grouped together to form a coherently diffracting domain. If the cells are not identical but show a variation in atomic position destroying long-range order, the material is called amorphous. It is observed from the pattern that the powders are mainly amorphous in nature with no incipient formation of crystals as is to be expected for any glassy material. In the present study, this lack of incipient crystallization is considered desirable for actual in-vivo application, since it could be correlated with the presence of phosphate and silicate network and the possible phase separation even in microscale.

Scanning Electron Microscopy (SEM)

The preparation conditions of as-prepared bioactive glass powders before observing under SEM was the same as that for HAP powders as stated in Section 2.2.2. The SEM of the bioactive glass powders is shown in Fig. 2.10.

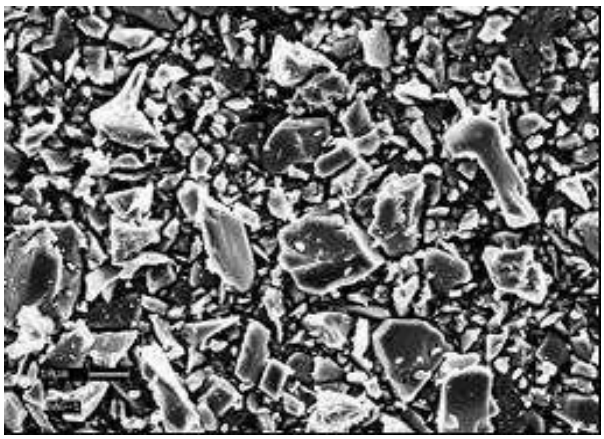

Figure 2.10: SEM of the as-prepared bioactive glass powders

Because of its amorphous nature and nano size (with associated high free energy) in the as-prepared formation, the bioactive glass powders were found to be much agglomerated with no definitive physical structure. As expected for any glassy material, there was no sign of any crystal throughout the microstructure. These observations corroborate the observations from the XRD.

Fourier Transformed Infra Red (FTIR) Spectroscopic analysis

FTIR spectroscopy of the prepared bioactive glass powder has also been studied for confirmation of the functional groups present. These were measured at room temperature (∼ 20◦)C in the wavenumber range of 4000-400 cm−1 at resolution 2 cm−1 using Spectrum 100 (PerkinElmer Instruments, USA). The samples were pulverized into fine powder, and then mixed with potassium bromide powder, a weight ratio of 1:100 (0.002 g:0.2 g, samples:KBr, respectively). The mixture was subjected to a load of 15 T cm2 in an evacuable die for 5 min to produce homogenous pellets. The spectra were measured immediately after preparing the pellets to avoid moisture attack.

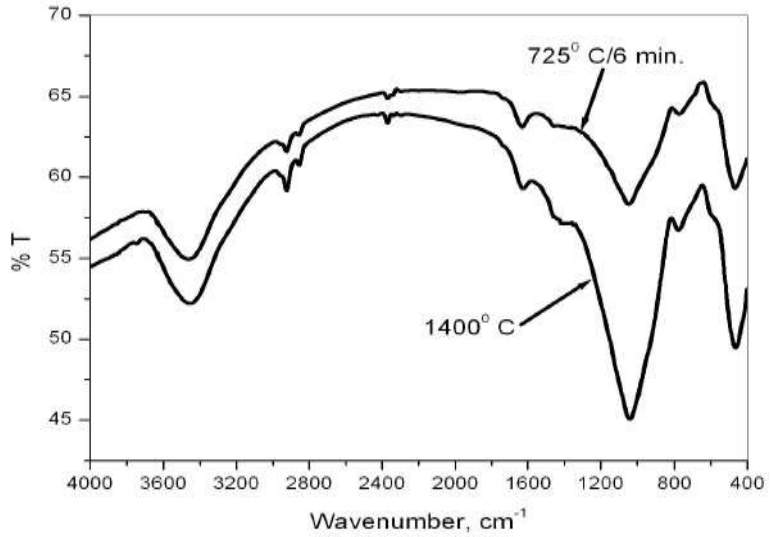

Figure 2.11: FTIR spectra of the bioactive glass powder prepared at 1400◦C and at 725◦C

The FTIR spectra of the bioactive glass powder in Fig. 2.11 shows well-defined transmission bands characteristic of the samples prepared at 1400◦C with sharp split bands. The IR transmission spectra show well-defined transmission bands at around 1094, 776 and 416 cm−1 which might due to Si-O-Si asymmetric stretching of bridging oxygen atoms within the tetrahedra, Si-O-Si symmetric stretching of bridging oxygen atoms within the tetrahedral and Si-O-Si bending, respectively. This observation could be correlated to the observation of Hench [74]. The weak inflection at 1627 cm−1 can be assigned to the presence of molecular water. The broad band centered at 3455 cm−1 can be assigned to hydroxyl group (-OH) or silanol group (Si-OH) which is indicative of bioactivity.

Differential Thermal Analysis (DTA)/ Thermo-Gravimetric Analysis (TGA)

DTA-TGA of the as-prepared bioactive glass powders was performed using the same instrument and parameters as described in Section 2.2.4 except for the final temperature (800◦C in this case) and much higher heating rate (20◦C/min) mainly to ascertain the thermal profile of the powders and estimation of glass transition temperatures. The DTA-TGA curve thus obtained is given in Fig. 2.12.

The glass transition temperature was calculated from the differential DTA in Fig. 2.12 and was found to be about 750◦C. It was also found that there was about 5% gradual total weight loss upto 800◦C which include removal of both adsorbed and surface water from the powder surface. Also, there was

no conversion to any crys- talline phase upto that temperature which is desirable for subsequent heat treatment, as required for the use of these powders as coatings of metallic substrates.

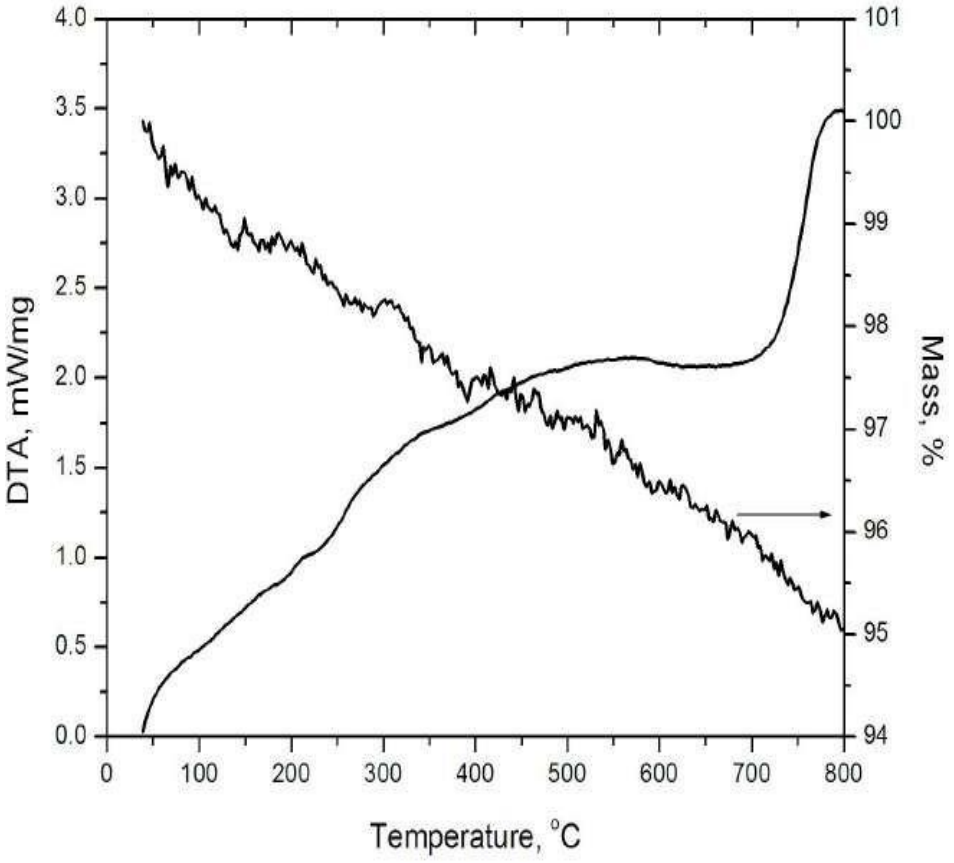

Figure 2.12: DTA-TGA plot of the as-prepared bioactive glass powders (from room temperature to 800◦C)

Discussions

In this Chapter, the HAP and bioactive glass powders indigenously prepared at the CSIR-Central Glass and Ceramic Research Institute (CSIR-CGCRI), Kolkata have been considered for the feasibility of their use in this study for dental implantation purposes. Hence, it is necessary to analyse the powder characterizations in terms of a) the ability of these bioceramic powders to obtain physico-chemical attachment to the bone by means of their bioactivity; and b) the usability of these powders as coating material on metallic implant surfaces in terms of their bonding strength.

The presence of high peaks of Ca and P ions in the XRD patterns of both HAP and bioactive glass powders are indicative of the bioactive capability of these powders when in contact with the bone. This

capability of the powders is further substanti- ated from the structural information received from SEM micrographs as well as the information about the presence of critical functional groups from the FTIR spec- trum, albeit in different ways. In case of the HAP powder, both the SEM and the FTIR results confirm the crystallinity of the powder even at temperatures as high as 1250◦C. This is known to improve the bioactivity of the HAP powder [74].
On the other hand, bioactive glass exhibits a non-crystalline glassy amorphous character, as evident in the SEM micrographs as well as the FTIR spectrum. However, the confirmed presence of the hydroxyl group (-OH) in the FTIR spectrum of bioactive glass powder is indicative of its bioactivity [74].

For use of these powders as coatings on the metallic implant surfaces, it is necessary to ensure high bonding strength under high temperatures. The results of the DTA-TGA confirm that HAP powders calcined at 800◦C are suitable for use as implant coatings. The corresponding results for the bioactive glass powder indicate that the glass transition temperature is about 750◦C and there is no crystalline phase formation till 800◦C, hence these powders are also usable as coatings. Furthermore, as expected for both these types of bioceramic powders [170], there is no water ab- sorption, thus leading to better adherence capability of these powders when used as implant coatings within the bone.

DESIGN OF BIO-CERAMIC AND GLASS BASED DENTAL IMPLANTS

A successful dental implantation requires an union between the implant and the surrounding hard tissues, often referred to as the implant-bone interface. This is also referred to as the bone-implant contact (BIC) in current dental literature [135]. The success of dental implants depends upon the quality and quantity of the harbouring bones. It also depends on the surface topography of the dental implant, for example, whether it is micro sand-blasted or acid-etched. For most of the implant designs, roughened titanium is adopted as the material of choice since it is generally accepted that the surface roughening increases the possibility of points of contact at the implant-bone interface and thus improves the early process of osseointegration [135].

An equally important factor for the improved BIC is the macro design of the dental implant, specifically involving the designs of the shape of the implant, the thread form, the neck geometry and similar details. The shape of the implant is typically cylindrical or tapered [135] while various thread geometries have been considered by different researchers [5] since it has been proven that thread geometric variations affect the mechanical locking [135].

The present work focusses on the effects of the implant macro-design on the implantation process in humans. In this Chapter, Section 3.1 reviews the bone quality and type in the human jaw, Section 3.2 gives an overview of the standard implant macro-design based on roughened Ti alloy implants [130, 135]; while a new, simpler, cheaper yet effective metallic (typically Ti alloy or stainless steel) implant with a smooth surface topography and certain modifications in the macro-design has been proposed in Section 3.3.

As stated earlier, increasing the surface roughness of implants is another important concern since this further enhances the BIC. In order to do so, the two types of bioactive materials: namely HAP and bioactive glass powders, whose preparation and characterization have been discussed in Chapter 2, have been used as coatings on the newly designed implant. The HAP and bioactive glass coatings and their characterizations have also been done at the CSIR-Central Glass and Ceramic Research Institute (CSIR-CGCRI), Kolkata, as reported by Dey et al. [39] and Soundrapandian [184] respectively. The

details of the coatings used and their characterizations, which are relevant to dental implantation applications, have been stated for HAP and bioactive glass in Sections 3.4 and 3.5 respectively. The assessment of the effect of these coatings on the BIC of the dental implant has been stated in Section 3.6.

Human Jaw Bone: Quality and Type

A dental implant is generally used in human subjects under edentulous or partial edentulous situations, or in other words, in absence of all or some teeth in the mouth. The human jaw bone comprises of an outer cortical and an inner cancellous (or marrow) part. Aspects critical to dental implantation are the availability of a particular bone type and its density. These depend on the location in the human jaw bone, while the type of bone also varies with the age of the patient. The most dense part of the bone with cortical part is mostly seen in the lower or mandibular jaw bone. This is followed by the anterior part of the maxilla while the least density, with more marrow spaces, is found in the posterior part of the maxilla. Porous cortical part of the bone is found in the ridge portion of the jaw bone. Coarse and trabecular patterns are seen within the outer shell of the cortical bone. A classification of bone density according to Linkow [110] is stated in Table 3.1.

Classification	Characteristics of Bone	Clinical Importance
Class I bone structure	Ideal bone type consists of evenly placed trabeculae with small cancellated space.	Most ideal foundation for dental implant prosthesis.
Class II bone structure	The bone has slightly larger cancellated spaces with less uniformity of the osseous pattern.	Satisfactory for dental implants.
Class III bone structure	Large marrow-filled spaces exist between bonetrabeculae.	This type of bone results in loose fitting implant.

Table 3.1: Classification of bone density [110]

Another standard classification of the bone quality in cross-section by Lekholm and Zarb [105] is given in Table 3.2.

The available bone and its biological considerations decide the diameter, length, macro and micro (surface) form of the dental implant for an edentulous area as well as the number of implants to be used. For less dense bone, increasing the number of implants is an option to increase the functional load bearing area, and thus reduce the effective stress on the region. Within the biological limits, increasing the diameter of the implants may increase the surface area and in such cases, the length of the implant can be reduced. Implants designed for D4 bone should have highest surface area. This can be achieved by changing the implant macro design. A threaded endo- osseous root form implant has 30% more surface area than a cylindrical root form implant. The surface area increases proportional to the number of threads. The depth of surface also can be altered according to the demand. Moreover the surface area can be increased by 500 times using different surface treatments, like coating of the dental implant.

In view of these considerations, an alteration of the dental implant macro-geometry is proposed in Section 3.3. The surface treatment of this implant is then done using the HAP or bioactive glass coatings on the implant, as stated in Sections 3.4 and 3.5.

Quality	Characteristics of bone	
D1	Homogenous Compact Bone	
D2	Thick layer of compact bone surrounding a core of dense trabecular bone.	
D3	Thin layer of cortical bone surrounding a core of dense trabecular bone.	
D4	Thin layer of cortical bone surrounding a core of low density trabecular bone.	

Table 3.2: Classification of bone quality in cross-section [105]

Typical Macro-Design of Dental Implant

In order to appreciate the modifications proposed in the macro-design of the dental implant, a detailed analysis of the standard structure of a dental implant [130] is stated here after.

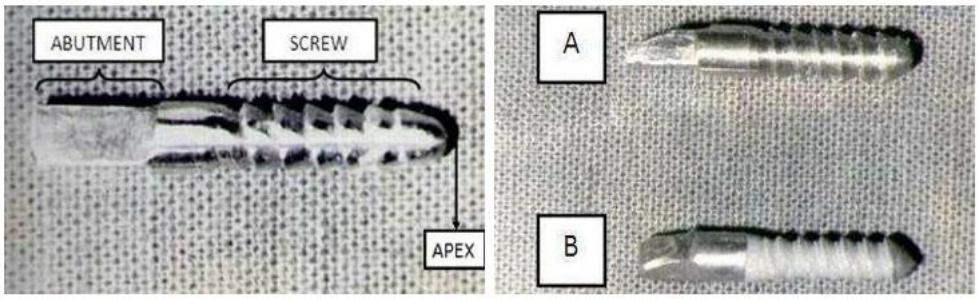

Figure 3.1: Single stage dental implant and variants [24]

Dental Implant Body

The dental implant body replicates the root form of a natural tooth and hence, is retained permanently in the jaw unlike a typical denture. This is usually drilled into the hole socket within the bone. As stated earlier, an implant is typically made of Ti or Ti-alloy and maybe cylindrical or tapered in form.

Dental implants used by the clinicians may be single-stage or two-stage implants. The single stage implant is traditionally a single structure composed of the implant body and the abutment as shown in Fig. 3.1. Of these, the abutment projects outside the transmucosal or gingival part of the jaw bone after implantation. Variants of such single stage, also called stage I, implants were designed and developed in an earlier work [24]. In this design, the implant body has an apical tapered part without any thread. This minimizes the damage to the underlying bone while placing the implant into the drilled hole.

However, modern day dental surgeons prefer the use of the two-stage, also called stage II, dental implants. The typical structure and components of the standard two-stage dental implant, as stated in Misch [130], is shown in Figure 3.2. It is to be noted that in this design, a combination of the implant body and the abutment shown in Fig. 3.2(a) forms an equivalent single-stage implant. The body of a stage II implant usually has an internal thread but depending on the manufacturer, in some designs,

there might be an external thread. Both internal and external threads are typically designed in the hex thread form in order to provide an anti-rotational function. These threads are provided in (on) the implant body since it has to be covered by a screw after the placement of the implant in the jaw.

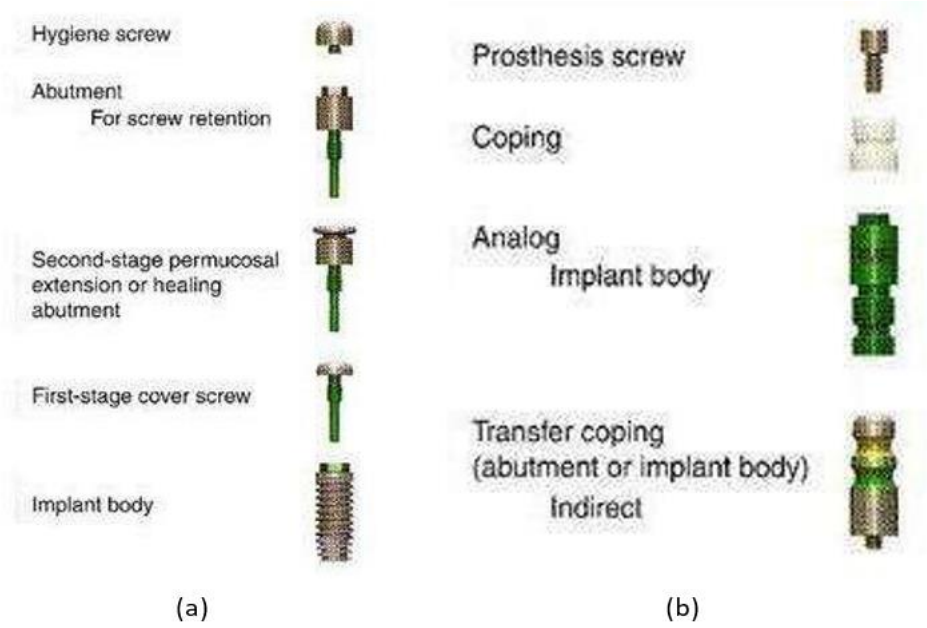

Figure 3.2: Dental implant components a) for two-stage implant in situ b)for prosthetics [130]

First Stage Cover Screw or Healing Screw

At the time of insertion of a stage II implant body, a first stage cover screw, more commonly referred to as a healing screw, has to be screwed into the top of the implant to prevent bone, soft tissue or debris from invading this area during healing. This thus keeps the internal thread portion free of any intrusion/growth and facilitates the insertion of the prosthetic abutment into the predetermined transmucosal region.

Healing Abutment

After a predetermined healing period to allow for sufficient tissue growth, it is necessary for the clinician to perform a surgical intervention. This is required to expose the stage II implant in order to attach a transepithelial portion to the implant body. So, when the clinicians decide that the bone

regeneration is sufficient, typically after 3 months of the implantation, they get an X-ray done of the implant and its associated region and certain clinical observations are also noted. If the X-ray report is within normal limits and clinical observations show that there is no infection or mobility or bleeding on probing, then the healing screw is removed and the second stage per- mucosal extension, commonly referred to as the healing abutment, is inserted in its place. As the name suggests, this extends the implant above the mucosal soft tissue and results in the development of a permucosal seal which helps in the formation of the soft tissue structure around the implant. This is usually retained in the jaw of the patient for 7 to 10 days.

Hygiene Screw

The structure of the healing abutment shown in Fig. 3.2 has a protruding top surface which is similar in form to a screw head. In some other designs, the healing abutment has an internal hex thread form. In such designs, the hygiene screw is placed over the permucosal healing abutment. The functionality of the hygiene screw is similar to that of the first stage cover screw, that is, it provides an interim cover on the healing abutment and thus prevents any unwanted growth of soft tissue in the internal thread region.

Abutment

When the clinician has ascertained that the bone regeneration has reached the stage where the implant can be structurally as well as functionally loaded with the pros- thetics, typically after the 7 to 10 days mentioned earlier, then the healing abutment is unscrewed from within the implant body and is replaced by the abutment. The abutment has a threaded screw form at the lower end for screwing it into the implant body while the hygiene screw is retained initially for providing the interim covering for the abutment.

Prosthetic Abutments

A set of prosthetic abutments, as shown in Fig. 3.2(b), are used in the case of a stage II implant in order to prepare the final prosthesis. This is usually prepared using one of the two commonly prevalent approaches, namely prosthesis fabrication by the clinician or laboratory fabrication of the prosthesis.

In both cases, the overall final structure of the implant, which is permanently inserted in the jaw of the patient, consists of the inserted implant body into which the superstructure is screwed in. This superstructure essentially has a lower part which has a form similar to the top of the abutment shown in Fig. 3.2(a) and an upper part similar to the coping shown in Fig. 3.2(b). This may be available as a single structure, called the analog. In such cases, the abutment is replaced by the transfer coping for preparing the final prosthesis. The clinician obtains an impression of the implanted region including the implant and transfer coping with a rubber based impression material. This is sent to the laboratory so that a master cast can be prepared in which the analog of the implant can be placed for final fixation of the crown. However, in several implant designs, the superstructure may have three separate sub-components. These are the abutment, as discussed earlier, onto which a coping is screwed in using a prosthesis screw. This prosthesis screw typically has two threaded forms, upper and lower, of different diameters in which the upper threaded form is used for the mechanical attachment of the crown. In all cases, the crown is either screwed onto the superstructure or is cemented onto it.

Figure 3.3: Designed Dental Implants

Proposed Design Simplification

As stated at the outset, the objective of the work presented in this thesis is to design and develop an indigenous, affordable dental implant for the Indian population. This would nevertheless provide most of the functional benefits obtained in the existing commercially available implants, without sacrificing

patient comfort. Such a simplified, yet effective version of the standard stage II implant was developed at the Coatings Division of CSIR-Central Glass and Ceramics Research Institute (CSIR- CGCRI), Kolkata. The overall dental implant structure was minimally reduced to three basic components an implant body, a healing screw and an abutment as shown in Fig. 3.3. A picture of the overall implant fitted with the prosthetics (crown) is also shown in the figure.

In this case, the clinician inserts the implant body into the jaw of the patient and covers it with the healing screw for the period required for bone regeneration. Thereafter, typically after about 3 months, the surgeon performs the necessary in- cisions to access the region. As in the standard case, this is done on the basis of X-rays of the region and clinical observations in order to ascertain that sufficient soft tissue growth has taken place. On ensuring that proper growth has taken place, the clinician temporarily screws in the abutment into the implant body, in place of the healing screw, in order to take a rubber impression of the region. This impression, along with the abutment, is sent to the laboratory for the design and cementing of the prosthesis, commonly called crown, on the abutment. This takes a time of typically 7 to 10 days, during which the healing screw is screwed back onto the implant to enable further tissue growth. Once the abutment with prosthesis is received from the laboratory and the clinician reassures himself/herself that the patient jaw is healed sufficiently for functional loading, the healing screw is removed and the abutment with crown is screwed in securely into the implant body, thus permanently replacing the missing tooth.

It can thus be seen that the proposed design simplification does not hamper the functionality of the implantation process or the implant. Instead, the operating costs can be reduced drastically due the overall simplicity of the design and the reduction of the additional components pertaining to the prosthetic abutments and also the healing abutment and hygiene screw as shown in Fig. 3.2. Thus, the next step in the research involves determining the design specifications for each of the individual components. These are shown in Fig. 3.4 and are discussed in detail hereafter.

Implant Body Design

The proposed macro-design of the dental implant is shown in Fig. 3.4(a) and (b). The material of implant used in this case is Ti alloy (alternatively stainless steel, only for some ex-vivo trials). A cylindrical smooth blank, as shown in Fig. 3.4(b) is used for designing the implant body. But, smooth

implants can have poor primary stability and BIC since variable roughness is the only factor to hold the implant in situ. So, to gain more stable attachment, threads have been generated partially on the exterior of the cylindrical form, as shown in Fig. 3.4(a).

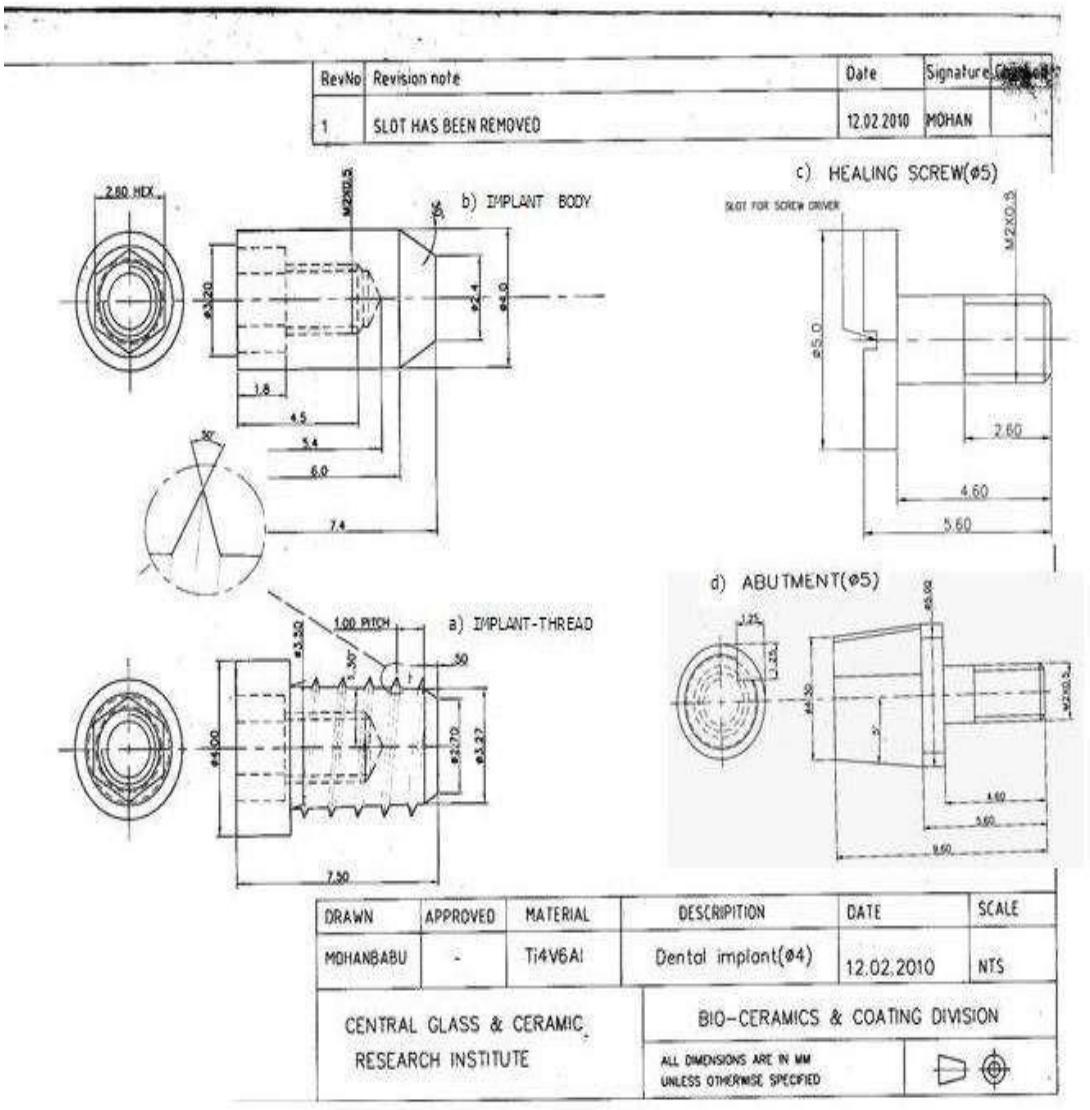

Figure 3.4: Modified Design of Dental Implant

The total length of the implant is maintained at ~ 7.5mm. Of this, the upper portion (shown leftmost in Fig. 3.4(a) in solid lines) is a smooth region ~ 2mm long without any thread, which forms the implant crest module. Next comes the threaded portion which is ~ 4mm long. The remaining ~ 1.5mm

smooth tapered region (seen rightmost in Fig. 3.4(a) and (b)) forms the apical part of the implant body. The diameter of the threads is ∼ 3.5mm as shown in Fig. 3.4(a). The threads allow the growth of gingival mucosa, which will attach the implant to the surrounding bone. This design of the implant can be easily screwed into the bone using only a round bur drilled hole.

Thread Shape: The shape and face angle of the thread modify the direction of the occlusal load [132, 22]. Usually, implant threads have 30◦ angulation for obtaining better implant attachment during insertion [135]. However, it must be noted that when using a particular implant, the effect of a single feature could be washed out by other elements of the particular design of the selected implant [5]. Hence, in the present design, 25◦ face angle has been used which increases the angulation to 50◦. This is done with the objective of achieving similar level of primary attachment of the coated implant as in the case of the typical uncoated implant, since any coating of the bare Ti threaded surface is expected to reduce the effective angulation of the implant thread. Thus, typical parabolic 'V' shaped threads have been used for this design, but with 25◦ face angle. A single pitch of the thread has been shown in a circular insert in Fig. 3.4(a).

Thread Pitch: The thread pitch used in this implant design is 1mm as shown in Fig. 3.4(a). In this design, a single threaded implant body with more than usual number of pitches have been used to get more amount of bone-implant contact re- lationship. Furthermore, 2◦-5◦ gradual taper with linear isotropic law has been used in the threaded portion of the implant body, from apical part to crest module, in order to make the implants self tapped in nature.

Apical Part: The apical part of the implant body is of length ∼ 1.5mm. As in the typical case, the apical part is blunt to avoid injury during insertion. This also works as an anti-rotational part at the apical region and helps in bone formation.

Implant Body Crest Module: In Fig. 3.4(a), the implant body crest module is seen as the leftmost part of the implant body, beyond the threaded region. This is 4mm in diameter and ∼ 2mm long. The implant body crest module is basically flat and smooth with a platform at the alveolar ridge. An internal hex is provided in the crest module as an anti- rotational component for insertion of the healing screw. Fig. 3.4(b) shows that this internal thread has a total length of 5.4mm with a maximum diameter of 3.2mm at the top.

Healing Screw Design: The proposed design of the healing screw, shown in Fig. 3.4(c), is such that it prevents the formation of soft tissue, debris or bone within the internal threaded region of the implant. The healing screw, which is also made of Ti alloy, has a total length of 5.6mm. The top portion is of length 1mm and diameter of 5mm, with a slot on top to hold the screw-driver during its insertion. This portion sits flat on the implant crest module after insertion of the healing screw. The lower parallel portion is 4.6mm in length, of which the lowest 2.6mm has external threads cut into it for secure placement into the implant. The apical portion of the healing screw is kept flat.

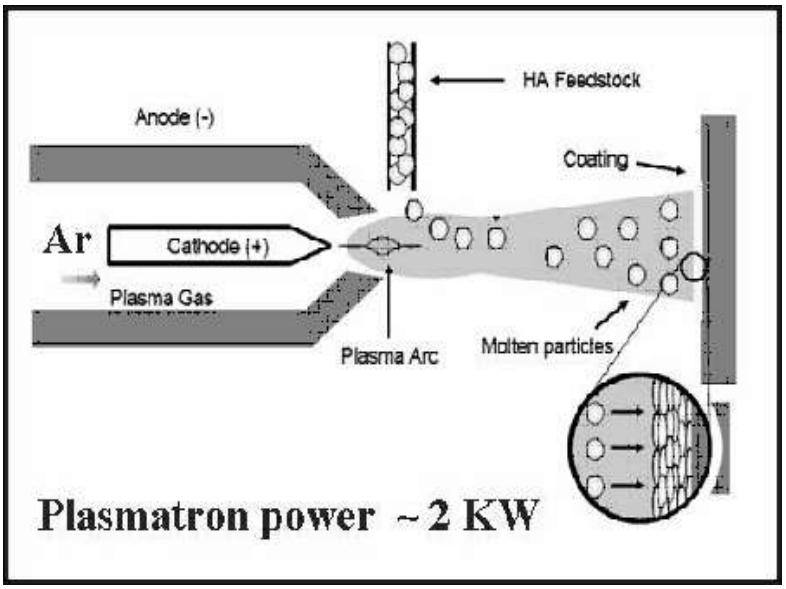

Figure 3.5: Schematic of Plasma Spray Process

Abutment Screw Design

The proposed design of the abutment screw is shown in Fig. 3.4(d). The abutment, which is also made of Ti alloy, has a total length of 9.6mm. The lower structure is identical to that of the healing screw while the top portion has an additional topmost part of length 4mm which is smooth and tapered. This topmost tapered region has a vertical slit as an anti-rotational device for proper cementing of the superstructure or crown.

HAP Coating: Plasma spray method

The designed dental implants were coated with HAP using a low power Argon (Ar) plasma spray method. The schematic of the process is illustrated in Figure 3.5. Due to high potential difference, a pilot arc is initiated between tungsten cathode and continuous water cooled copper anode. Argon (Ar) is used as the primary gas and is passed between the cathode and anode where it ionizes. This ionized Argon gas provides a continuous current path for the main transferred plasma arc. In this pro- cess, Argon was also used as the secondary gas to protect the sample from oxidation. Hot and partially molten externally fed powder was flown by Ar gas pressure and it stuck layer by layer on the substrate in the form of splats. Subsequently, the splats were air cooled to affect the coating development.

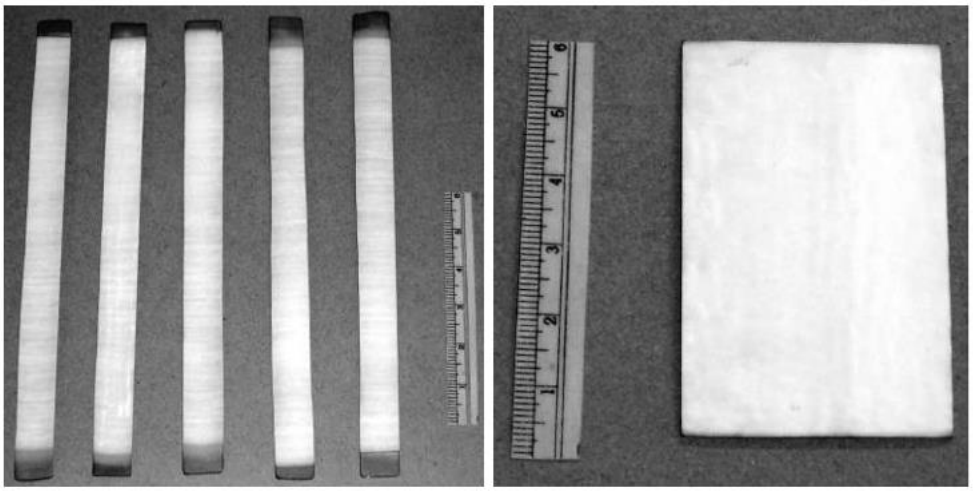

Figure 3.6: HAP coated SS316L substrates (test pieces) with dimensions (a) 155 mm x 20 mm x 2 mm (b) 25 mm x 25 mm x 2 mm

As test piece, commercially available SS316L were cut into rectangular strips of sizes 155 mm x 20 mm x 2 mm and 25 mm x 25 mm x 2 mm. These were then used as the metal substrates for the HAP coating as shown in Fig. 3.6. The same SS316L was also used to prepare stainless steel base HAP coated dental implants with the specific macrodesign. HAP granules in the size range of 53-64µm with good flowability (flow rate of ~ 0.5g/s) measured using Hall flowmeter (Lloyds, India), ASTM B 212 [1], were used for plasma spraying [36, 37] of both the test pieces and the designed dental implants. Prior to plasma spray treatment, the substrates were roughened by blasting the surface with about 200-

250µm alumina grits to a centre line average (CLA) of about 2.5µm (Taylor Hobson I-120, UK). Atmospheric plasma spray was carried out using a commercial instrument (Miller Maxstar 200 SD 2.5kW, USA) at a low plasmatron power of 1.5-2kW with external powder feeder chamber. The plasma spray parameters used in the present study for coating on the substrate are given in Table 3.3. The coating thus obtained was subsequently annealed at 600◦C for 2h to modify the coating properties and adherence to the substrate.

Parameters	HAP coating
Primary Gas Pressure (N_2)	4 bar
Secondary Gas Pressure (H_2)	4 bar
Primary Gas flow rate	471/min
Secondary Gas flow rate	4.71/min
Current	500 A
Voltage	70 V
Power	35kW
Stand-off distance	75mm
Number of passes	5

Table 3.3: HAP Coating Parameters

Phase analysis using XRD

The phase purity and degree of crystallinity of the coatings were analyzed by X-ray diffraction (XRD; Philips PW 1710, Holland) technique using monochromatic CuKα1 radiation at 55mA and 40kV, following methods given in Klug and Alexander and Landi et al. respectively [91, 99]. Phase and crystallographic features of coating ob- tained after plasma spray treatment, both before and after heat treatments at 600◦C is given in Fig. 3.7. The data for the as-synthesized powders and powders/granules fired at 1250◦C is also incorporated in Fig. 3.7 for comparison. It is observed that the crystalline phase of HAP is retained after plasma spraying and post heat treatment of this coating material (Figs. 3.7c and 3.7d). In addition, the respective positions of the XRD peaks are found to be well matched with JCPDS 74-0566 (calcium hydroxide phosphate, Fig. 3.7a) or 09-0432 (crystalline hydroxya- patite, Fig. 3.7b). The degree of crystallinity for HAP granules, as sprayed and 600◦C heat-treated HAP coatings are ∼ 98%, 80% and 91% respectively. Initial re- duction in crystallinity of HAP granules can be ascribed to unmelted HAP particles in asprayed plasma spray coating while the later enhancement reflects the presence of more crystalline phase formation in the 600◦C heat-treated

coating. It is known that further increase of post heat-treatment temperature causes an adverse effect on the substrate SS316L [185] and also the coating crystallinity [27] and hence, has not been attempted in the present work.

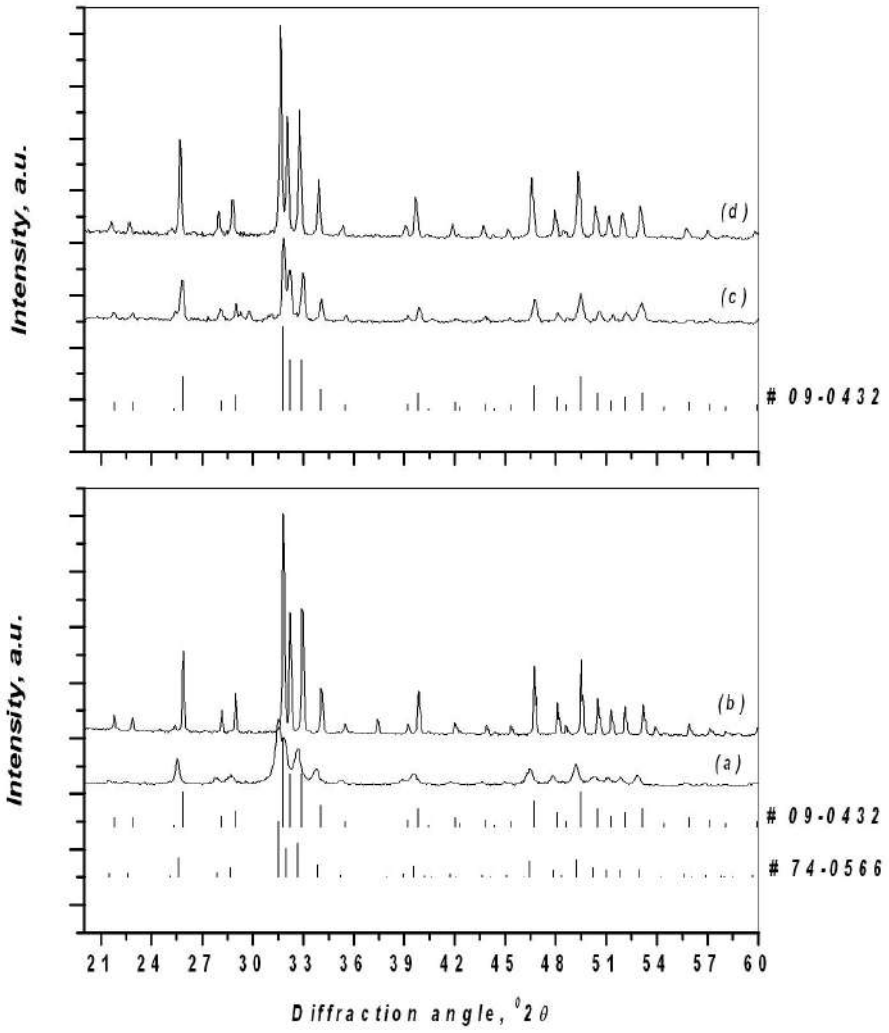

Figure 3.7: XRD patterns of HAP powders and coatings (a) as dried powder (b) sintered granule (1250◦C) (c) as sprayed coating and (d) heat treated (600◦C) coating

FTIR analysis for functional groups

FTIR of as-sprayed plasma spray coatings and coatings after heat treatment at 600◦C for HAP are given in Fig. 3.8. In addition, the spectrums of powders/granules fired at 1250◦C are also incorporated

for the purpose of comparison only. For the as-sprayed HAP coating (Fig. 3.8b), the strong peaks at 1039 and 1092 cm−1 correspond to the stretching mode of PO3− and those at 569 and 600 cm−1 relate to bending modes of PO3−. The peak at 877 cm−1 may be ascribed to a symmetric P-OH stretching vibration of HPO2− groups. There exists a weak band at 962 cm−1 attributed to absorbed OH−. The band at 3446 cm−1 might have come from lattice H2O because this band exists in the range of 3550-3200 cm−1 for hydrated H2O. Further, the additional peak at 3569 cm−1 band is assigned to the bulk

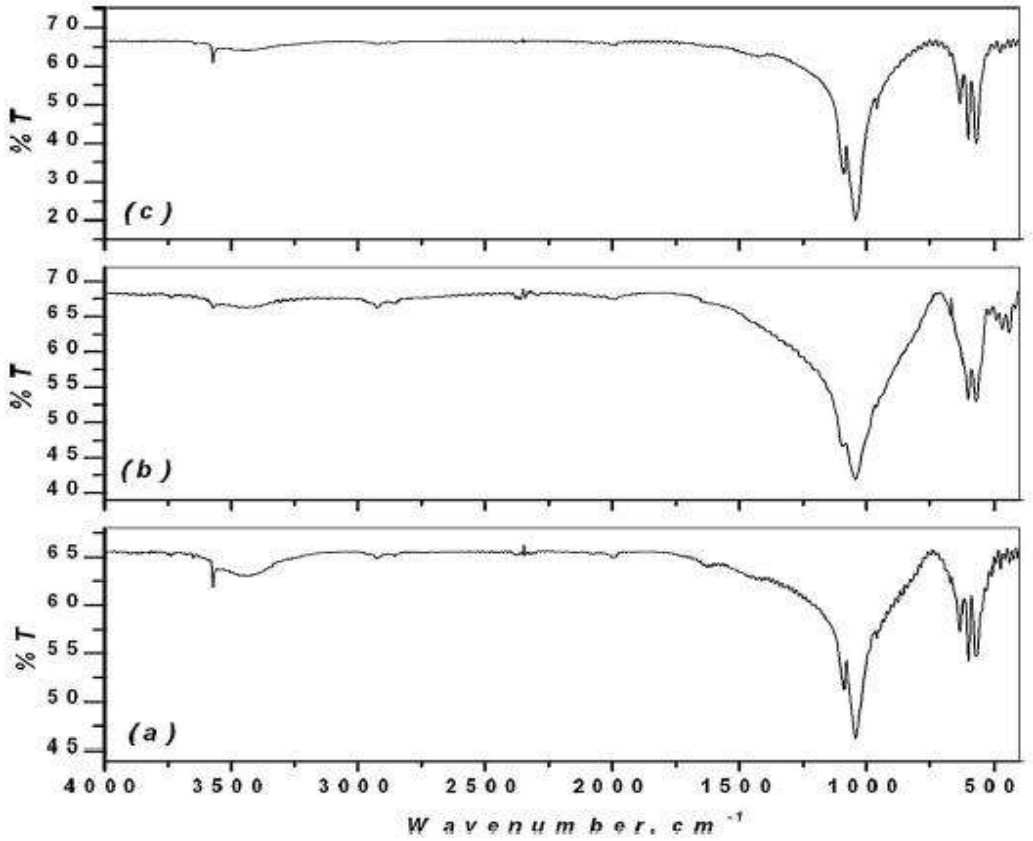

OH− ions in the fired compositions also. The FTIR spectra of HAP are consistent with those reported by Ota et al. for pure HAP powder [151]. The peak at 1092 cm−1 corresponding to PO3− band has merged giving rise to a broad band indicating the presence of other Ca-P compounds and most likely, formation of some amorphous HAP. The decrease in transmittance at 3446 cm−1 (Fig. 3.8b) for the as-sprayed coating indicates that some of the hydroxyl groups (OH−) were driven off during the high temperature process. This is probably due to dehydroxylation during spraying in which some plasma sprayed HAP might have been converted to oxyhydroxyapatite (OHAP) with the approximate formula Ca10(PO4)6(OH)2−2xOx x (= vacancy , x < 1) [27]. Heat-treatment however led to the recovery of transmittance value at 3569 cm−1.From both XRD and FTIR data, it is found that the as-prepared

powders are composed of calcium deficient hydroxyapatite, which when fired at their calcination temperature become poly-crystalline HAP, as reported earlier [217, 137].

Figure 3.8: FTIR spectrum of HAP powders and coatings (a) sintered granule (1250◦C) (b) as sprayed coating and (c) heat treated (600◦C) coating

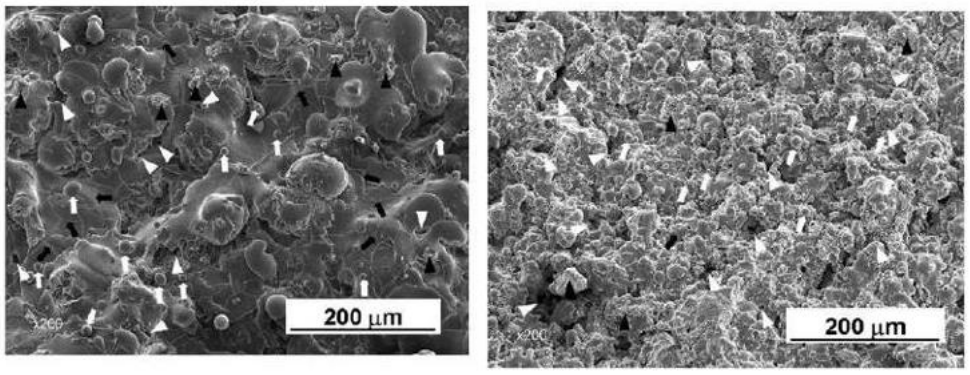

(a)

Figure 3.9: SEM photomicrograph of plasma spray coating for HAP; (a) HAP as sprayed: pores (white bold arrow heads), unmelted splats retaining a nonflattened core (white bold arrow), deformed splats (black bold arrow heads), splat cracks (black bold arrow), (b) HAP after post heat treatment: pores (white bold arrow heads), unmelted splats retaining a non-flattened core (white bold arrow), deformed splats (black bold arrow heads), splat cracks (black bold arrow)

Coating Surface Morphology from SEM

Microstructural characterizations and coating thickness measurements were carried out by scanning electron microscopy (SEM; s430i, Leo, UK). Samples were sputter coated with Au-Pd (∼ 50 − 70nm coating thickness) prior to insertion in the sample chamber of electron microscopy. Typical SEM image of heat-treated plasma sprayed HAP coating is shown in Fig. 3.9.

The microstructure of the coating is heterogeneous and highly porous. The av- erage volume percent open porosity has been determined to be ∼ 20% as measured using the Image Analyzer (Leica Q500MC, UK) applied to SEM photomicrographs. Splat size is ∼ 50 − 70µm, macropore size is ∼ 10 − 30µm and micropore size is

~ 1µm. Intra and inter-splat microcracks are observed to be distributed all over the as-sprayed coating (Fig. 3.9a) along with unmelted HAP particles. The pores could have formed because of poor bonding between adjacent splats and microcracking probably arose from shrinkage of the splat during quenching and subsequent differ- ential thermal contraction between substrate and coating. Post heat-treated plasma sprayed HAP coating microstructure, as shown in Fig. 3.9b, appears as if it is more densified than the as-sprayed coating shown in Fig. 3.9a.

The plasma flame coated HAP implants with roughness and porosities on the surface help in increasing the point contact of the implant with the surrounding hard tissues as compared to that of the uncoated implants. Furthermore, if the critical porosity level is maintained < 100µmm, then the resorption is more and so the physicochemical contact along the surrounding hard tissue structure is enhanced.

Bonding Strength

The bonding strength of the coatings was evaluated as per ASTM C633 specification using a universal testing machine (Instron 5500R, USA) [2] using the procedure reported in [36, 37, 38]. Briefly, plasma sprayed HAP coatings were put on SS316L cylindrical stubs (25.4 mm diameter and length 25.4 mm) (loading stub, L and the substrate stub, S). The coated stub (S) was joined to an uncoated stub (L) with a commercially available adhesive tape (FM 1000 adhesive film, Cytec Industries Inc., NJ, USA). The tape was made by a mixture of polyamide and epoxy resin with an appropriate curing agent. The stubs were then mounted on a snugly fitted fixture and kept in an oven for about 5h at 300◦C for curing purpose. Tensile test was carried out at a cross-head speed of 0.1 mm/min using a Universal Testing Machine (UTM Instron 5500R, USA) under ambient conditions.

The bonding strength of the coating was obtained by dividing the critical load at failure by the coated area. The measured bonding strength for HAP coating was found to be ~ 13 MPa. This is quite comparable with the reported values (~ 2 − 30 MPa) for the macro-plasma deposited coating [215, 216].

Owing to the high crystallinity, phase purity, less coating cracks, high adhesion strength and moderate-to-high amount and distribution of micropores, plasma spray coated and heat treated HAP substrates have been found to be suitable for further in vivo studies.

Bioactive glass Coating: Conventional dip coating

Due to the inherent amorphous nature of the bioactive glass, using it as a coating on any load bearing metallic implants, whether stainless steel or any titanium alloy, necessitates matching their thermal expansion coefficients in order to achieve a strong adhesion to the substrate. As a result, all characterizations in this case have been stated for coating of the titanium alloy surface itself.
In this case, the coating has been applied by conventional vitreous enamelling technique. For this, the coating material should possess a softening temperature below the α → β transition temperature (955-1010◦C) of titanium [113]. The glass composition was formulated from soda-lime-silica (Na2O.CaO.SiO2) glass system.
Boric acid is widely used in manufacture of different commercial glasses usually to reduce the thermal expansion coefficient and softening temperature of the glass. Since it has antiseptic, antifungal and antibacterial also, hence it is used widely in humans and animals. Another compound Titanium di-oxide, a bio-inert oxide always found on bare metal implants, is used to improve chemical bonding between coating and substrate. In this case, Boric acid (H3BO3) and Titanium di-oxide (TiO2) was added to the composition in such a way that the thermal expansion coefficient (α) matches that of the substrate (Ti6Al4V alloy, $\alpha = 9.5 - 10.5 \times 10{-}6/{\circ}C$ at room temperature to 400◦C).

The glass softening temperature was found to be < 750◦C from DTA results (Fig. 2.12) which helps prevent excessive oxidation of the alloy during enamelling. The linear coefficient of thermal expansion of the glass (α) was measured to be $10.93 \times 10{-}6/{\circ}C$ at room temperature to 600◦C, which is very much comparable with that of the base metal.

Thick slurry of glass powder was prepared first using fine glass powder and coat- ing of bioactive glass was applied by normal enamelling technique on mechanically roughened and cleaned Ti6Al4V substrates of flat coupons of size 20mm x20mm x2mm and round small rod of diameter 2-5 mm. However, for characterization and evaluation of bioactive glass coating, small flat coupon samples were used. Homo- geneous slurry of glass powders was applied to obtain uniform coating by spraying or dipping technique. The coated samples were thoroughly dried in an air oven at 60-80◦C overnight, which were subsequently heat treated at 820◦C for 5 min. (suitable for small coupons and rods) under reduced pressure using a dental fur- nace (VITA,VACUMET). The heat treatment schedule was established by analyzing a number of trials in the temperature range of 800-850◦C for different time

which matches well with the firing schedule of other reported work [64] in order to obtain defect free, adherent coating.

Phase analysis using XRD

Phase analysis of the coating was performed using the XRD shown in Fig. 3.10. The XRD analysis shows the glass and the resultant coating to be amorphous in nature. After heat treatment at 650◦C for 1h, some crystallites form with peaks corresponding to quartz and Na2Ca2Si3O9 crystalline phases.

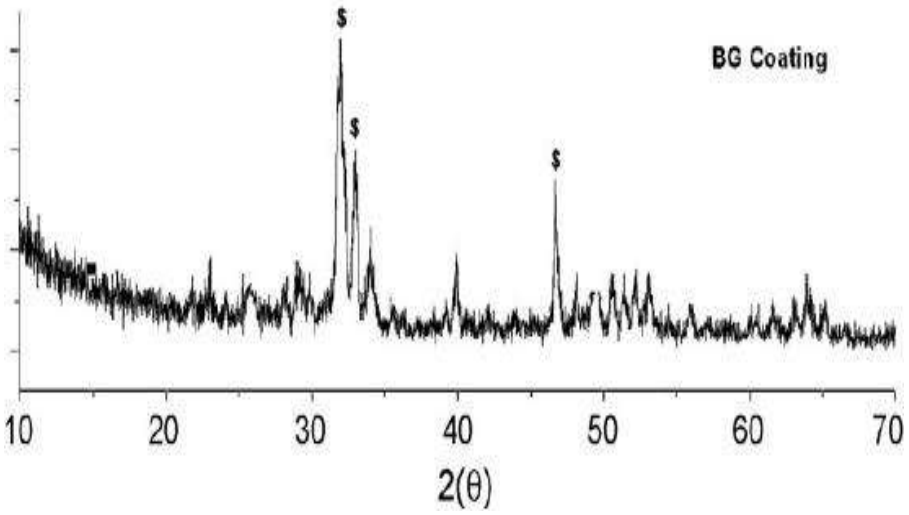

Figure 3.10: XRD pattern of bioactive glass coating

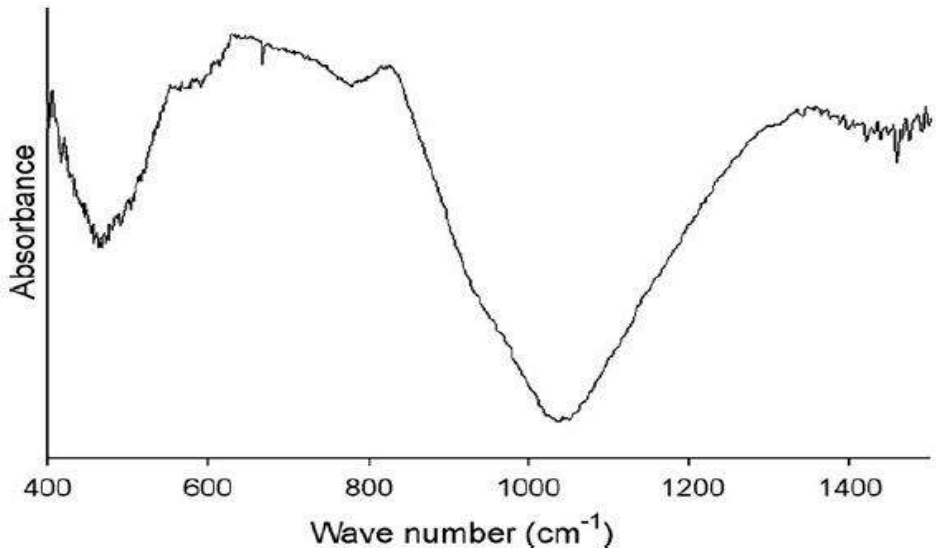

Figure 3.11: FTIR spectrum of bioactive glass coating

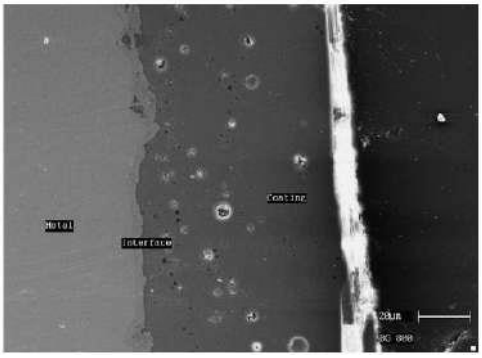

Figure 3.12: SEM micrograph of cross section of bioactive glass coating on Ti6Al4V

FTIR analysis for functional groups

In order to analyze the presence of various functional groups, FTIR spectroscopic analysis was performed for the bioactive glass coating also. The FTIR spectra (Fig. 3.11) shows two broad strong absorption bands at ~ 1050 cm−1 and 480 cm−1 which can be assigned to Si-O and P-O vibrations, respectively. B-O stretching of BO3 units may be assigned to the weak broad band at 1300-1450 cm−1 [7]. However, the existence of different groups like borate and phosphates cannot be pin pointed accurately because of superimposition of different peaks.

Coating Surface Morphology from SEM

Microstructure of the coatings were studied using a SEM (LEO 430i, UK) along with quantitative EDAX analysis using Si-Li detector to identify different area and phases in the microstructure. In vitreous enamelling technique, the thickness of the applied glassy or composite coating is easily controllable with a good degree of accuracy. Coating thickness can be controlled by controlling some of the process parameters like rheological properties of the coating material slurry which is applied on the metal and also by controlling the green coating thickness and number of applications.

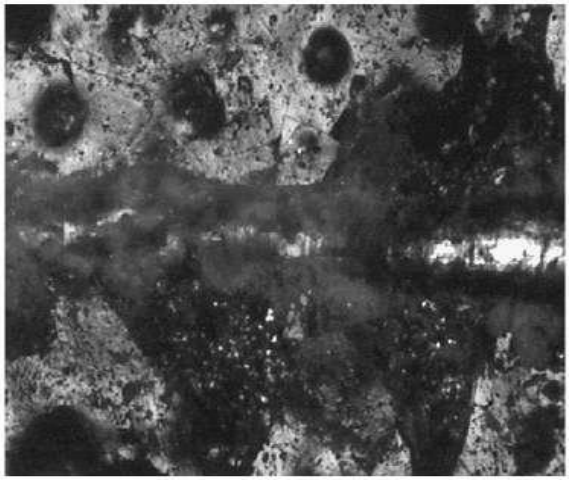

Figure 3.13: Optical micrographs of the scratches of BG coating

The coating thickness obtained on the surface of Ti6Al4V (as in case of dental implants) was ~ 80µm. The coating is almost uniform over the surface and the interface is rough and relatively thick (~ 4µm) indicating strong chemical bonding (Fig. 3.12). The small defects present in the coating metal interface are some trapped gas bubbles which normally occur in case of titanium and its alloy enamelling, as reported by other authors [113]. The thickness of the coating metal interface (~ 4µm) is indicative of the extent of inter diffusion of resulting low valent metal oxide in the molten glass matrix, which indirectly quantifies the chemical bonding as reported in the literature [42, 175].

Bonding Strength

Hardness, fracture toughness and elastic modulus of the coating were measured and found to be 6.52 GPa, 0.74 MPa√m and 72 GPa respectively.Thus, hardness and Young's Modulus values achieved are found to be superior compared to other bioactive glass coating compositions already reported by other researchers [65]. Adhesion of the coating was estimated by scratch testing of the coating using a Ducom Scratch Tester TR-01 attached with a load cell of 200 N and using a Rockwell diamond indenter. Scratch testing of the coated samples was carried out at an increasing load with loading rate 2-5 N/mm, scratch speed 0.1 mm/s and stroke length varying from 5-7 mm. Optical micrographs of

the scratches were taken using an image analyzer (Correct, Seiwa Optical, Tokyo) to observe the failure of the coating.

In case of hard and brittle bioactive glass coating on compliant metallic substrate of Ti6Al4V alloy, three different types of failure mode can operate simultaneously, Through-thickness cracking, (ii) coating detachment and (iii) chipping within the coating. From the scratch test results, it was observed that the critical load (adhesion strength) for bioactive glass coating was ~ 21 N. With increasing load, all the coating failed by chipping off from the metal substrate. The glassy coating fractured as the normal load was increased by coming out as flakes. Fig. 3.13

Discussion

In this Chapter, an acceptable, simple, affordable yet effective design of the dental implant has been proposed. The macro-design of the modified dental implant was done at the CSIR-Central Glass and Ceramic Research Institute (CSIR-CGCRI), Kolkata in the scope of the present work.

The proposed indigenous dental implant has only three essential components- the implant body, the healing screw and the abutment screw instead of the multiple components listed in literature [130] for a standard stage II implant. The combination of these three elements suffice to provide all required functionalities without causing patient discomfort or affecting the aesthetics. The healing screw is used in place ofthe first stage cover screw and/or the hygiene screw while the single abutment screw is used in place of the healing abutment and/or abutment screw. As in the case of certain popular implant designs, the implant body has 'V' shaped parabolic threads on the essentially smooth, cylindrical, tapered implant surface in order to provide more physical attachment for the implant. But, a typical feature of the proposed design is the increased angulation of 50◦, which specifically addresses the reduction in effective angulation due to coating of the implant.

In order to assess the increase in the biocompatibility of this implant, the HAP and bioactive glass coatings of suitable metallic substrates and their characterizations as reported by Dey et al. [39] and Soundrapandian [184] respectively, have been analyzed. This work was also done at the CSIR-Central Glass and Ceramic Research Institute (CSIR-CGCRI), Kolkata.

The feasibility of the use of the HAP and bioactive glass powders as coatings on the proposed dental implant was assessed using stainless steel SS316L substrates coated with HAP powder, which were further heat treated at 600◦C [39]; and Ti alloy surfaces coated with bioactive glass powder, further heat treated at 650◦C [184]. In case of HAP coatings, the use of SS316L, in place of Ti alloy, reduced the trial costs while retaining the utility of the experiments. This was not possible in case of bioactive glass since, in this case, the matching of the thermal coefficients of coating and substrate plays a major role in the adhesion of the coating to the substrate. It must be stated that all in-vivo trials, whether on uncoated or coated implants, were done using Ti alloy implants. It is further to be noted that the heat treatment temperatures were decided based on the DTA-TGA results obtained for the respective powders, as stated in Chapter 2.

The XRD of the HAP coated SS316L substrates affirm the crystallinity of the coating while the FTIR analysis indicates the presence of Ca-P compounds necessary for bioactivity. The coating surface morphology revealed from the SEM micrographs exhibit roughness and porosities in the coating of sizes less than 30μm, thus enhancing the resorption and subsequent physicochemical contact. This fact is further validated from the bonding strength value of ∼ 13 MPa.

A similar study of the bioactive glass coated Ti surface reveals the retention of the essential amorphous nature of the glass with some additional peaks corresponding to quartz and Na2Ca2Si3O9 crystalline phases. Although Si-O and P-O groups could be identified from the FTIR spectra, yet borates and phosphates, which further aid the bioactivity, could not be definitely pin pointed. The SEM micrographs, however, are observed to be uniform with a desirable rough and relatively thick interface (∼ 4μm). The hardness and elastic modulus of the coating (6.52 GPa, and 72 GPa) respectively are found to be superior compared to other bioactive glass coating compositions reported by other researchers [65].

Thus, a suitable macro-design of the dental implant has been proposed in this Chapter along with two possible bio-active coatings, the bio-ceramic HAP and the glass based bioactive glass, for this implant. The coated modified implant design can be expected to provide the required surface roughness and increase the points of contact at the implant-bone interface. Furthermore, the biocompatible material is expected to enhance the bioactivity in the surrounding tissues favourably and provide faster healing and/or stronger BIC in the long run.

IMPLANTATIONS IN RABBIT BONE TO STUDY TISSUE REGENERATION

Prior to use of the newly developed implant (detailed in Section 3.3) in humans, it is necessary to evaluate the performance of the two varieties each of the uncoated implants and the implants coated with the bioactive materials (discussed in Sections 3.4 and 3.5) in terms of their capability to enhance the tissue regeneration at the implanted sites in in-vivo applications. An evaluation of the bioactivity of the pow- ders discussed in Chapter 2 may be expected to provide key insights into the overall performance of the coated implant systems.

For this purpose, animal studies are often an essential stop prior to clinical use in humans. However, in most cases, testing in any one particular animal species cannot ensure the fulfilment of all the requirements of the ideal model. In the scope of the present work, several stages of animal studies have been done for the benefit of human beings. In all cases, animal experiments were done following the guidelines by Indian National Science Academy, 2000, after constituting an Institutional Animal Ethics Committee (IAEC) following the guidelines specified by the Committee for the Purpose of Control and Supervision of Experiments of Animals (CPCSEA).

Two sets of studies were done on rabbits, as discussed in this Chapter, to deter- mine the osseous regeneration capability in relation to the in-vivo situation. Rabbit as an animal was chosen in this first stage of the animal testing primarily because of availability. Furthermore, since rabbit meat is acceptable as a food product, so clear- ance from the ethical committee is easier to obtain for bulk testing as well as euthana- sia based analysis on rabbits. This was essential since SEM-EDAX, histopathological tests and push-out tests had to be performed to obtain some conclusive analysis of the bony tissue regeneration using the implant design modification, without or with the two proposed coatings.

The first study, detailed in Section 4.2, was primarily done with the objective of studying and characterizing the effects of the following in bony tissue regeneration: a)Ti (screw) implant macro-design vis-a-vis b)Ti (smooth) implant and also c)HAP powder (discussed in Sections 2.1 and 2.2) as a filler material. In the second study stated in Section 4.3, 4 coated implant systems, specifically HAP or bioactive glass coated, Ti (smooth) and Ti (screw) implants have been considered and their relationship with surrounding hard tissues have been observed. The results of these studies performed

on the Ti (screw) implants and the bioactive coating materials and the detailed analysis of their bioactivity have been stated in Section 4.4.

Implant Design for Rabbit Studies

For the implantation studies on rabbits, the implants were placed into the drilled hole socket of the mid-metaphyseal region of their hind legs. This particular surgical site has been chosen because of the anatomically flat surface, which makes it easier to place the implant. Since this region has a typical cross sectional diameter < 3mm, so it was not possible to use the design of the implant as discussed in Section 3.3 and shown in Figures 3.3 and 3.4. Instead, the implant design had to be modified/ simplified to accomodate the requirement for a much smaller size.

Since these are in-vivo trials, so the raw material used for the implants is Ti alloy (Ti6Al4V procured from M/s Mishra Dhatu Nigam, Hyderabad, India), as discussed at the outset in Chapter 3 from the point of view of bio-tolerance. Cylindrical shaped rods of tap drill size 2.5 mm were used to make the single stage implants with dimensions which have been reduced to a diameter of 1.5mm to 2mm and length of only 2mm, as shown in Fig. 4.1, at the CSIR-Central Glass and Ceramic Research Institute (CSIR-CGCRI), Kolkata. Two sets of implants were prepared for the various experiments: sets without any thread, henceforth denoted as Ti (smooth) implants, and sets with standard metric M3 × 0.5 V-shaped thread, henceforth denoted as Ti (screw) implants. As in the case of the proposed implant macro- design in Section 3.3, these implants are also self tapped with a taper of 2◦ in order to generate less stress at the surgical site during implant insertion. For further simplification of the implantation process, no abutment or hygiene screw were used for this study. Instead, the implant head had a slot engraved on it for the insertion of the implant using the hand-driven screw driver, as seen clearly in Fig. 4.1(a). Uncoated implants (Fig. 4.1(a)) were used for the first set of rabbit studies while coated forms of these implants, having the same basic design, (Fig. 4.1(b)) were used for the second set of rabbit studies.

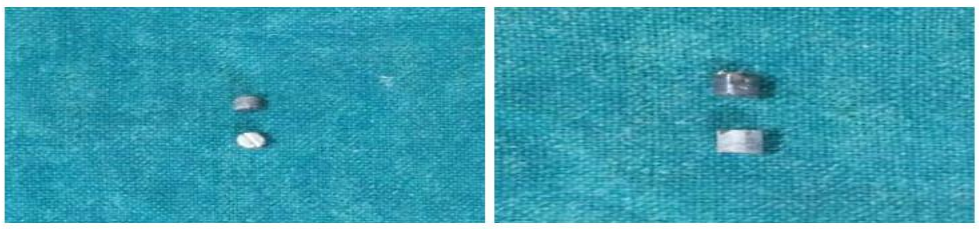

(a) (b)

Figure 4.1: Single stage rabbit implant: a)typical (uncoated) implant and b)coated implants

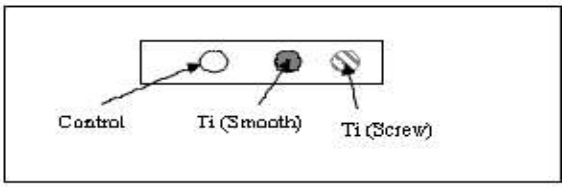

Figure 4.2: Schematic diagram showing HAP filler (control) and implants placed in rabbit leg.

Comparative studies 1: HAP filler, Ti (smooth) and Ti (screw) Implants

For the first in-vivo study, 3 numbers of male white Australian Chinchilla rabbits, each of about 7 months of age, were chosen. These have been hereafter designated as M1, M2 and M3 and all of them were in the weight range of about 1.2 kg. In this study, 2 designs of uncoated implants have been chosen for implantation purpose, namely Ti (smooth) and Ti (screw).

The basic scheme of the surgery involved making three holes in the mid-metaphyseal portion of the tibia of both hind legs of each of the rabbits M1, M2 and M3 using round burs of diameter around 2 mm. HAP powder was used as a filler material in one of these holes, while the Ti (smooth) and the Ti (screw) implants were inserted into the other two holes successfully, as shown in schematic form in Fig. 4.2. The hole filled with HAP powder has been treated as a positive control to observe the healing in the absence of any implant, but in presence of bioactive powder.

Surgical Method

The surgery was done under general anesthesia using 90% alcohol. The surgical area was further anesthetized with local anesthetic agent (2% Lignocaine with adrenaline) to achieve a bloodless field during surgical procedure. The incision was given after surgically cleaning that area by shaving off the hairs. Subsequently, the incision was given through the skin and muscle layer with surgical blade to expose the raw bone surface. Then the 3 holes were made over the bone surface for the placement of the Ti (smooth) and Ti (screw) implants and the HAP filler. Finally, the cut surfaces were sutured with Catgut(3-0).

Post-operative Evaluation

Post-operatively, the rabbits were medicated with the antibiotic Taxim (IM) and the analgesic injection Voveran (IM) for 3 consecutive days. The dosage was adjusted for the rabbit on the advice of the veterinary surgeon. One day prior to the surgery and thereafter for 7 days subsequent to the surgery, all the rabbits had to undergo routine body temperature measurements, haematological studies and also biochemical studies. Haematological studies include the measurements of haemoglobin %, TC, Neutrophil %, Lymphocyte %, Monocyte %, Eosinophil % and Basophil %, while biochemical studies were done to determine the quantity of calcium and al- kaline phosphatase present in the serum in post-operative situations. The routine body temperature of all the animals, both pre- and post-operatively, is shown graph- ically in Fig.4.3, while the haematological and biochemical study results are shown in Fig.4.4.

All the rabbits implanted with different materials showed some limping on the very first day of surgery. This resulted in inflammation in the region of surgery from the second day, which continued for another 2 days. There was evidence of pain associated with the redness of the region and swelling. With the application of proper and suitable medication, the limping as well as the inflammation decreased from the 5th day onwards. In case of M2, in addition to the limping and inflammation, there was a nasal obstruction, which could be due to some cold infection of that species. From Fig.4.4(a), it is observed that the body temperature of all the animals are in the normal range. The haematological reports, as shown in Fig.4.4 for this duration, also show that any kind of adverse responses with the Ti-alloy inserted into the system, whether immunological or allergic or acute inflammatory, is absent.

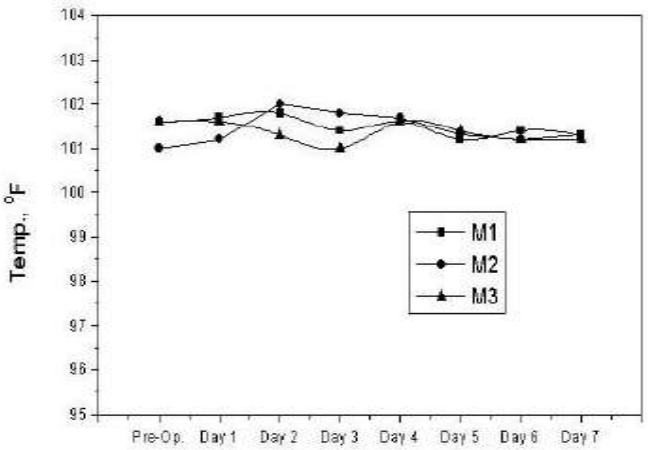

Figure 4.3: Body temperature in ◦F of M1, M2 and M3 for 1 day pre-operative and 7 days post-operative.

In all the cases, the alkaline phosphatase content of serum has increased from their respective pre-operative values, while the calcium content has gradually decreased during the observation period. The primary importance of measuring alkaline phos- phatase is to check the possibility of bone disease or liver disease. It has also been seen that the serum alkaline phosphatase enzyme level and the calcium level, as shown in Fig 4.4(d), act as blood markers to assess the bone-repairing process. After any bone injury, serum alkaline phosphatase level increases. This helps locally by depositing phosphate directly and/or it helps in the formation of collagen matrix in such a way that calcium can precipitate at that site [69]. So, evidence of elevated serum alkaline phosphatase, which is typically produced by bone-forming cells called osteoblasts, and/or the subsequent decrease of calcium in the serum can be ascribed to the rapid growth of bone.

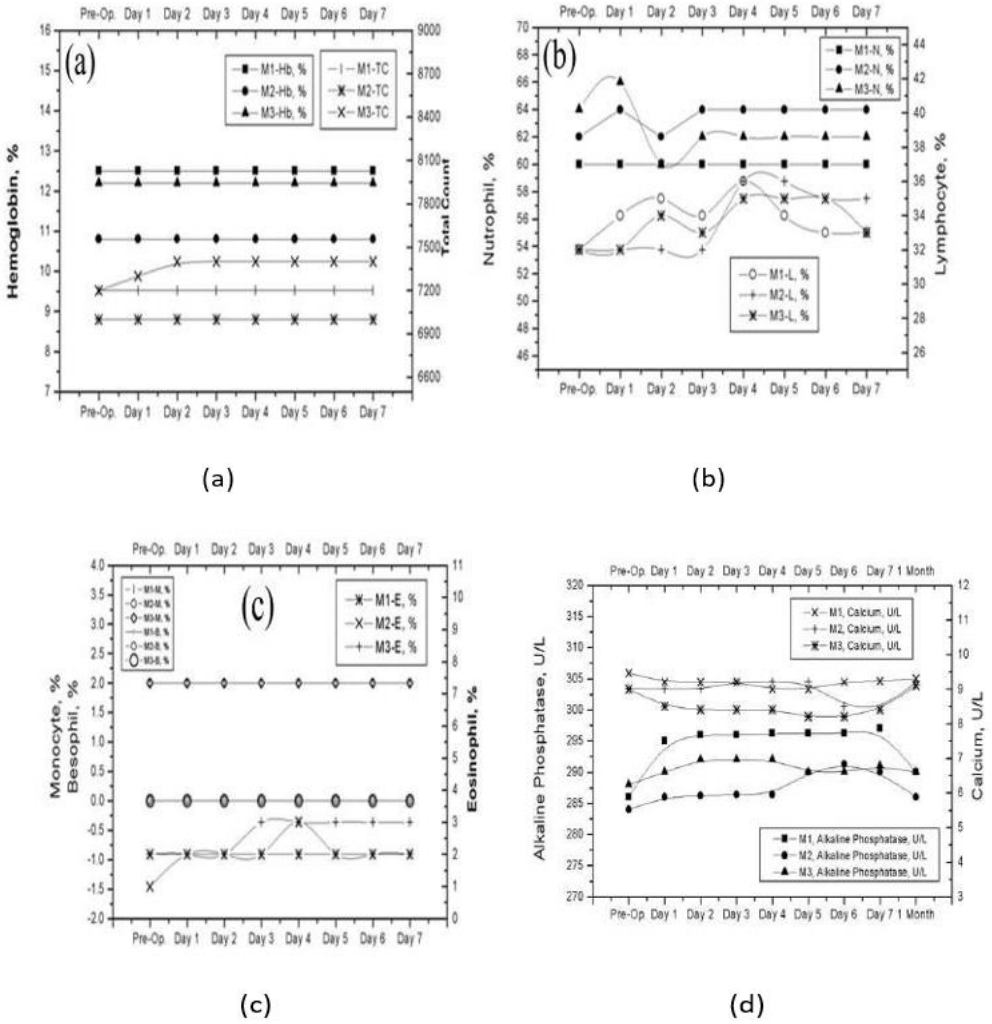

Figure 4.4: Haematological and Biochemical Report of M1, M2 and M3 for 1 day pre-operative and 7 days post-operative: (a) Haemoglobin (b) Neutrophil, Leucocyte (c) Monocyte, Basophil, Eosinophil (d) Alkaline phosphatase and calcium

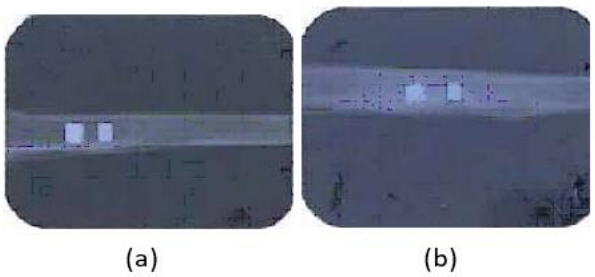

Figure 4.5: Implants in-situ in the rabbit hind leg: a)1 month b)3 months

Post-Euthanasia Evaluation

As stated at the outset, the studies were conducted for a period lasting a maximum of 3 months. The 3 rabbits used for the study, identified as M1, M2 and M3, were sacrificed after 1, 2 and 3 months respectively in order to study the various stages of the tissue regeneration at the implant-bone interfaces. Implanted regions in the right hind leg for M1 and M3 can be seen in Fig. 4.5.

Certain key studies were done after euthanasia of the rabbits in order to analyze the tissue regeneration at the implanted or powder filled regions. It is known that ion exchange between the implant and the surrounding tissue is indicative of the bone formation at the site [84]. Accordingly, SEM-EDAX studies were done in order to observe and compare the ion-exchange at the implanted region, the implant-bone interface and over the bone. Histopathological evaluation of the living tissue, which was obtained from the hind legs of the rabbits right after euthanasia, was also done in order to assess the interfacial zone. The attachment strength at the implant- bone interface is intricately linked to the surface roughness at the interface. This was measured using push out tests. The detailed procedures of these tests and the results obtained have been stated hereafter.

Figure 4.6: SEM Instrument Set up at CGCRI, Kolkata

SEM-EDAX

SEM-EDAX permit the analysis of the interfaces between biomaterials and bone tissues at the required resolution [97]. For these studies, the portion of the femur bone, where the implantation had been made, was cut from the three rabbits M1, M2 and M3. These were mounted in a resin block (10:1 of the Araldite AW 106 Standard Epoxy Resin (Huntsman, Delaware, USA) and hardener XY 95 (Vantico, Switzerland)) in such a way that each of the surface of the specimens of M1, M2 and M3 were exposed. In cases where the surface were covered with the woven bone, the surfaces were fine ground with a diamond wheel (grit size of 100 mesh). The resin-mounted specimens were then vacuum dried for sufficiently long time to ensure the dehydration of the specimens. The SEM was done in LEO 430 STEROSCAN,

U.K. instrument as shown in Fig. 4.6. Thereafter, the samples were cleaned ultra- sonically and subsequently sputter coated with carbon of coating thickness 5-20nm for observation. Qualitative EDAX were then performed as spot on the different parts of the resin block. The detector used in EDAX was the Lithium drifted Silicon detector operated at liquid nitrogen temperatures.

Fig. 4.7 shows the SEM-EDAX of the HAP filled regions for M1, M2 and M3 along with their interfaces with the surrounding tissues and the woven/matured tis- sues. Fig. 4.8 and Fig. 4.9 show the corresponding SEM-EDAX for Ti (smooth) and Ti (screw) implants respectively. The position in which the EDAX have been taken have been indicated by arrows in the SEM photomicrographs.

SEM-EDAX of HAP filled surface (positive control):

•Fig. 4.7a shows the SEM of the HAP granules in-situ over the material after 1 month under ×100 magnification. The typical sizes of these granules are in the range of 250-350 μm. The corresponding EDAX shows high peaks of Ca and P ion release from the HAP granules.

•Fig. 4.7b shows the SEM of the bone-HAP filler contact after 1 month under ×500 magnification, which is evidently very less. In few areas, gaps are also visible. As in the earlier case, in this case also, high Ca and P peaks are visible in the EDAX, though Ca release is more in this region.IOO insoluble

cytoskeleton compartment and together with p 130^{cas} is found in the sealing zone required for osteoc1astic bone resorption.(43)

• It is observed in Fig. 4.7c that after 2 months, the surrounding tissues are almost attached to the HAP material. EDAX of this contact area shows lower Ca and P peaks than in the earlier cases.

• Fig. 4.7d shows the SEM of the bone-HAP filler contact after 3 months under ×500 magnification. In this case, the Ca and P peaks observed in the EDAX are higher than those in case of the results after 2 months. This is indicative of the bioactivity of HAP in the region.

• Fig. 4.7e shows the SEM over the bone in the HAP filled region after 3 months under ×500 magnification. It is evident from the SEM that there is almost no gap in between the HAP material and the surrounding tissues. The EDAX also shows very high peaks of Ca and P in this region.

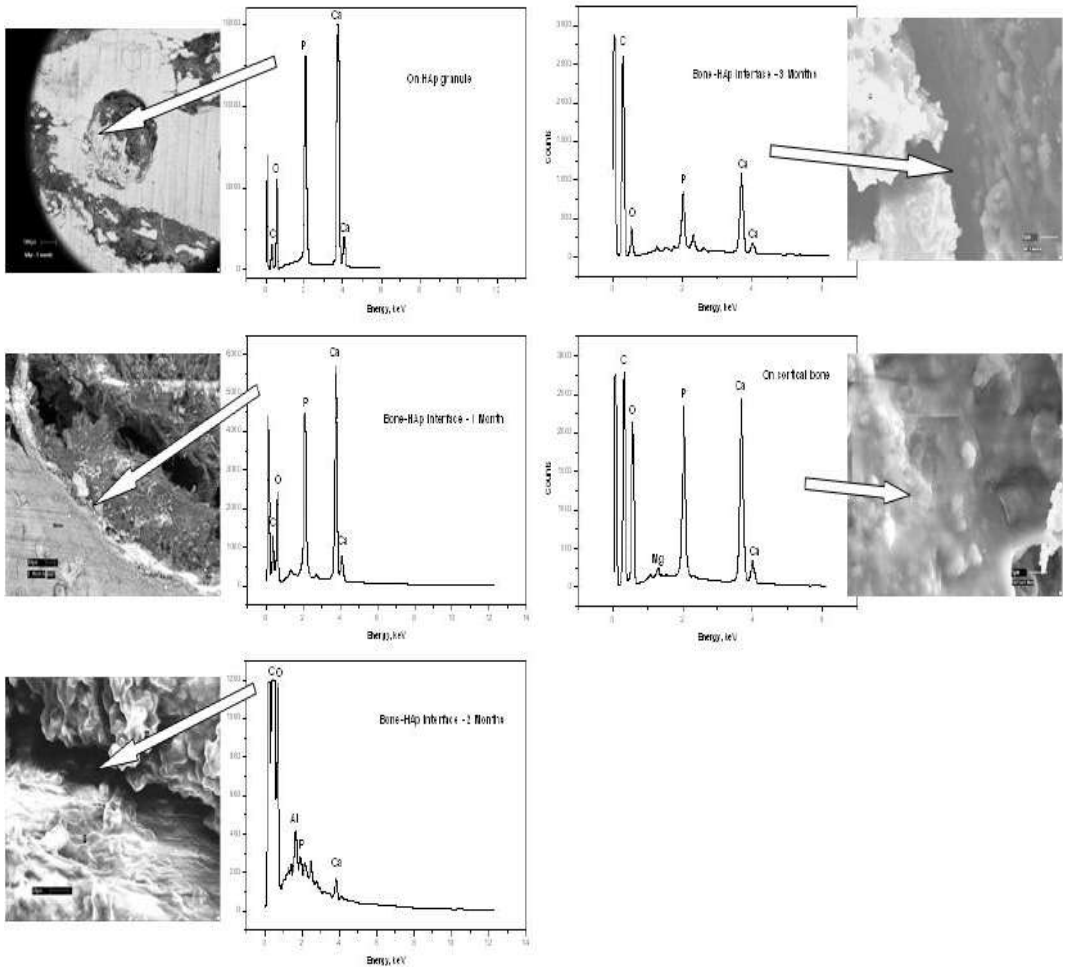

Figure 4.7: SEM and EDAX of HAP filled surface (positive control) a)HAP granules in-situ x 100 after 1 month b)HAP granules in-situ x 500 after 1 month c)HAP granules in-situ x 500 after 2 months d)HAP granules in-situ x 500 after 3 months e)HAP granules in-situ over bone surface x 500 after 3 months

Thus, it can be inferred that HAP granules in the range of 250-350 μm are highly bioactive and help in the formation of hard tissue in in-vivo conditions.

SEM-EDAX of Ti (smooth) implanted region:

• Fig. 4.8a shows the SEM of the Ti (smooth) implant in-situ over the material after 1 month under ×100 magnification. It is observed that after 1 month of insertion of the implant, it is well within the cancellous bone. The correspond- ing EDAX shows high peak of Ti.

• Fig.4.8b shows the SEM of the bone-Ti (smooth) implant interface after 1 month under ×500 magnification. The implant is observed to be in close contact with the bone. As in the earlier case, in this case also, high peak of Ti is visible in the EDAX. Peak of Ca, attributable to the bony surface, is also observed during this healing phase.

• Fig. 4.8c shows the SEM of the bone-Ti (smooth) implant interface after 2 months under ×500 magnification. It is observed that the implant is in-situ after 2 months, with lower peaks of Ti (from the implant) as well as Ca (from the bone) being visible in the EDAX.

• Fig. 4.8d shows the SEM of the bone-Ti (smooth) implant interface after 3 months under ×500 magnification. The implant-bone interface still shows a gap between the implant and the surrounding hard tissues. As in the earlier case, in this case also, low peaks of Ti (from the implant) as well as Ca (from the bone) are visible in the EDAX.

• Fig. 4.8e shows the SEM over the bone in the Ti (smooth) implanted region af- ter 3 months under ×500 magnification which clearly show the gaps in between the implant and the bone, although the implant seems to be moving towards the bony surface. Low peaks of Ti (from the implant) as well as Ca (from the bone) are visible in the EDAX in this case also.

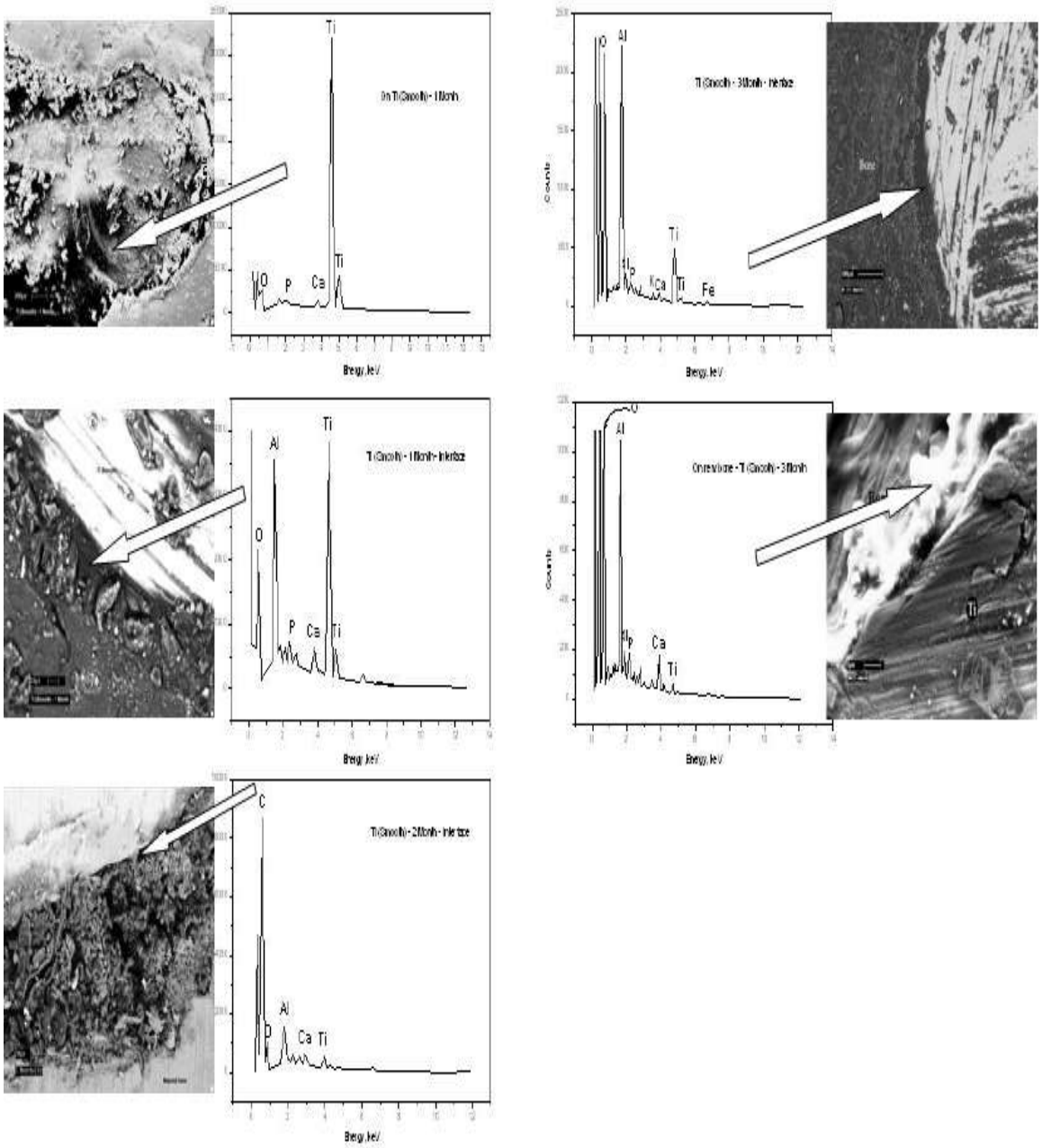

Figure 4.8: SEM and EDAX of Ti (smooth) implant in rabbit hind leg a)in-situ x 100 after 1 month b)interface x 500 after 1 month c)interface x 500 after 2 months d)interface x 500 after 3 months e)over bone surface x 500 after 3 months

The implant-bone interface in the case of implantation using the Ti (smooth) im- plant shows the existence of gaps even after 3 months of placement of implant. This may be due to the smooth structure of the implant which does not provide any en- hancement of point contact between the bone and the implant.

SEM-EDAX of Ti (screw) implanted region:

• Fig. 4.9a shows the SEM of the Ti (screw) implant in-situ over the material after 1 month under ×100 magnification. It is observed that after 1 month of insertion of the implant, there is no fracture within the bone. The correspond- ing EDAX shows high peak of Ti.

• Fig. 4.9b shows the SEM of the bone-Ti (screw) implant interface after 1 month under ×500 magnification. Collagenous tissue formation is observed in this case. The high peak of Ti is visible in the EDAX in this case also. A very low peak of Ca, attributable to the bony surface, is also observed.

• Fig. 4.9c shows the SEM of the bone-Ti (screw) implant interface after 2 months under ×500 magnification. Low peaks of Ti (from the implant) and Ca (from the bone) are visible in the EDAX.

• Fig. 4.9d shows the SEM of the bone-Ti (screw) implant interface after 3 months under ×500 magnification. The gap between the implant and the surrounding hard tissues is clearly visible in this case along with the presence of some fibrous tissue. As in the earlier case, in this case also, low peak of Ti (from the implant) is observed in the EDAX. However, the high peak of Ca ion released from the bone indicates the natural healing.

• Fig. 4.9e shows the SEM over the bone in the Ti (screw) implanted region after 3 months under ×500 magnification which shows a mechanical locking. EDAX of this region shows significantly high peaks of both Ca and P ions.

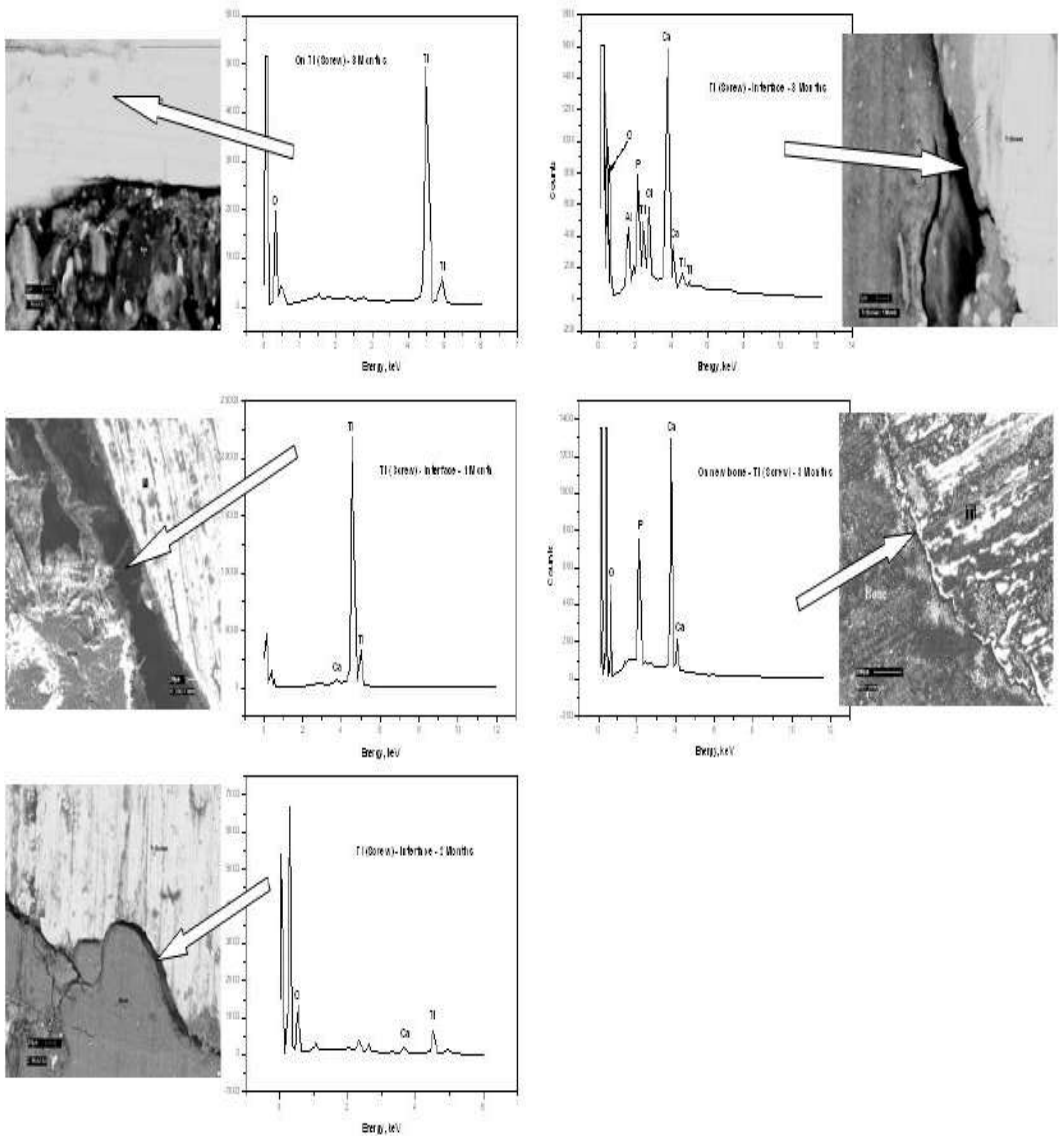

Figure 4.9: SEM and EDAX of Ti (screw) implant in rabbit hind leg a)in-situ x 100 after 1 month b)interface x 500 after 1 month c)interface x 500 after 2 months d)interface x 500 after 3 months e)over bone surface x 500 after 3 months The healing process is clearly observed in the case of implantation with the Ti (screw) implant. The process shows natural healing with the gradual release of Ca and P ions as seen through the EDAX.

Analysis of interfacial gap

A quantitative comparison of the interfacial gaps, as measured from the SEM pho- tographs, are stated in Table 4.1 for the HAP filler, the Ti (smooth) implants and the Ti (screw) implants.

Table 4.1: Interfacial gap between Ti (screw) implant/ Ti (smooth) implant/ HAP granules and the surrounding bone.

	Interfacial gap for Ti (screw), μm	Interfacial gap for Ti (smooth), μm	Interfacial gap for HAP granules, μm
1st Month	57.33-62.64	26.57-35.82	5.22-8.18
2nd Month	7.31-8.91	7.17-7.7	-
3rd Month	1.79-6.99	3.09	-

It is observed that in both the cases where Ti implants were inserted, the in- terfacial gaps between the implant and the hard tissue are significantly high after 1 month of insertion. The gap is almost double in case of the Ti (screw) implant as compared to the Ti (smooth) implant. In both cases, the gaps reduce drastically by the 2nd month and considering the amount of reduction in the gap, it may be inferred that the healing is more in case of the Ti (screw) implant during this period. Interestingly, the interfacial gaps observed after 1 month in case of the HAP filler, which is used as the positive control, are similar to the gap sizes measured for both the implants after 2 months of insertion. In case of the HAP filler, the gaps are no longer measurable beyond the period of 1 month since they were almost in contact with the surrounding hard tissue. After 3 months of insertion, the interfacial gaps in case of the Ti (screw) implants vary over a larger range with the maximum value being almost double that of the average gap in case of the Ti (smooth) implant, although the lowest gap is much lesser. This is probably dependent on the amount of trauma incurred at the particular site during implant insertion.

Overall, it may be inferred that although the Ti (screw) implant needs more torque to insert the implant, but it provides more points of contact between the surrounding bone and the implant in comparison to the Ti (smooth) implant due to its macro-geometry. This leads to an initial high value of the interfacial gap in case of the Ti (screw) implant but also leads to the maximum reduction of the same in the subsequent phase. Furthermore, it is observed that the use of the bioactive HAP filler by itself also

enhances the natural healing in the bone by lending itself to the physico-chemical attachment with the viable bone.

Histopathological Evaluation

Histopathological observations provide a qualitative evaluation of the implant-bone interfacial region and thus provide an effective diagnostic criteria for deciding the comparative effectiveness of the two types of implants used in this study. Hence, histopathological evaluation of the femur samples obtained from M3, which was sac- rificed after 3 months, have been performed in order to observe the cellular activity at the implantation sites of the Ti (smooth) and Ti (screw) implants. The typical procedure to be adopted for the histopathological evaluation is listed hereafter, fol- lowed by the evaluation of the implanted regions.

Procedure:

Step 1 Fixation of samples in 10% formalin for 24 hours. Step 2 Washing of tissue in running tap water.

Step 3 Decalcification of samples in 5% nitric acid to soften the implant-bone contact for easy removal of implant.

Step 4 Decalcification of samples containing impression of the implant, with formic acid. Solution changed over 2 consecutive nights.

Step 5 Washing of samples in running tap water.

Step 6 Dehydration of samples in ascending grade of alcohol.(50-100%) Step 7 Cleaning in two changes of xylene, 1 hour each.

Step 8 Infiltration in two changes of molten paraffin, 1 hour each. Step 9 Embedding in molten paraffin.

Step 10 Microtome sectioning at 4 μm thickness and staining with H&E stains.

Histopathological Evaluation of Ti (smooth) Implanted Region: Histopathological specimen of M3 where Ti (smooth) implant was placed is shown in Fig 4.10(a). The immunological cells are observed to be less in number in this case. The figure also shows that the amount of contact of the bone with the surface of the implant is less.

Histopathological Evaluation of Ti (smooth) Implanted Region: Histopathological specimen of M3 where Ti (screw) implant was placed is shown in Fig 4.10(b). The figure shows the lamellated bone surrounding the implant, which is seen on the right side. In this case, a low amount of bone formation is observed surrounding the implant.

These findings support the inferences from the SEM-EDAX studies in Section 4.2.4.

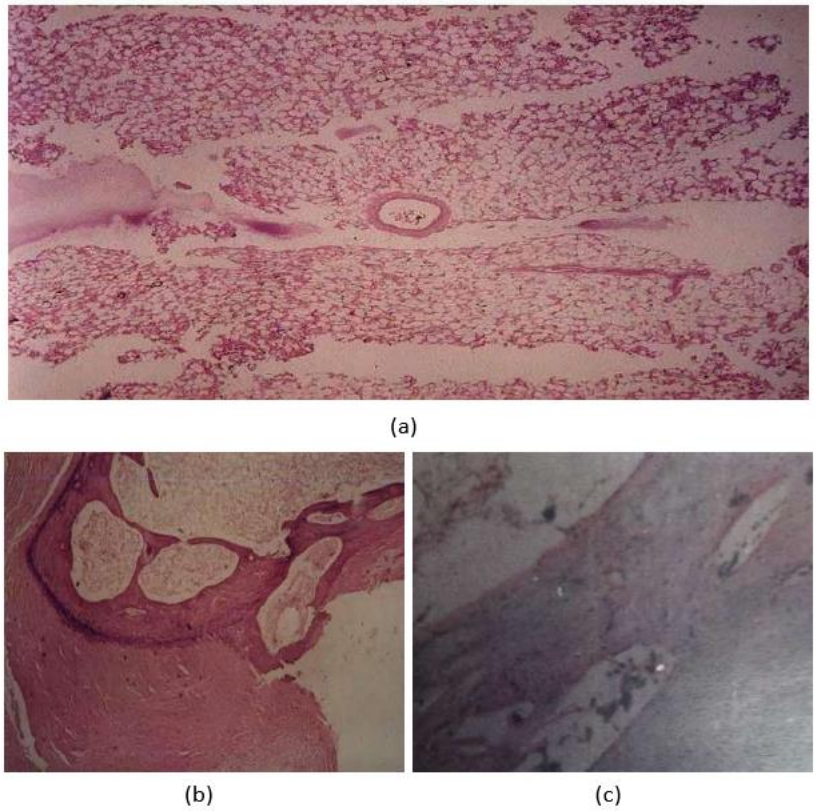

Figure 4.10: Histopathology of Rabbit Hind Leg after 3 months. (a) On removal of Ti (smooth) Implant (b) On removal of Ti (screw) Implant (c) In HAP filled region

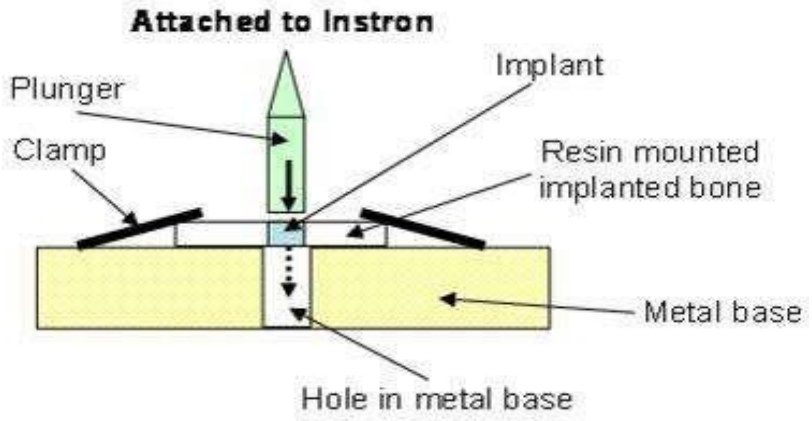

Figure 4.11: Push out Set-up (schematic view)

Push Out Tests

The strength of the interface between a biomaterial and bone is critical to the long- term performance of any load-bearing implant and this is commonly determined using push-out tests [10]. In this case, push out tests have been performed on the sacrificed rabbit bone in order to assess the interfacial shear strength developed between the respective Ti implant and the bone with time. It is obvious that the HAP filler positive control being a powder, there is no relevance of a push out test in this context.
The maximum load applied over the implant in-situ for the push out has been detected using the Instron machine. A representation of the push-out test set-up is shown in Fig. 4.11. To obtain the specimens for push-out testing, femurs were retrieved and sectioned immediately following the death of the rabbits while ensuring that the long axis of the specimen was parallel to the axis of the implant. The rabbit femur sections were then resin mounted. Such a sample was placed on the machine and then clamped to keep it in place. A specific plunger was used to apply an increasing load over the specific area in order to debond the implant. The applied load which led to complete debonding of the implant from the associated bone has been considered for calculating the push out strength in terms of the shear stress. The push-out tests were carried out with a cross-head speed of 0.5 mm/min.

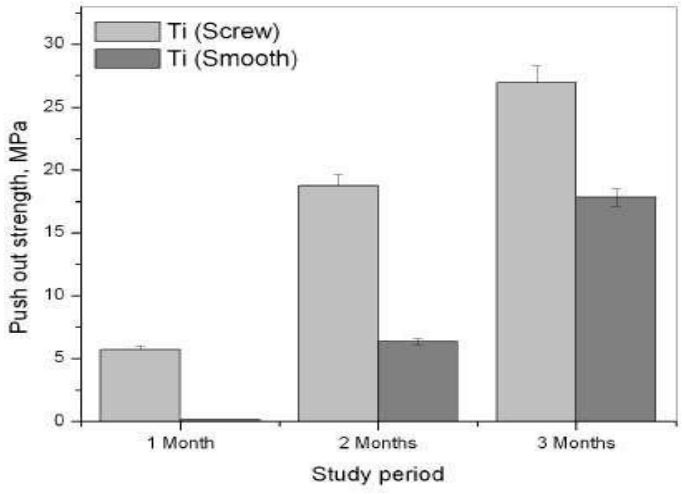

Figure 4.12: Bar diagram showing the push out strengths of Ti (screw) and Ti (smooth) implants for 1-3 months.

Implant Type	1st month	2nd month	3rd month
Ti (screw)	5.71	18.75	26.95
Ti (smooth)	0.177	6.365	17.86

Table 4.2: Average Interfacial strengths (in MPa) for Uncoated Implants

The interfacial strengths, measured in MPa, are shown in the form of a bar diagram in Fig. 4.12 and listed in Table 4.2. It is observed that the initial stability of the Ti (smooth) implant was very poor compared to that for the Ti (screw) implant. The average interfacial strengths increase significantly with time in both cases, but were consistently higher in case of Ti (screw) implants.

Interpretation of Results

It is evident from the SEM photomicrographs that the Ti (screw) and the Ti (smooth) implants as well as the HAP granules were well placed within the mid-metaphyseal portion of the tibia of the rabbit in the holes made with drill-bits of same diam- eter. In due course of time, the growth of the fibrous tissue along the marginal part of the respective implants and filler is also observed. According to Maloney et al.(1990) [119], the placement of Ti (smooth) and Ti (screw) type of implants into the mid-metaphyseal region of the rabbits causes osteolysis. In the present study also, respective EDAX pictures in the interface show that the quantity of Ca and P ions decrease from 1st to 2nd month for both types of implants, indicating the osteolysis process. However, there is a marked increase of Ca ions in the 3rd month in case of Ti (screw) implants indicating natural healing. It is further observed that the rate of woven bone to lamellated bone formation during this period is satisfactory and increases steadily in all cases, thus establishing the bioactivity of all these materials and in particular, of the Ti (screw) implants.

Supportive analysis is obtained from the study of the interfacial gaps in all these cases. It is observed that after 1 month of implant insertion, the interfacial gap is larger in case of the Ti (screw) implant than the Ti (smooth) implant. This can be ascribed to the initial predominance of bone osteolysis phenomena as a traumatic consequence of the torque applied during insertion of the Ti (screw) model. This is subsequently observed to be covered by the woven bone and the interfacial gap is found to be almost the same after 2 months for both the Ti (smooth) and the Ti (screw) implants. As the surfaces were not chemically treated, it is expected that the bone apposition in the close proximity of the implant should be the same and that is observed in these cases also.

A comparison of the interfacial gap (from SEM) and interfacial strengths (from push out tests) in these two cases show that while the interfacial strength is much more in case of the Ti (screw) implants, yet the average interfacial gaps are lesser in case of the Ti (smooth) implants. It can also be inferred from

this that the regeneration of bone along the Ti (smooth) type of implants was faster than that of the Ti (screw) type while the stability or mechanical locking provided by the threaded macro-design of the Ti (screw) is more. In case of HAP filler, the interfacial gap between the bone and HAP granule was visible only after the 1st month. Thereafter, as the bone grew, the gap was uniquely absent indicating the acceptability of the HAP powder for tissue regeneration. Histopathology in all three cases proves the bio-tolerance of the HAP filler and Ti implants.

Thus, this first study establishes that these materials are acceptable for use in biological bodies in terms of tissue regeneration. Furthermore, all the studies establish that a duration of 3 months can be treated as a substantial time period for hard tissue formation around the abutment.

Comparative studies 2:HAP and bioactive glass coated implants

It is observed in the first set of studies that both Ti (smooth) and Ti (screw) implants lead to bone formation eventually, yet Ti (screw) implants are more acceptable than Ti (smooth) implants. The next step in research is to study the effect in rabbit models of the use of two types of coatings, namely HAP and bioactive glass. The effect of these coatings were studied for both cases, on the Ti (smooth) implants as well as on the Ti (screw) implants.

For this in-vivo study, total 6 numbers of white Australian Chinchilla rabbits, both male and female, were chosen. Each of these were about 7 months of age and they all weighed about 1.2 kg. In this study, a set of 4 implants have been implanted in each rabbit. Two Ti (smooth) and two Ti (screw) implants have been taken. As shown in schematic form in Fig. 4.13, in each pair, one is coated with HAP, while the other is coated with bioactive glass (BG in figure). Thus, in this case, the basic scheme of the surgery involved making 4 holes in the mid-metaphyseal portion of the tibia of the right hind leg of each of the rabbits using round burs of diameter around 2 mm and then placing the HAP coated

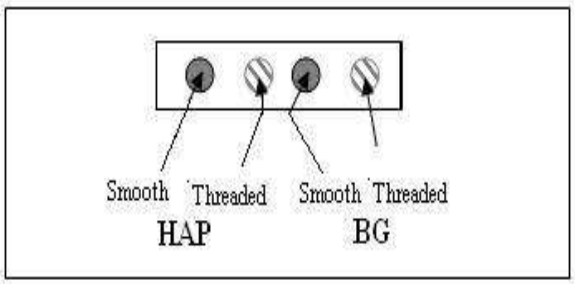

and the bioactive glass coated Ti (screw) implants as well as the HAP coated and the bioactive glass coated Ti (smooth) implants into each of the holes successfully.
Figure 4.13: Schematic diagram showing HAP and bioactive glass coated Ti (smooth) and Ti (screw) implants.

Surgical Method and Post-operative Evaluations

The surgical method followed for this study was similar to that used in the previous study stated in Section 4.2.1. In this case also, the rabbits were anaesthesized. The surgical area was shaved and sufficient incisions were made to drill 4 holes. The 4 varieties of implants mentioned above were placed and tightened with hand-driven screw driver. The area was sutured with 4-0 vicryl suture and proper dressing of the implantation sites were done.

Post-operatively, the rabbits were kept in separate cases. The rabbits were given normal diet and allowed to move during this whole period. Since the implantations were done in the hind leg, so this ambulatory status allowed the load to be borne by the bone-implant in in-situ condition. As in the previous case, clinical observations were done periodically where the body temperature, movement and appetite of the rabbits were monitored. Routine blood examinations were done in this case also to monitor the biochemical and haematological parameters. Dressings were also changed during the observations.

SEM-EDAX

The SEM-EDAX of all 4 implanted regions for each of the 6 rabbits were done. Representative SEM micrographs along with associated EDAX results for the HAP coated Ti (smooth), HAP coated Ti (screw), bioactive glass coated Ti (smooth) and bioactive glass coated Ti (screw) implants are shown in Fig.4.14, Fig.4.15, Fig.4.16 and Fig.4.17 respectively. In each case, 3 EDAX plots are shown pertaining to the implant, the implant-bone interface and the bony region, as marked by arrows to the SEM micrograph.

HAP coated Ti (smooth) implant: Fig.4.14 shows the SEM micrograph (×500 magnification) of the HAP coated Ti (smooth) implanted region. It is observed that after 3 months of insertion of the implant,

the surrounding bone has moved towards the coated implant surface. Furthermore, the resorption of the coating has taken place in certain areas and woven bone formation is observed at the 10'o'clock position. However, most of the area of the implant- bone interface is not directly in contact with the matured bone.

EDAX of metal: Large peaks of Ti and Al are observed. The peak for Al is probably due to the polishing agent used during sample preparation. EDAX on bone: High Ca and P peaks are seen as is usual for a bony structure. EDAX on interface: In the specific region under observation, peaks of Ca and P can be detected. However, since these peaks are low, strong bone-implant contact is not confirmed.

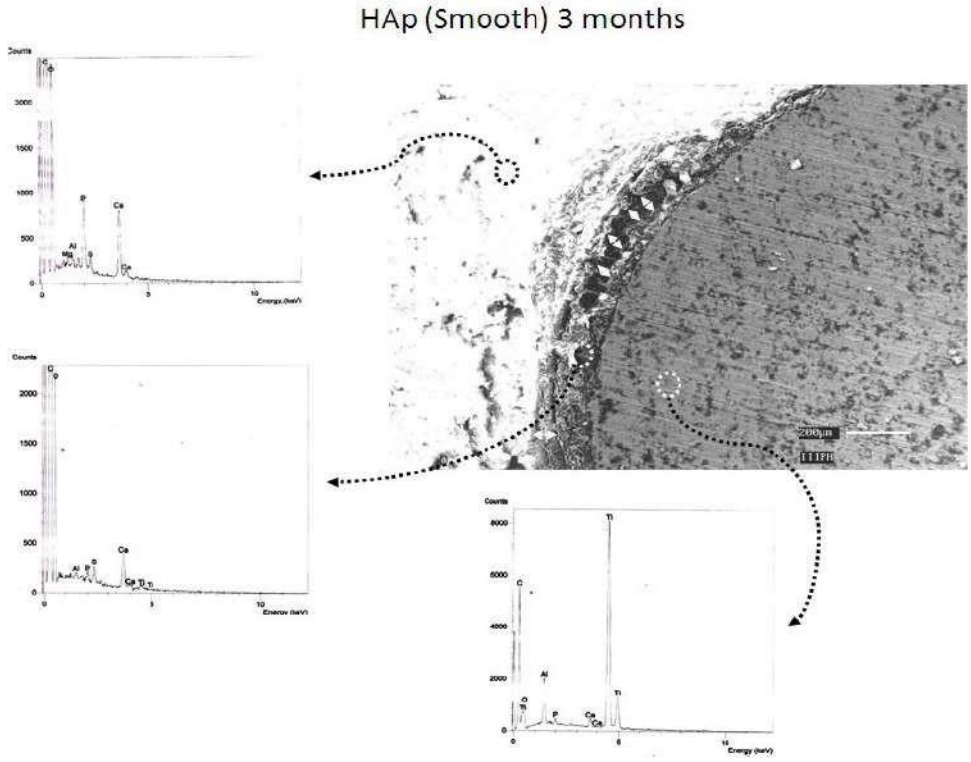

Figure 4.14: SEM showing HAP coated Ti (smooth) implant after 3 months.

HAP coated Ti (screw) implant: Fig.4.15 shows the SEM micrograph (×500 magnification) of the HAP coated Ti (screw) implant in situ, after 3 months of implantation. This SEM picture clearly shows a radio-opaque Ca and P rich interfacial zone. Well laminated bones are present around the implant. Furthermore, crystalline HAP particles are visible in the bony regions indicating resorption and formation of bone along the implant structure.

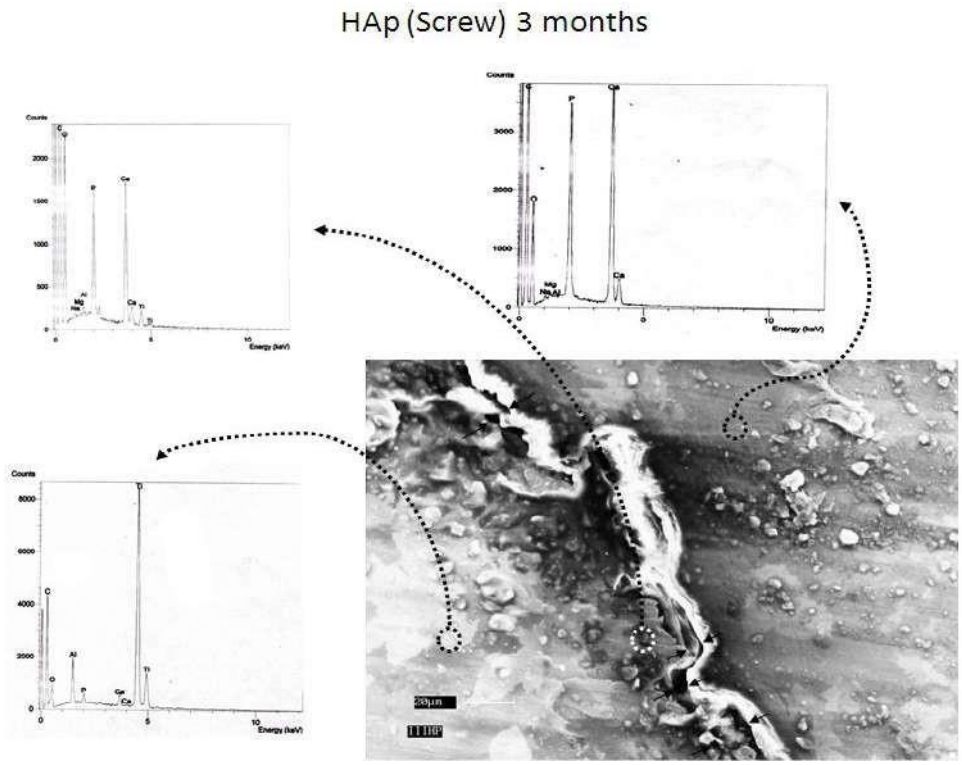

Figure 4.15: SEM showing HAP coated Ti (screw) implant after 3 months.

EDAX of Metal: Large peak of Ti is observed along with Al and Ca peaks of insignificant levels.
EDAX of Bone: Significantly high peaks of Ca and P are visible, as is expected due to the presence of crystalline HAP particles.
EDAX of Interface: High peaks of Ca and P are seen, confirming an acceptable level of bone-implant contact.

•Bioactive glass coated Ti (smooth) implant: Fig.4.16 shows the SEM micrograph (×500 magnification) of the bioactive glass coated Ti (smooth) implanted region after 3 months in rabbit hind leg. This SEM shows rapid dissolution of HAP coating from the implant surface. The dissolution can be seen from 11'o'clock to 3'o'clock position. Therefore, bone-implant contact is poor. Woven bone is seen below the upper surface.
EDAX of Metal: Ti peaks pertaining to the implant is visible. The presence of high Ca peak confirms the rapid dissolution of the HAP coating.
EDAX of Bone: The bone is immature, as indicated by significantly low peaks of Ca and P.

EDAX of Interface: Ca and P peaks are very low, as may be expected due to the dissolution of the coating.

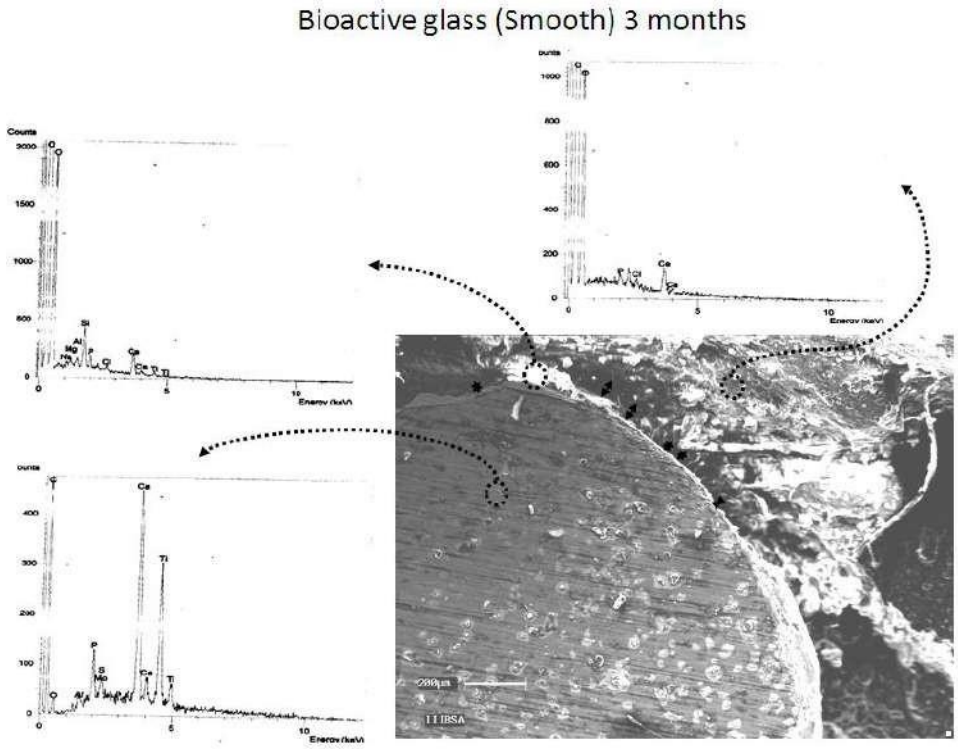

Figure 4.16: SEM showing bioactive glass coated Ti (smooth) implant after 3 months.

• Bioactive glass coated Ti (screw) implant: Fig.4.17 shows the SEM mi crograph (×500 magnification) for the bioactive glass coated Ti (screw) im- plant, after 3 months in the bony environment. As in the previous case, this picture also shows the rapid dissolution of the coating at 2'o'clock and above positions in the metallic region. In the interfacial region, larger than usual interfacial gap is observed along with woven bone formation. Bone-implant contact is also low. These observations indicate less than usual bone formation at the interface in this duration. However, bioactive glass particles are visible over the bony surface.

EDAX of Metal: Ca peaks though present, are lower than that in the previous case.
EDAX of Bone: Ca peak is observed, as is usual in a bony region.
EDAX of Interface: Ca peak is observed, indicative of coating dissolution and/or surrounding bone formation.

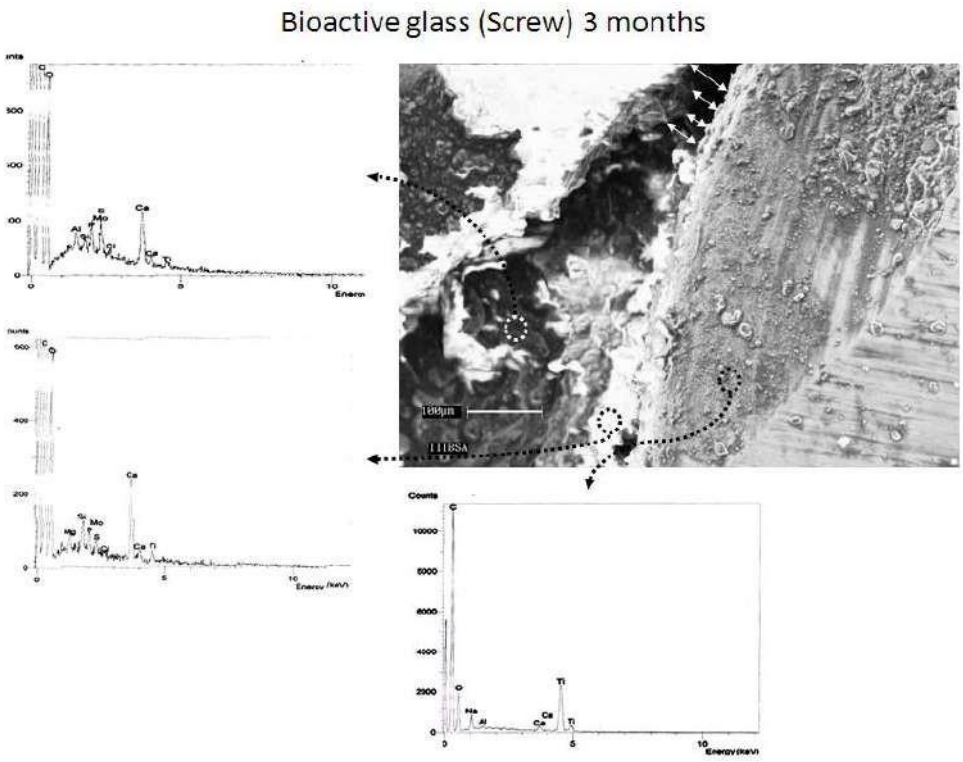

Figure 4.17: SEM showing bioactive glass coated Ti (screw) implant after 3 months.

Analysis of Interfacial Gap

In all cases, interfacial gaps are visible between the coated implants and the surrounding hard tissues. The interfacial measurements have been obtained from the SEM micrographs for all 4 varieties of implants for each of the 6 rabbits after 3 months of healing phase. These are stated in Table 4.3 and shown in Fig. 4.18.

The coated interfacial bar diagrams show that the minimum gap between sur- rounding bone and implant is observed for the HAP coated Ti (screw) implant. This is probably due to the presence of threads as well as the gradual resorption of porous HAP coating, leading to bone formation.

The macro-design of the Ti (screw) implants increase their points of contact with the surrounding bone. This is a possible reason for the bioactive glass coated Ti (screw) implant also showing less interfacial gap. As expected, both the coated Ti (smooth) implants show larger interfacial gaps, with the bioactive

glass coated Ti (smooth) implants showing the maximum distance between the implant-bone interface. This can be ascribed to the higher dissolution rate of the bioactive glass coating in comparison to the HAP coating.

Implant Type	Interfacial Gap (in μm)	
	Mean	STD
bioactive glass coated Ti (screw)	20.49	1.02
bioactive glass coated Ti (smooth)	61.08	3.66
HAP coated Ti (screw)	14.21	0.43
HAP coated Ti (smooth)	44.27	1.77

Table 4.3: Interfacial Gap in Coated Implants

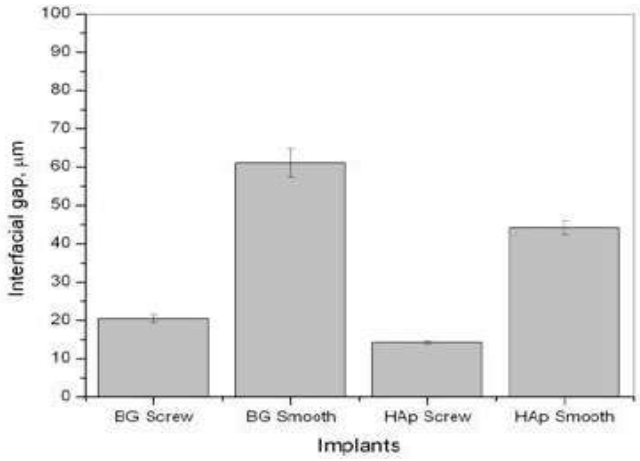

Figure 4.18: Bar chart showing interfacial gaps for bioactive glass coated Ti (screw), bioactive glass coated Ti (smooth), HAP coated Ti (screw) and HAP coated Ti (smooth) implants after 3 months.

Histopathological Evaluation

The histopathological photomicrographs shown in Fig. 4.19 for all the 4 varieties of the coated implants show the regions with the osteoblastic activities in relation to immunological or host defence mechanisms. Any injurious site is vulnerable to immunological cells creeping into the site. The histopathological tests of such sites typically show inflammatory responses which are expected to reduce with time and healing. In the present work, it has been assumed that the bone regeneration

process is almost completed in a period of 3 months and so any inflammation due to the primary injury caused by the insertion of the implant into the bone is expected to heal in that duration.

For histopathological evaluation, the implant has been removed from the respec- tive location on the hind leg after euthanasia of the rabbit. Thereafter, as in the first set of rabbit studies, slides have been prepared for the tissue surrounding the implant using haematoxylin and eosin (H&E) as the stainer in this case also. The observations for all cases are stated hereafter.

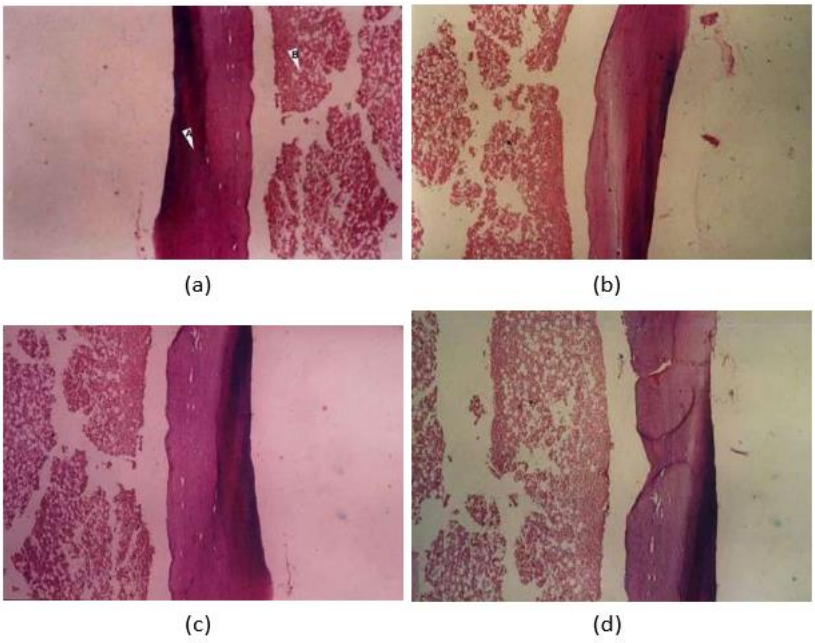

Figure 4.19: Histopathology of rabbit hind leg, after removal of: a) HAP coated Ti (smooth) implant (b) HAP coated Ti (screw) implant (c) bioactive glass coated Ti (smooth) implant (d) bioactive glass coated Ti (screw) implant

• HAP coated Ti (smooth) implant: Fig. 4.19(a) pertains to the HAP coated Ti (smooth) implant. In this case, the slide shows the immunological cells in the marrow spaces. The impression of the implant is noted over the bone and the marrow spaces. However, the region after the cortical bone, marked as A in the figure, does not show any impression of the implant. It can thus be inferred that bioactivity was present within the marrow, but primary or secondary stability was not achieved till acceptable levels, although a faint impression of implant contact is observed in a small area in the 9o'clock position of the slide.

• HAP coated Ti (screw) implant: Fig. 4.19(b) pertains to the HAP coated Ti (screw) implant. This slide shows an intact cortical bone but an impression of the thread geometry can be observed on the right side of the slide over the entire bone area. Thus, it is inferred that bone-implant contact (BIC) is more in this case as compared to the earlier case. The marrow spaces are observed to have immunological cells and the osteoblastic activity is also observed to be satisfactory, at acceptable levels.

• Bioactive glass coated Ti (smooth) implant: Fig. 4.19(c) pertains to the bioactive glass coated Ti (smooth) implant. The tissue observed in this slide shows marrow with dense cellular portion, which can possibly be ascribed to the dissolution of the bioactive glass coating surface. In this case, the cortical bone is observed to be intact and no adhering part over the bone surface is visible. Thus, the bioactive glass coated Ti (smooth) implant does not show any characteristic changes even after 3 months of insertion, as might be expected due to the roughness of the coating over the implant.

• Bioactive glass coated Ti (screw) implant: Fig. 4.19(d) pertains to the bioactive glass coated Ti (screw) implant. The marrow space shows dense cells with bioactivity and the mid-portion of the right side of the cortical bone shows a faint impression of the implant thread. However, both the bioactivity and the BIC are observed to be less than those in Fig. 4.19(b) for the HAP coated Ti (screw) implant.

Thus, in this case also, the inferences from the histopathological evaluation sup- port the observations from the SEM-EDAX studies.

Push Out Tests

As in the previous study using uncoated implants, in this case also, the histological sections of the rabbit femurs were obtained for the push out tests after sacrificing the rabbits. In this case also, it was ensured that the long axis of the specimen was parallel to the long axis of the implants. These were then used for mechanical testing to evaluate the bone-biomaterial interface using the push out tests. The mean and standard deviations of the interfacial strengths recorded using push out tests for all 4 varieties of coated implants have been listed in Table 4.4.

Implant Type	Interfacial Strengths (in MPa)	
	Mean	Std. deviation
bioactive glass coated Ti (screw)	63.29	3.1645
bioactive glass coated Ti (smooth)	38.517	1.54068
HAP coated Ti (screw)	93.02	4.651
HAP coated Ti (smooth)	40.006	1.60024

Table 4.4: Interfacial Strengths (in MPa) of Coated Implants

The results show that the HAP coated implants, both Ti (smooth) and Ti (screw), have consistently higher levels of push out strength as compared to the bioactive glass implants. It is also evident that both the varieties of coated Ti (smooth) implants exhibit low bonding strengths while the performance of the Ti (screw)

coated implants are significantly better. Among the two Ti (screw) implant varieties, the HAP coated Ti (screw) implant shows significantly higher bonding with the hard tissue. Thus, it can be inferred from the push out results also that the coated Ti (screw) implants are more acceptable than the coated Ti (smooth) implants, with the HAP coated Ti (screw) implant being the most acceptable of all 4 varieties of implants.

Interpretation of Results

SEM-EDAX as well as histopathological observations clearly show that the effective- ness of the bio-active coatings, whether HAP or bioactive glass, are more in the case of Ti (screw) implant design, as compared to the Ti (smooth) implants. This can be interpreted as follows. In case of the coated Ti (smooth) implants, the mechanical locking feature of the thread is absent and this inhibits the development of intimate contact between the implant and the bone and hence results in poor primary sta- bility. The presence of threads in the implant macro-design retain the mechanical locking feature in spite of some surface smoothening due to the coating and hence, this enhances the BIC when coatings are used on the Ti (screw) implants. The inferences from the SEM-EDAX and histopathological observations are supported quantitatively from the push out results.

The observations also establish that of the two coated Ti (screw) implant varieties, the HAP coated Ti (screw) implant is more effective than the bioactive glass coated Ti (screw) implant, specifically in terms of the increased BIC and interfacial strength. Thus, the HAP coated Ti (screw) implant is the most acceptable of all four varieties of implants. On the basis of the SEM-EDAX results for the HAP coated Ti (screw) implant, this can be ascribed to the roughness of the coating feature. Additionally, it can be inferred from the SEM-EDAX of the sacrificed rabbits with implants that another factor for the acceptability of the HAP coated Ti (screw) implant is that the formation of bone in the specific environment matches that of the implant, while the bioactive glass coatings on the Ti implants exhibited rapid dissolution unmatched by the rate of (cancellous) bone formation in the rabbit tissue.

Discussions

The aim of the two sets of in-vivo studies on Australian chinchilla rabbits discussed in this Chapter was to investigate the relationships and interactions between the bone and the Ti-alloy implant, without or with bioactive coatings. In addition to evaluating the tissue regeneration capabilities of the different implant systems, these studies were expected to provide a qualitative and quantitative evaluation of the interfacial bone response and interfacial biomechanical strength with time in the various cases. For this purpose, the first study was done using uncoated Ti (smooth) and Ti (screw) implants, along with HAP filler as a positive control; while the second study was done with HAP or bioactive glass coated, Ti (smooth) and Ti (screw) implants. In all cases, the rabbits used were sacrificed at predetermined durations and SEM-EDAX, histopathological evaluations and push out tests were performed on the hard tissues.

Post-operative evaluations in all cases established the absence of any kind of adverse responses with the Ti-alloy based implants inserted into the system, whether immunological or allergic or acute inflammatory, establishes the bio-tolerance of these implants. SEM-EDAX as well as histopathological observations clearly show that in terms of tissue regeneration capability, the uncoated Ti (screw) implant design is more effective as compared to the uncoated Ti (smooth) implants. This observation holds true for the respective coated forms of these implants also, whether HAP coated or bioactive glass coated. The analysis of the interfacial strengths of these implant varieties, as obtained from push out tests, also support this observation. It can thus be interpreted that the absence of the mechanical locking feature of the thread in case of the Ti (smooth) implants inhibits

the development of intimate contact between the implants and the bone in spite of the comparatively lesser trauma induced during implant insertion. These observations primarily establish that the proposed implant macro-design of the Ti (screw) implant will provide enhanced tissue regeneration as compared to any Ti (smooth) implant of similar dimensions.

A comparison of all the results for the uncoated and coated forms of both the Ti-alloy implants shows that the BIC as well as bone formation increases with the use of coatings on the implant surface, whether HAP or bioactive glass. This can be ascribed to the increased surface roughness of the implants due to the coatings. Overall, it is observed that the HAP coated and bioactive glass coated Ti (screw) im- plants exhibit maximum bone formation with high interfacial strengths as compared to any of the other implant varieties. It can thus be inferred from these that the presence of threads in the Ti (screw) implants retain the mechanical locking feature, in spite of some surface smoothening due to the coating, thus enhancing the BIC.

The SEM-EDAX of the bioactive glass coated Ti (screw) implants, however, show rapid dissolution of the coating associated with lesser bone formation in the rabbit tissues while the HAP coated Ti (screw) implants show more bone formation. This result, coupled with the significantly high interfacial strength of the HAP coated Ti (screw) implants, establishes that the HAP coated Ti (screw) implants are most acceptable in terms of tissue regeneration. However, in general, all uncoated and coated varieties of the Ti (screw) implants are found to be suitable in terms of bioac- tivity and interfacial strength. So, taking into account the differences in bony tissues of rabbits and humans, all further studies have been conducted using uncoated, HAP coated and bioactive glass coated Ti (screw) implants.

This study also establishes the effectiveness of the use of the indigenously devel- oped HAP powder in (Chapter 2) as a filler material, alongside its use as a coating on the proposed Ti (screw) implant. A possible interpretation for this may be that in spite of an absence of chemical bonding between the HAP coating and the gingival mucosal tissue, the time of dissolution of this particular type of bioactive material matches that of the (cancellous) bone formation around the implant in rabbits.

IMPLANTATIONS IN CANINE JAWBONE TO STUDY FUNCTIONAL RESTORATION

Subsequent to the validation of the tissue regeneration capability of the newly de- veloped implant systems as discussed in Chapter 4, it is necessary to ensure the functional restoration capability of the implants, prior to their use in humans. This can be done by studying the (in-vivo) bio-compatibility of the implants and are in- tricately linked to the proper match of the implant systems to the underlying bone structure.

Dogs are standardly classified as the companion group of animals, and so their highly tractable nature can be beneficial for conducting in-vivo studies, though macrostructurally there are obvious differences in bone loading for animals with quadrupedal gait. Their bones also have slightly higher mineral density than human bone [204] but it is found that there is most similarity in bone composition between dog and human jaw [120]. The food habits of dogs being quite different from that of humans, the functional loading characteristics of their teeth varies from that of humans. In spite of this, canine models are used in dental implant studies primarily due the availability of both cortical and trabecular bones, thus mimicking the case in humans.

Resonance frequency (RF) measurements can provide information about the in- vivo bone-implant interfacial bonding [126] and the impact of loading on the bio- compatibility of the implants. In this Chapter, Section 5.1 details the in-vivo im- plantations performed in dog jaw bones, while Section 5.2 provides details of the RF analysis (RFA) done to ascertain the bio-compatibility of the implants. The overall inferences from this study are stated in Section 5.3.

In-Vivo Study

In-vivo studies were conducted on mongrel dogs at the West Bengal Animal and Fisheries College, Kolkata under the supervision of veterinary surgeons for a total duration lasting less than 60 days. A preliminary implantation of a single uncoated threaded Ti-alloy implant was conducted on a brown mongrel dog, which was then monitored for a period of 2 weeks while being to allowed to remain in its natural habitat. In this duration, it was assured that no adverse effects took place in the dog.

Thereafter, the comparative in-vivo study involving three other mongrel dogs was undertaken to assess the functional restoration in the dog jaw.

Implant Design for Dog Jaw Bones

Since this in-vivo study was performed to observe the functional restoration in the non-human jaw bone, hence the V-shaped threaded dental implant macro-design de- veloped in Section 3.3 was used in this case also. However, two similar yet nominally different diameters of the implants were used, specifically 3.5mm and 4.0mm and two different lengths, 7mm and 9mm, were chosen for the implants. Thus in this case, 3 varieties of the Ti-alloy implants developed in Chapter 3: specifically un- coated threaded, HAP coated threaded and bioactive glass coated threaded varieties of implants, were used.

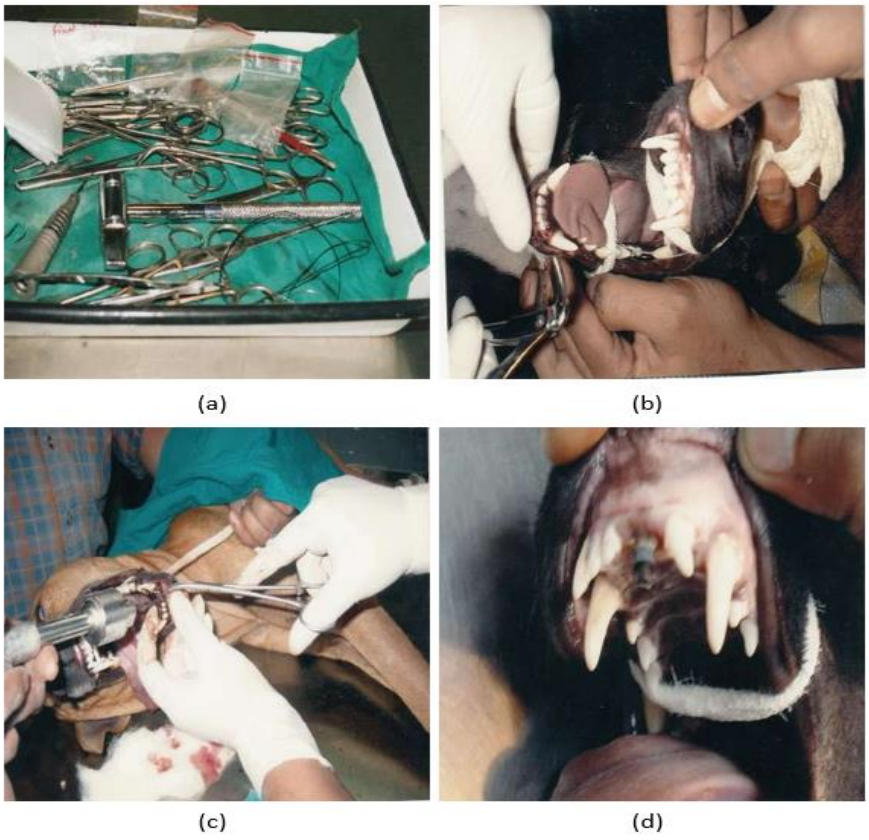

Figure 5.1: Implantation in dog jaw a) armamentarium b) tooth extraction c) drilling socket d) implant in situ

Surgical Procedure

Three number of mongrel dogs, two black (labelled as Black and Black New) and one brown, were chosen for the canine study and the surgeries was performed at West Bengal Animal and Fisheries College, Kolkata. Prior to this set of surgeries, a pre- liminary implantation was done on a brown dog, labelled as brown (old) dog, to test the feasibility of the procedure. The surgical procedures were undertaken on these dogs under the supervision of a veterinary surgeon in an operation theatre where standard surgical protocols for animal surgery were followed. The armamentarium used for the surgery is shown in Fig. 5.1(a). Each dog was given general anaesthesia during surgery. The implants were inserted after the removal of the tooth, typically located in the anterior regions of both upper and lower jaws. Anterior region were chosen because of presence of leeway space in the dog jaw bone. This is small partial edentulous area. Incisor region was also taken into account, after removal of the teeth and immediate insertion of implant with finger wrench. In each case, anterior teeth were removed with forceps as shown in Fig. 5.1(b) and thereafter, sockets were drilled using round burs in a micromotor as shown in Fig. 5.1(c), while copious water was used to clean and cool the region. Thereafter, one uncoated threaded implant, one HAP coated threaded implant and one Bio-glass coated threaded implant were placed into these sockets with a finger wrench as shown in Fig. 5.1(d). Care was taken to keep the superstructure exposed. This was done in order to avoid the re- quirement for subsequent surgery to expose the implant top for in-vivo monitoring. Thus, although the two-stage implant was used, yet in terms of the surgical proce- dure, it may be considered effectively as a single-stage one. After the procedure, the dogs were allowed to move normally within their habitat.

Clinical Observations

During surgery, it was observed that the quality of the dog jaw bones, particularly the cortical bone, was much harder than that of humans. However, primary stability achieved in each case of implantation was observed to be within normal limits, as ensured clinically. The dogs were found to be clinically normal and healthy in post- operative evaluations, both on the day of surgery and for a subsequent period of 7 days. They were found to behave normally in their natural habitat and did not reject food, which indicated that they did not have any foreign body reactions.

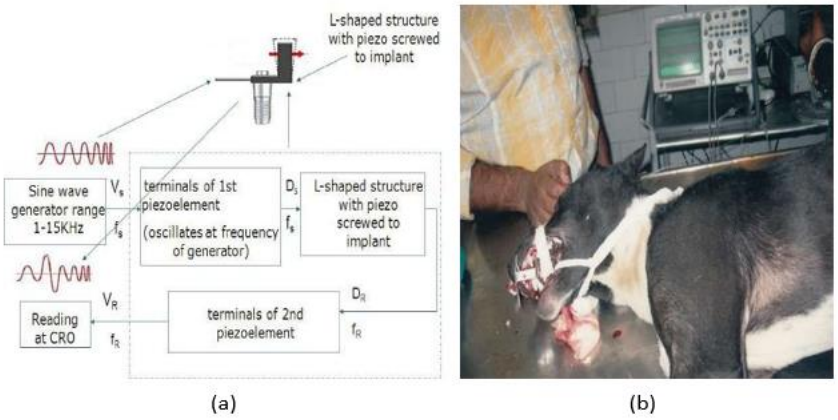

Figure 5.2: RFA measurement (a) schematic diagram (b) of implant placed in situ in dog jaw showing resonant output (top) and corresponding sinusoidal input (bottom) voltages on CRO

Resonance Frequency Analysis (RFA)

In this particular study, the resonance frequency analysis (RFA) technique was used to obtain a non-surgical, non-invasive contact based method to determine the quan- titative analysis of implant-bone interface in relation to time. The RFA was done to observe the stability of the implant with time in terms of its change of association, or integration, with the associated structure. Commercially available instruments are typically used to observe the stability of implant at primary level after insertion of the implant and also to get a measure indicative of the subsequent implant stability so that the clinician may then proceed for the immediate loading [126]. However, the use of these instruments are often prohibitively costly for most of the Indian populace.

The RFA technique based instrument adopted in this study has been developed indigenously and has been tested in several in-vitro trials [26, 168]. The schematic of the instrument is shown in Fig. 5.2 (a). The principle of operation of this instrument involves monitoring the change of the resonance frequencies of the overall system with the change of the bonding of the dental implant with the surrounding bony medium during its setting. The sensor for this particular application is based on a piezo element. As shown in the schematic, a forced vibration is transmitted to the dental implant through the piezo element. The implant-bone interface offers mechanical impedance, which is recorded by the piezo sensor as an equivalent electrical output. This resultant electrical output voltage of the piezo sensor changes with the frequency of the input signal. At particular frequencies,

resonances occur depending upon the bonding at the implant-bone-surrounding tissue interfaces. As a result, changes in the implant bonding with time cause corresponding changes in the resonance frequencies. This change in the resonance frequencies is used to monitor the changes at the implant-tissue interface during healing, when all other conditions remain the same.

In [26], the implant was inserted in frozen butter as part of an in-vitro study using the developed instrument, in order to mimic the osteolysis process. In this case, a significant drop in the RF is observed with time as the butter dissolves and finally the RF attains a steady value when no further dissolution of the butter is possible. In comparison, the changes in RF for an implant inserted in a hardening dental plaster mixture are more varied [26, 168]. This can be ascribed to the variations in the interactions of the dental plaster mixture with the implant attached to the sensor in the different trials. Yet, once the dental plaster hardens fully, the RF stabilizes to a fixed value and this phenomena can be considered indicative of the implant stability in the dental plaster. Thus, in both cases, the attainment of a fixed value of RF is indicative of the end of any systematic changes. Based on these results, the instrument was used in the present study as shown in Fig. 5.2 (b) to obtain in-vivo information regarding the hard tissue formation around the implant in case of the insertion of dental implants in mongrel dogs.

RFA Observations:

The three mongrel dogs, two black and one brown, have been labelled in the study as Black, Brown and Black (New) while the readings corresponding to the two sensors used for the study have been labelled as set1 and set 2. The frequency at which the maximum resonance is recorded during an experiment using the instrumentation system, as shown in Fig. 5.2(b) has been considered as the RF value. Typically, the RF value of the sensing system was noted each day before attaching it to the implant. This was considered as the reference RF for the day for the particular sensor, denoted as RF (open). Thereafter, multiple readings of the RF was recorded while the sensor was attached to the implant within the dog mouth. The average RF of these readings for a particular sensor was considered as the representative RF recorded from the implant using that sensor on that particular day, denoted as RF (sensor). In order to offset the variations in RF (open) recorded by the sensor on different days, all observations have been based on the change of the average RF (sensor) from the reference RF (open), which was recorded as the respective change in RF for the day, denoted as ΔRF.

The change in RF have been recorded using two sensors labelled as piezo 1 and piezo 2. The values of ΔRF recorded on each day have been stated in Tables 5.1-5.4 and plotted in Figs. 5.3-5.5. Fig. 5.3(a)-(c) and Table 5.1 depict the results for uncoated implant in the three dogs: black, brown and black new respectively, the respective results for HAP coated implant are shown in Fig. 5.4(a)-(c) and listed in Table 5.2 and those for the bioactive glass coated implant are shown in Fig. 5.5(a)-(c) and listed in Table 5.3. In these plots, day 1 refers to the first value of change in RF, which was recorded just after the insertion of the dental implant. Subsequent change in RF readings were recorded from the implants at approximately regular intervals, by putting the dogs under general anaesthesia. During this total period, the dogs were kept in their normal habitat while antibiotics and analgesics were administered to them under the supervision of the veterinary surgeon.
The observations from the RFA values for each type of implant are listed hereafter.

1. Uncoated threaded implants: The pattern of RF in Fig. 5.3(a) for the black dog showed initial stability. The implant was retained in the dog mouth for almost 3 weeks and the records are available for 19 days. But, primary stability comes down after the 6th day of insertion. Again, the osseous natural healing helps the implant to be present for BIC.

In Fig. 5.3(b) for the brown dog, the RF plot shows a lowering in case of piezo 1 till the 6th day, which is similar to that of both piezos in the black dog. However, in case of piezo 2, there is an initial rise in RF. Furthermore, in case of both piezos in this dog, a plateau like pattern is observed during the period from 6th till 13th day. Thereafter, the implant has been displaced from the specific site.
Fig. 5.3(c) for the black new dog shows the same nature of primary stability followed by osteolysis on the 6th day as in case of the black dog. The piezo 1 values exhibit clearly the improved BIC in this case which leads to implant stability by the 27th day as evident from the plot.

Overall, it is observed from Fig. 5.3 that the primary stability was achieved for all the uncoated implants put in all the 3 dogs. Following this, osteolysis is observed typically till the end of the 1st week as a drop in the ΔRF. After the osteolysis, both sets of piezo readings show that the nature of the ΔRF changes to an increasing pattern, although the pattern varies quite widely for each dog and each sensor. However, all the ΔRF values have a tendency of stabilizing with time. This stabilizing pattern is most evident in the uncoated threaded. implant used for feasibility study in the brown dog as shown

in Figure 5.6 and stated in Table 5.4. However, in all other cases, the uncoated threaded implant was typically removed by the dog within a period typically lasting about 20 days.

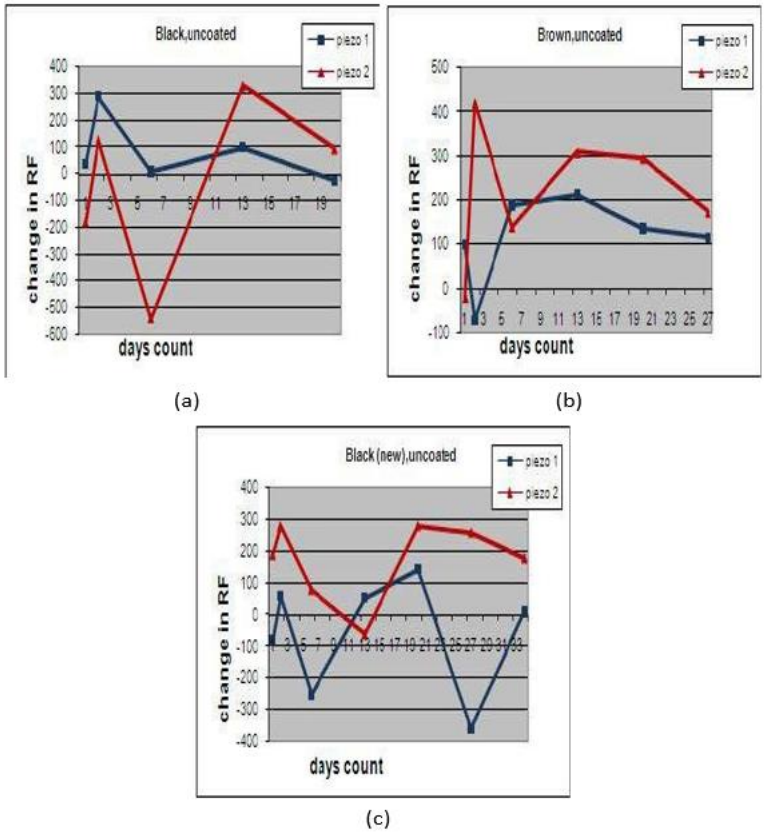

Figure 5.3: RFA change for uncoated implants in situ in dog jaw a) black dog b) brown dog c) black new dog

2. **HAP coated implants:** In Fig. 5.4(a), it is observed that both patterns of RF, for piezo 1 and 2, for the black dog showed initial stability, followed by osteolysis from the 2nd day onwards. Again, the osseous natural healing helps the implant to be present for BIC as in case of uncoated implant. However, a comparison indicates faster healing in case of the HAP coated implant. This is also clearly evident in case of the HAP coated implant in the black new dog as shown in Fig. 5.4(c).

Primary stability was attained for all the HAP coated implants in all the 3 dogs as evident from the finite RF change values on day 1. Thereafter, the osteolysis phase is observable for the similar duration of 6 days in all these cases also. This was followed by a phase of healing where the stability increases in the case of the two black dogs but the brown dog ejected the implant some time after 6 days. It is to

be noted that in all 3 dogs, the use of the HAP coating on the Ti-alloy implant leads to similar natures of ΔRF changes over time for both piezos, although the values differ.

Bioactive glass coated implants: From Figs. 5.5(a)-(c), it is observed that in this case also, the RF values fall off soon after insertion. It can thus be inferred that the onset of osteolysis is faster than that for the uncoated implant, leading to early loss of surrounding hard tissue from the sides of the implants. However, from Fig. 5.5(c) for the black new dog, it can be inferred from the positive changes that the process of regeneration of surrounding bone has begun after the 6th day onwards. However, this does not prevent the final rejection of the implants by the dogs.

In these cases also, the primary osteolysis phase is observed within the initial 6 days. Thereafter, a small phase of increasing stability was observed. However, the dogs rejected these implants also within 20 days.

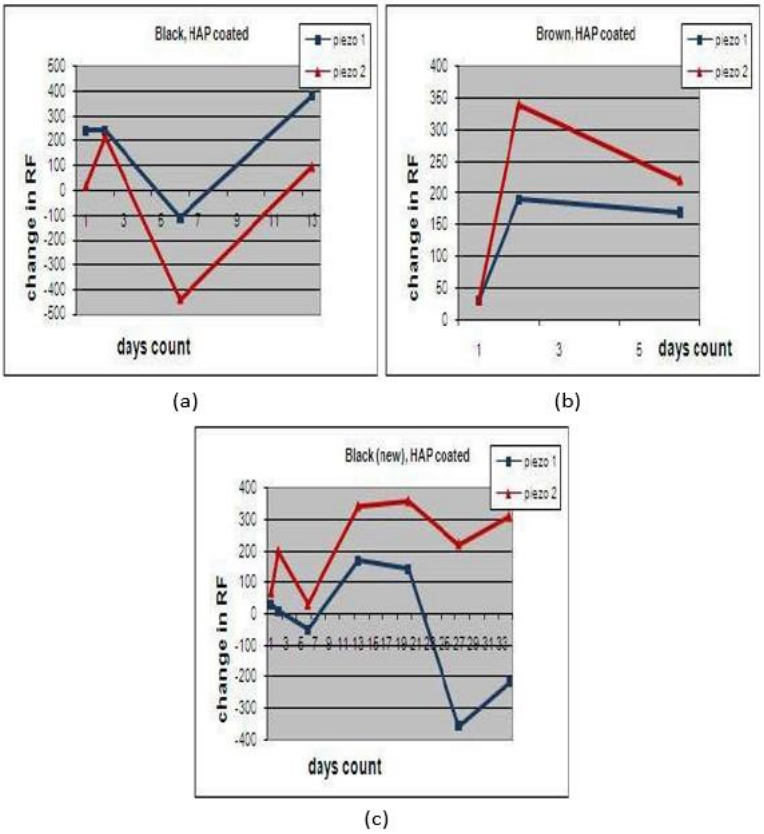

Figure 5.4: RFA change for HAP coated implants in situ in dog jaw a) black dog b) brown dog c) black new dog

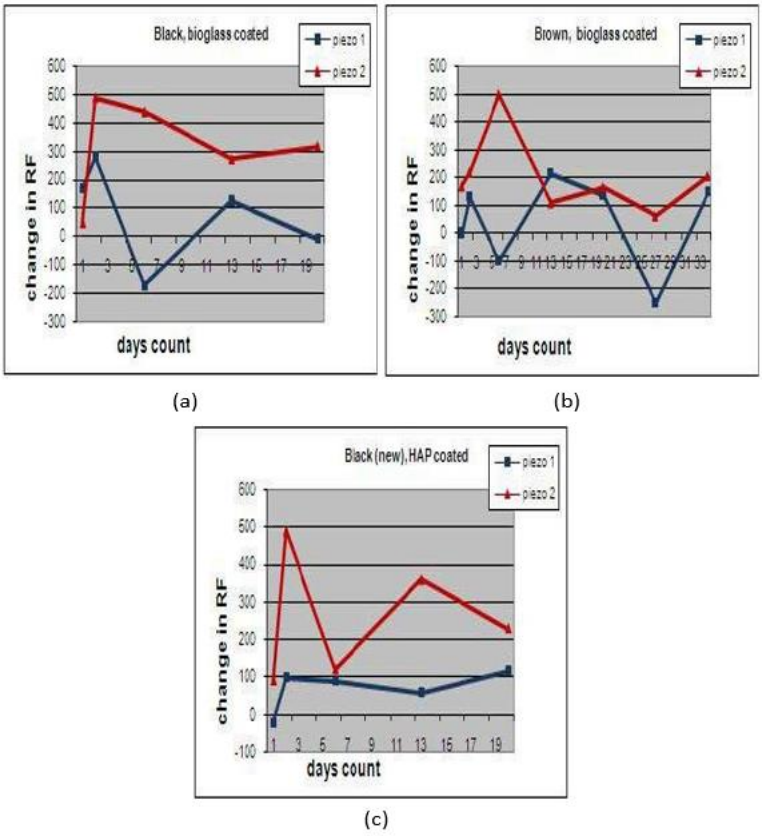

Figure 5.5: RFA change for bioactive glass coated implants in situ in dog jaw a) black dog b) brown dog c) black new dog

Interpretation of Results

From this study, it can be inferred that in case of insertion of all the 3 varieties of implants in the dog mouth, the traumatic injury caused initial osteolysis. Although subsequent functional restoration was observed in all cases, yet since the dogs were allowed to remain in their natural habitat and maintain their usual lifestyle, without any restrictions on their diets or licking habits, so the implants were mostly removed by the dogs as irritants.

In the duration that the implants were retained within the dog mouth, it is significant to note the similar natures of the subsequent functional restoration in case of the uncoated threaded and the bioactive glass coated threaded implants. Although the marrow spaces of the mongrel dogs are different from

those of humans, yet a similar response at the cellular level may be expected in humans also, specially in the D1 and D2 types of bones. The HAP coated implants seem to have triggered more irritation in the dogs, because of which these implants were ejected earlier. However, since the humans are more geared to the final benefit, it might be that their tolerance to the local irritation caused by the HAP coated implants is more. This is an aspect to be investigated in detail during the human experimentations.

Furthermore, in all cases, the implants have shown definite osteolytic changes followed in some cases by a short phase of secondary healing. The RF patterns indicate the retention has been better, in terms of the number of days, in case of uncoated implants. This may be due to better binding of the uncoated thread with the surrounding bone as validated from the successful retention of an uncoated implant in a brown dog for 49 days as seen in Fig. 5.6. It is also evident that both types of coated implants lead to faster natural healing than the uncoated implant with the process being slower in case of the HAP coated implant. Overall, it may be inferred that positive bone-formation is to be expected at the bone-implant contact in case of any in-vivo implantation using the present design of implants, both uncoated as well as coated.

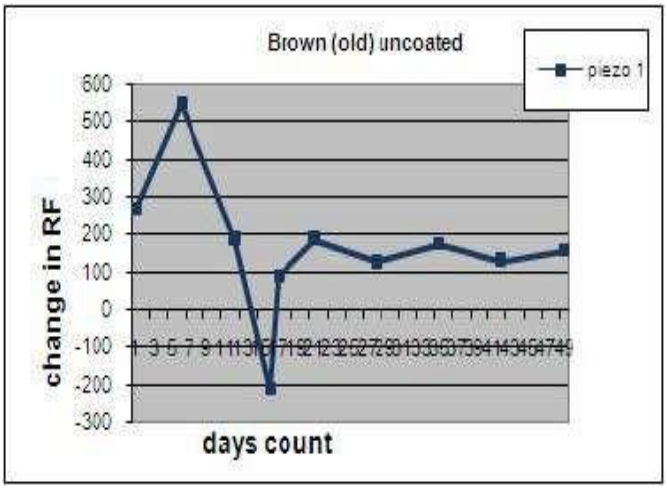

Figure 5.6: RFA change for uncoated implant in situ in brown (old) dog jaw

Discussions

The objective of the implantation study in the canine model, discussed in this Chap- ter, is to evaluate the functional restoration of the implant system in the mandible. For this, the uncoated, HAP coated and bioactive glass coated Ti-alloy threaded implants are placed in in-vivo situation of dog jaw bones and changes of resonance frequency (RF) have been measured.

The loading of the RF sensors by the implant placed within the bone changes the unloaded resonance frequencies of the sensors, which is denoted as ΔRF. The functional restoration of implants are expected to cause changes in these ΔRF values over time. The positive and/or positively changing nature of ΔRF in the first two days of implantation indicate primary acceptability of the uncoated, HAP coated as well as bioactive glass coated threaded implants. The bone osteolysis, which forms an integral part of the implantation process [119], prior to functional restoration and tissue regeneration, is also indicated in each case by a subsequent fall in ΔRF.

The functional and para-functional loading of the bone in the implanted region also affect the ΔRF values. The dominance of these effects on the ΔRF values is most consistently observed in the HAP coated implants with both sensors showing similar natures of changes in ΔRF with time. This can be ascribed to a good match between the HAP coated implant macro-design and the quality of jaw bone. On the other hand, the changes in ΔRF measured for uncoated and bioactive glass coated implants using the 2 piezo sensors are not always consistent. This may be due to the fact that the absence of any bioactive coating or a mismatch of the bioactive glass coating dissolution rate with the bone formation rate in the particular implanted re- gion in the canine model fails to dominate the RF response of the sensor(s). However, this inconsistency is not necessarily a contra-indication of the functional restorative ability of the particular implant as is evident from the results for a single case per- taining to the use of an uncoated threaded implant. The RFA results for this case provides a classical example of functional restoration followed by successful tissue regeneration, with the implant being retained in the dog jaw bone for more than 49 days.

It is evident from all these observations that the proposed implant macro-design, without or with the proposed HAP or bioactive glass coatings, ensures (in-vivo) bio- compatibility and provides functional restoration of the implant in the mammalian jaw. It is also noted that in case of the canine model, the HAP coated threaded implant macro-design provides the most consistent results in terms of functional restoration.

Day	RF (open) in kHz	RF (sensor) in kHz	ΔRF in Hz	RF (open) in kHz	RF (sensor) in kHz	ΔRF in Hz
	Black dog, Piezo 1			Black dog, Piezo 2		
1	8.500	8.460	40	6.620	6.800	-180
2	8.500	8.210	290	6.440	6.310	130
6	7.500	7.490	10	6.190	6.730	-540
13	7.435	7.335	100	6.400	6.070	330
20	7.392	7.416	-24	6.430	6.336	94
	Brown dog, Piezo 1			Brown dog, Piezo 2		
1	6.620	6.520	100	6.450	6.470	-20
2	6.440	6.510	-70	6.720	6.300	420
6	6.190	6.000	190	6.660	6.520	140
13	6.400	6.186	214	6.330	6.022	308
20	6.430	6.293	137	6.390	6.095	295
27	6.405	6.288	117	6.320	6.146	174
	Black (new) dog, Piezo 1			Black (new) dog, Piezo 2		
1	8.500	8.580	-80	6.450	6.260	190
2	8.500	8.440	60	6.650	6.370	280
6	7.500	7.750	-250	6.660	6.580	80
13	7.435	7.380	55	6.330	6.392	-62
20	7.392	7.248	144	6.390	6.108	282
27	7.430	7.786	-356	6.320	6.060	260
34	7.580	7.570	10	6.220	6.040	180

Table 5.1: RFA change for Uncoated Implants in situ in dog jaws

Day	RF (open) in kHz	RF (sensor) in kHz	ΔRF in Hz	RF (open) in kHz	RF (sensor) in kHz	ΔRF in Hz
	Black dog, Piezo 1			Black dog, Piezo 2		
1	8.500	8.260	240	6.620	6.600	20
2	8.500	8.260	240	6.440	6.220	220
6	7.500	7.610	-110	6.190	6.630	-440
13	7.435	7.056	379	6.400	6.303	97
	Brown dog, Piezo 1			Brown dog, Piezo 2		
1	6.620	6.590	30	6.450	6.420	30
2	6.440	6.250	190	6.720	6.380	340
6	6.190	6.020	170	6.660	6.440	220
	Black (new) dog, Piezo 1			Black (new) dog, Piezo 2		
1	8.500	8.470	30	6.450	6.380	70
2	8.500	8.490	10	6.650	6.450	200
6	7.500	7.550	-50	6.660	6.630	30
13	7.435	7.265	170	6.330	5.986	344
20	7.392	7.248	144	6.390	6.030	360
27	7.430	7.788	-358	6.405	6.183	220
34	7.580	7.800	-220	6.220	5.910	310

Table 5.2: RFA change for HAP coated Implants in situ in dog jaws

Day	RF (open) in kHz	RF (sensor) in kHz	ΔRF in Hz	RF (open) in kHz	RF (sensor) in kHz	ΔRF in Hz
	Black dog, Piezo 1			Black dog, Piezo 2		
1	8.500	8.330	170	6.450	6.400	50
2	8.500	8.220	280	6.720	6.230	490
6	7.500	7.670	-170	6.660	6.220	440
13	7.435	7.310	125	6.330	6.056	274
20	7.392	7.400	-8	6.390	6.070	320
	Brown dog, Piezo 1			Brown dog, Piezo 2		
1	8.500	8.500	0	6.620	6.450	170
2	8.500	8.370	130	6.440	6.220	220
6	7.500	7.600	-100	6.190	5.690	500
13	7.435	7.220	215	6.400	6.290	110
20	7.392	7.255	137	6.430	6.263	167
27	7.430	7.680	-250	6.405	6.343	62
34	7.580	7.430	150	6.360	6.153	207
	Black (new) dog, Piezo 1			Black (new) dog, Piezo 2		
1	8.500	8.520	-20	6.450	6.360	90
2	8.500	8.400	100	6.650	6.160	490
6	7.500	7.410	90	6.660	6.540	120
13	7.435	7.376	59	6.330	5.970	360
20	7.392	7.275	117	6.390	6.160	230

Table 5.3: RFA change for Bioactive glass coated Implants in situ in dog jaws

Day	RF (open) in kHz	RF (sensor) in kHz	ΔRF in Hz
	Brown dog, Piezo 1		
1	7.040	6.770	270
6	6.850	6.300	550
12	6.630	6.440	190
16	6.620	6.830	-210
17	6.440	6.350	90
21	6.190	6.000	190
28	6.400	6.273	127
35	6.430	6.256	174
42	6.405	6.273	132
49	6.360	6.200	160

Table 5.4: RFA change for Uncoated Implant in situ in brown (old) dog jaw

HUMAN CLINICAL TRIALS

As detailed in Chapter 5, in-vivo studies in dog jaw bones have been performed us- ing both uncoated and coated variants of the proposed dental implant system. The studies established the functional restorative ability of all 3 varieties of these dental implants, when used in the mammalian jaw. In this case, the HAP coated implant system appeared to exhibit the most consistent results although in one case, the uncoated implant system showed functional stability and subsequent tissue regener- ation.

Specific in-vivo studies were performed in rabbits using uncoated and coated vari- ants of smooth and threaded implants, as detailed in Chapter 4, to study the tissue regeneration aspect of the different varieties of the proposed dental implant. These studies establish the merits of using a threaded implant system in tissue regener- ation, as opposed to smooth implants. It has been further established that both the HAP coated and the bioactive glass coated implant systems perform better in this aspect as compared to the uncoated threaded implant, with the HAP coated threaded implants exhibiting maximum and stable tissue regeneration.

Based on the success achieved in these animal studies, the HAP and bioactive glass coated dental implants, proposed in Chapter 3, were selected for human trials, as discussed in this Chapter. As in case of the animal studies, necessary clearances from the Ethical Committee have been obtained in these cases also. Section 6.1 provides a comprehensive listing of the inclusion and exclusion criteria for the se- lection of human subjects suitable for dental implantations. Thereafter, a review of the implantation site selection has been provided in Section 6.2. This has been been followed in Section 6.3 with a detailing of the radiographic techniques used in the present study for the evaluation of the surgical region. In cases where the quantity of bone had to be increased prior to implantation, the effect of use of HAP powder for tissue augmentation has also been studied. A case study illustrating the procedure and the results of multi-patient trials have been presented in Section 6.4. Section

6.5 contains details of various aspects of dental implantations, as performed in the scope of the present study, along with a case study. Comparative evaluations of the various studies done on human subjects using standard techniques have been stated in Section 6.6 while a subjective evaluation to ascertain the patient satisfaction, fol- lowing and further extending the ICMR guidelines available online, has been detailed in Section 6.7. Discussions are stated in Section 6.8.

Human Subject Selection

The recent epidemiological survey report [158] shows that more than 87.6% of the Indian population in the age group of 35 to 44 years are suffering from gum diseases that lead to the loss of tooth, irrespective of the socio-economic status. The loss of tooth may be due to common dental problems like poor oral health maintenance. The carious or grossly mutilated tooth also becomes an important factor for oral re- habilitation through dental implant procedure. Accidental injury may cause avulsion or fracture of tooth or teeth, while other causes may be facial or dental congenital deformities and morbid diseases like carcinoma etc.

In the present study, suitable patients for dental implantation have been screened based on certain inclusion and exclusion criteria. Since dental implantation is a sensitive procedure, so it is important to take into account the age and socio-economic condition of the patient and also judge the biological aspects or even the implant design which can be used. These have led to the formulation of comprehensive lists of certain inclusion and exclusion criteria in the present study, as stated in Table 6.1. It must be stated here that some of these criteria are available in standard literature also [129].

Inclusion Criteria	
Periodontal cause leading to bone defect, following which loss of tooth or teeth.	
Hopeless prognosis of tooth or teeth.	
Exfoliated or extraction of teeth.	
Partial edentualism due to anodontia.	
Regeneration of jaw bone due to congenital defect.	
Exclusion criteria	
General	Defects
Children below tooth eruption age.	Periodontal bone defects
Presence of infection.	Mobile teeth
Malignant diseases (high mortality risk).	Exfoliated/Extracted tooth
Patients with negative bone factor due to systemic diseases.	Edentulous mouth with different bone quality
Patients with psychosomatic diseases.	Regeneration in congenital defects

Table 6.1: Inclusion and Exclusion Criteria for Dental Implantation

Implantation Site Selection

The proper selection of the implantation site is an important criteria in any human implantation. The site selection depends on few biological factors as well as the demand of the patient. The criteria for

which the natural tooth has been lost has to be factored into the choice since this gives an idea of the systemic conditions and/or the oral health maintenance habits of the patient [129].

As discussed in Section 3.1, the bone quality and bone type are important bio- logical factors to be considered because the type of implant, the surgical procedure to be used as well as the healing phase depend on these. Another important factor which needs to be observed prior to dental implantation is

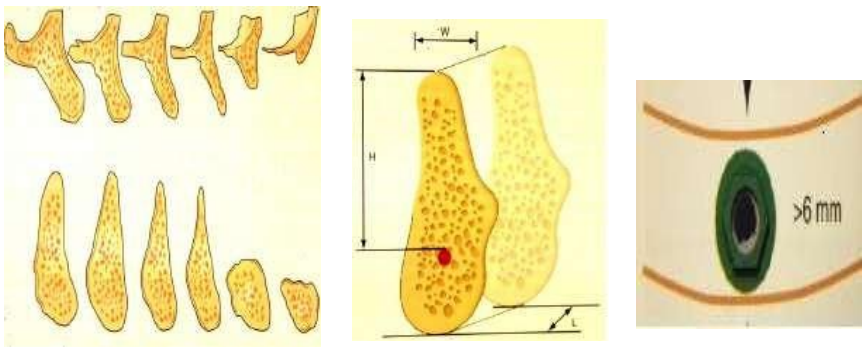

the bone volume, since it also decides the macro-geometry of the implant to be used. Various researchers have provided various classifications for the bone type and quality as stated in the review article by Nayar et al. [142], from which some relevant details are stated hereafter.

(a) (b) (c)

Figure 6.1: a) Sections of Mandible and Maxilla bone, b) Width, height and length in available bone, c) Width of available bone. [131]

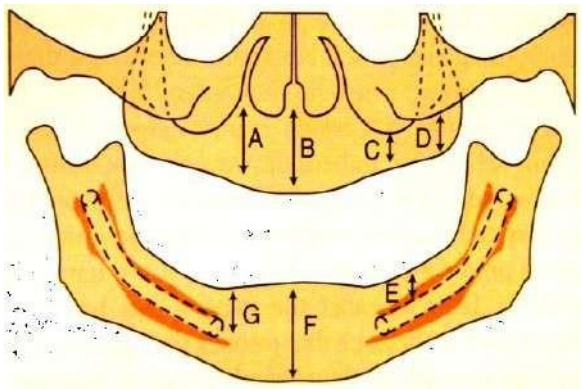

Figure 6.2: Anatomical landmarks to determine height of available bone. [131]

Prior to dental implantation, it is also necessary to determine the quantity of the jaw bone, or the bone volume. The typical structure of the bone in the human.

Division	Width	Height	Length	Angulation	CHS
A(abundant)	> 6 mm	> 12 mm	> 7 mm	< 25°	<= 15 mm
B(barely sufficient bone)	2.5 mm to 6 mm	> 12 mm	> 6 mm	< 20°	< 15 mm
C(compromised bone)	0 to 2.5 mm	< 12 mm		> 30°	> 15 mm
D(deficient bone)	Severe atrophy, flat maxilla, pencil thin mandible				> 20 mm

Table 6.2: Quantification of bone volume for implantation [134]

mandible and maxilla are shown in Fig 6.1(a) [131]. The width, height and length (Fig 6.1 (b)) of the bone are 3-dimensional features which need to be specified for the proper placement of the implant into the jawbone. From the prosthetic point of view, future crown height space (CHS) and angulation of bone are also taken into consideration during the pre-surgical analysis of the bone to be implanted. The quantitative characterization of the required bone volume in terms of these features, for different categories of the human bone, as available in literature [134] is listed in Table 6.2. A discussion of these features is provided hereafter.

The width of available alveolar bone, as shown in Fig. 6.1(c), is measured between the facial and the lingual plates at the crest of the potential implant site. There should be at least 1mm bone available on each side of the implant at the crest so that the blood supply to the jaw is adequate.

The height of the available bone is measured from the crest of the edentulous ridge to the opposing landmark. The anatomical landmarks to determine height of available bone are shown in Fig. 6.2. The anterior regions are limited by the maxillary nares (lower part of nostrils) or the inferior border of the lower jaw or mandible. The posterior regions of maxilla are limited by the maxillary sinus. The opposing landmarks, as marked in Fig. 6.2, may be the maxillary canine regions (A), floor of the nose (B), maxillary sinus (C), tuberosity (D), bone above the inferior alveolar canal (E), anterior mandible (F) and mandibular canine region (G).

The mesiodistal length of available bone is often limited by adjacent teeth or implants. As a general rule, the implant should be at least 1.5mm from an adjacent tooth and 3mm from an adjacent implant. In edentulous condition, the angulation of alveolar bone changes due to resorption process. While selecting an implant, it should be remembered that the final prosthesis can attain a divergence of angle upto 25◦, or in other words, the acceptance of bone angulation is 25◦.

The crown height space (CHS) is defined as the vertical distance from the crest of the ridge to the occlusal plane. For an ideal treatment plan, the CHS should be equal to or less than 15mm.
The implications of the available bone volume on dental implantation are specified in Misch [131]. It is known that when there is Division A bone, root form large diameter endosseous implants are inserted without any modifications of the ridge. In case of Division B bone, modifications are needed either to subtract or augment the bone to make it a Division A bone. If not possible then small diameter implants may be the choice. In cases of Division C bone, augmentation, nerve repositioning, sinus lifting should have to be considered for root form implants or else subperiosteal, ramus form or transosseous implants can be considered. Division D warrants a use of autogenous graft for augmentation of the available bone but comes with frequent complications related to grafting and early implant failure.

Patient Evaluation

Patients selected for dental implantation have been counselled detailing the proce- dures to be adopted in the particular case. Depending on the availability of bone in 6.3. PATIENT EVALUATION 141 the implantation site, as discussed in Section 6.2, the dental implantation procedure has to be preceded by the regenerative osseous procedures.
In both cases of osseous regeneration and/or dental implantation, certain pre- operative and post-operative clinical evaluations are mandatory to assess the condi- tion of the patient and ascertain the success of the procedure. A major evaluative technique in present times is that of radio-imaging, since it offers a direct non-invasive method of observing the operated region. It is needless to state that all pre-operative and post operative documentations have to be maintained carefully for proper anal- ysis.

Radiographic analysis

The pre-operative and post-operative radio-imaging procedures help develop and implement a comprehensive treatment plan for any dental surgical procedures. The pre-surgical imaging is done in order to gather all necessary surgical and prosthetic information to determine the quality, quantity and

angulation of bone, the relation- ship of the critical structures to the prospective implant site and the presence or absence of disease at the proposed surgical site. The purpose of the imaging system is thus to assist the surgical team in restoring the patients occlusion and function by providing reliable diagnostic information. The post-operative imaging, on the other hand, allows for a comparative evaluation and monitoring of the efficacy of the procedure.

The imaging techniques used in this study are primarily the Orthopantomogram (OPG) view and Intra-oral periapical (IOPA) x-rays, though few cases have been done with the help of Conventional Tomography (CT) scan as a pre operative diag- nostic tool.

OPG: Orthopantomogram (OPG) is characterized by a single image of the jaws and provides a vertically and horizontally magnified image of the same. The initial assessment of the vertical height and opposing landmarks is thus very easy and smooth, and it provides the advantage of evaluating the gross anatomy of the jaws, where the insertion site can be seen along with the vital structures like I/D canal in the mandible [90].

IOPA: The Intra-oral periapical (IOPA) x-ray provides a high resolution planar image of a limited region of the jaws although it is highly technique sensitive. One of its major benefits being inexpensive, it is useful for ruling out local bone or dental disease and identifying critical structures in the local region.

CT images: Conventional Tomography (CT) is a digital imaging technology. The axial images formed by this non-invasive radio-imaging modality give a cross sectional view, with the advantage of constant magnification. CT scans are especially useful for evaluating the small, narrow regions of jaw bones in high detail. However, in the present study, CT scans have been rarely used due to its prohibitive cost. In fact, in a developing country like India with a large demographic in the lower socio-economic strata, the cost of this imaging technique often renders it unusable since it cannot be afforded by the patient.

Tissue regeneration using HAP Filler

In case the pre-operative clinical observation shows a lack of sufficient bone level at the implantation site, the clinician prefers going in for ridge augmentation in order to ensure adequate amount of bone, which can successfully accept the implant. The indigenously developed alloplastic HAP powder,

prepared and characterized in Sections 2.1, 2.2 and tested for use as fillers in Section 4.2, has been used in the present case as a scaffolding factor for the purpose of ridge augmentation.

Case Study

A case study illustrating this regenerative procedure has been stated hereafter. Al- though, the case study pertains to a case where the ridge augmentation was followed up with a fixed partial denture in

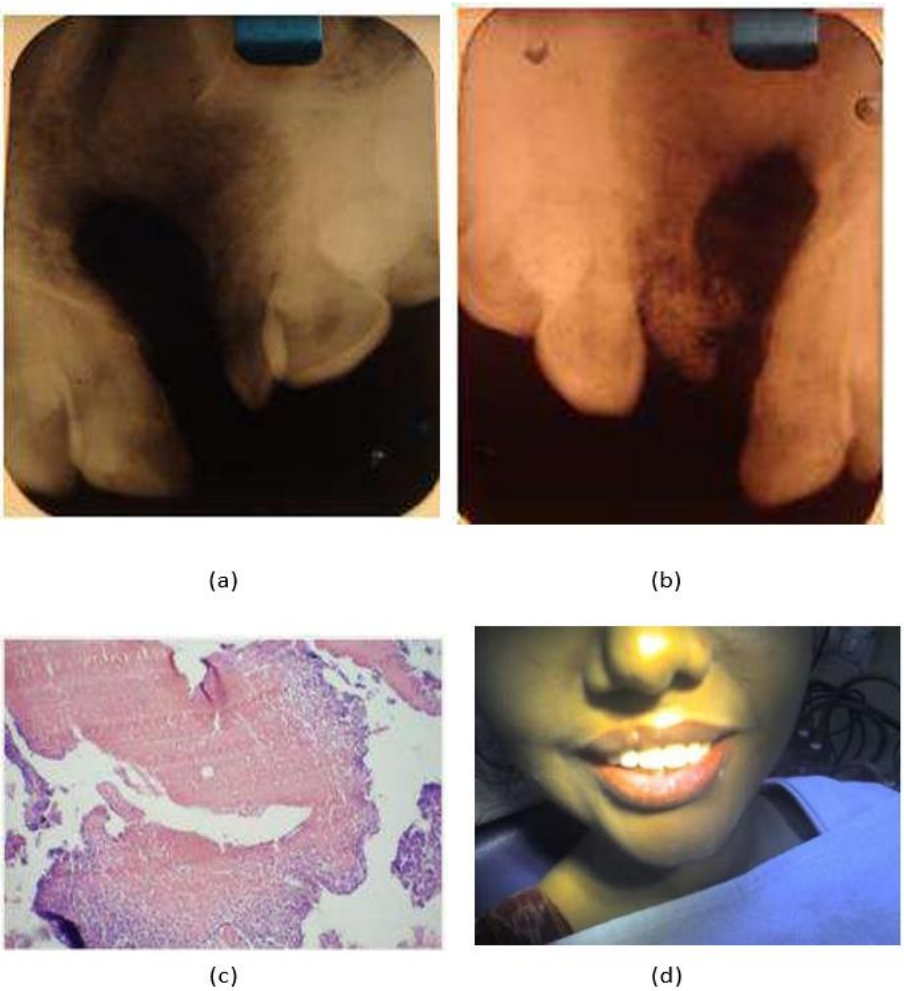

the area of initial loss of tooth, yet it must be noted that the same procedure is followed when the situation demands a follow-up dental implantation.

Figure 6.3: Bony tissue regeneration in human subject using HAP block (a) Intra oral X-ray of the defect (b) Postoperative X-ray (c) Histopathology showing osteoids (3 months) (d) Post operative patient mouth with denture in place (6 months)

- Material used:5mmx5mmx5mm HAP blocks have been used for the study. The range of porosity of the block was 200µm(approx).
- Patient profile:The patient named Piyali Mondal, 29/F, had the problem of oro-nasal communication. The patient was sent to correct the communication and for functional and aesthetic rehabilitation. The patient was properly diag- nosed and informed about the HAP block graft and the consent form was duly signed by the patient.
- Treatment procedure: Complete oral prophylaxis was undertaken. The material was then placed into the site of upper left anterior region, under local anaesthesia (2% lignocaine hydrochloride).
- Post-operative observations:Post operative period was uneventful and the sutures were removed after 7 days. Regular recall visits were undertaken in every 15 days.

Studies were done to clinically monitor the mobility of the tooth and tenderness on percussion in neighbouring teeth was also observed clinically. The radio- logical regular views were observed to determine the formation of bone in the surgical site.

An occlusal x-ray is shown in Fig. 6.3(a) of the pre-operative site. This shows radiolucency, which is probably due to the presence of non-vital tooth and an oro-nasal communication.

The osteoconductive HAP block has been utilized in this particular case to enhance the hard tissue formation. The augmentation of the lost hard tissue by the usage of this bony graft material within the bony cavities is observed in the post-operative X-ray shown in Fig. 6.3(b).

Normally, the presence of chronic inflammatory cells are not usually indicated even after 4 months of the study. In the present case, the presence of chronic inflammatory cells in the region is plenty, which proves osteoblastic activities. This is supported by the osteoid formation observed in the histopathological slide prepared using the material collected during the second surgical procedure after 3 months. This is shown in Fig. 6.3(c). As inferred in the rabbit study (Section 4.2.7), this can be ascribed to the fast dissolution of the inserted HAP particles (average pore size 200µm) within the bony tissue, leading to an early onset of the osteogenic activity in the underlying tissue.

However, since it was observed that the HAP block resorption was not total, hence a secondary surgical intervention was required.

- Second surgical procedure: The re-entry to the same surgical site was done after 3-months of the first procedure in order to shape the HAP block. The sample of HAP and tissue materials obtained during this procedure have been used for histological observations (Fig. 6.3(c)). Thereafter, the patient was given the denture in that particular site of surgery for the aesthetic purpose. The patient was given the crown and bridge (a variety of fixed denture pros- thesis) after 6 months as shown in Fig. 6.3(d).
- Second post-operative observations: The removed HAP block sample was taken and sent for the histopathological evaluation.

It has been observed from the radiological observation and histopathological evaluation in Figs. 6.3(b) and (c) that the HAP block, if placed securely, acts as a scaffold and helps in the formation of bone in situ in due course of time because of its osteoconductive nature and gradual resorption. Therefore, it has become an important material for the hard tissue formation. The functional restoration was achieved for the patient by delivering a fixed partial denture in the area of initial loss of tooth (Fig. 6.3(d)).

Results of Multi-Patient Trials

Several similar studies have been done in a total of 200 patients using HAP powder. In the present study, the clinical observations used to evaluate the tissue regeneration involve the the gain of loss of attachment (LOA), the gain of clinical attachment level (CAL) and the reduction in pocket depth. In order to appreciate the significance of these terms, a small discussion of the natural tooth structure is presented herewith.

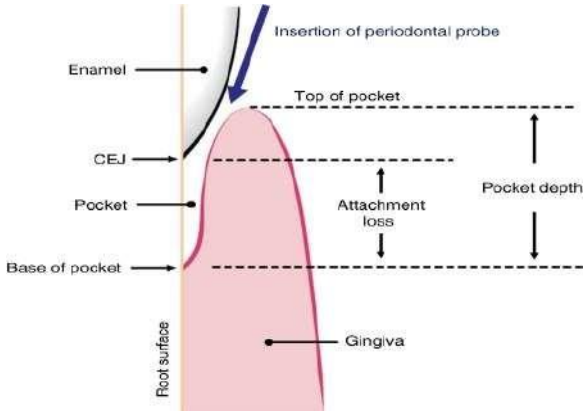

Figure 6.4: Schematic diagram of natural tooth with supporting tissues.

The supporting tissues of a natural tooth are compositely known as periodontium. This comprises of the gingiva and periodontal ligament fibres, which are the soft tissue components, as well as the cementum and the alveolar bone, which are the hard tissue components. The root surface of the natural tooth is covered with the cementum, the upper part comprises of the enamel and the junction of these two is called the cemento enamel junction (CEJ), as shown in Fig. 6.4. The CEJ is considered as a fixed line or point, depending on the situation.

The attachment loss, as shown in the figure, is also referred to as the loss of attachment (LOA). This is measured from the CEJ to the crestal part of the alveolar bone, which is represented diagrammatically as the horizontal line below the base of pocket. The clinical attachment level (CAL) is measured from the CEJ to the base of the soft tissue attachment, marked in the figure as the base of pocket. Improvement in the soft tissue attachment level with treatment is usually indicated by the gain of CAL. The periodontal pocket depth is defined as the clinical depth from the gingival crest to the base of pocket, as marked in the figure. Both the loss of alveolar bone and the apical movement of soft connective tissue attachment lead to increase in the pocket depth.

Parameters	HAP
Gain of loss of attachment (LOA)	92%
Gain of clinical attachment level (CAL)	26.1%
Reduction of pocket depth	64%

Table 6.3: Table showing osseous regeneration in 200 patients.

The gain of clinical attachment level as well as gain of loss of attachment level have been monitored in % in the present study. The reference level for the measure- ment is the pre-operative level. The clinician performs a pre-operative measurement of the absolute pocket depth. The reduction of pocket depth with the use of HAP filler and its subsequent resorption has been monitored in % in the present study. The results in terms of the gains in LOA and CAL and the reduction of pocket depth in the various cases are stated in Table 6.3. It is observed that there is 92% gain in the loss of attachment. This indicates the almost total recovery of bone level in the edentulous region in terms of the fixed point cemento enamel junction (CEJ), which is determined in this case with respect to the neighouring teeth. This is further supported by the observation of satisfactory (64%) reduction in the pocket depth. The gain in the clinical attachment level at 26.1% is not very acceptable in absolute terms. But, in

terms of the use of HAP as a filler material, it can be inferred that it assists the formation of bone in the particular region of implant insertion. Thus, the overall inference from these studies validate the claim of hard tissue regenera- tion and/or soft tissue formation at the site of dental implant placement using the bioceramic HAP filler.

Dental Implantation

In the scope of the present work, dental implantations have been done on human subjects using the proposed HAP and bioactive glass coated threaded dental im- plants, having nominal diameter of 3.5mm or 4.0mm and length of 7mm or 9mm or 11mm. In this case, the loading of the dental implant occurs primarily on placement of the acrylic based crown. A small summary of the implantations is stated hereafter, followed by details of the various procedures adopted in the subsequent subsections.

1. Sample:

- Threaded dental implants of HAP and bioactive glass coated varieties of diameters 3.5mm and 4.0 mm and lengths 7 or 9 or 11 mm have been used. Two stage technique has been followed. Total 40 numbers of implantation sites have been evaluated in a number of patients, where 20 in numbers are used in each of the 2 categories of HAP and bioactive glass coated implants.

2. Number of human patients in whom implants placed:

- HAP coated threaded implants: 16 patients/ 20 sites bioactive glass coated threaded implants: 19 patients/ 20 sites

3. Period of observation: 1, 3 and 6 months 4.Patient evaluation techniques used:

- Bleeding on probing
- Oral hygiene
- Mobility of the implants Clinical attachment level Tenderness on percussion
- Radio imaging (marginal bone loss)

Pre-operative Tasks

In case of dental implantation, the dental surgeon has to note the anatomical land- marks in the region of jaw bone where the implant is to be placed. This is so since the presence of the landmarks, namely blood vessels, nerves, sinus need to be as- certained so as to avoid them during the surgical procedures.

So, before implant insertion, it is important to perform the following tasks of thorough clinical examination, radio-imaging, preparation of study models and ridge mapping, which are described hereafter.

1. **Clinical Observation:** Clinical observation of the specific region of jaw bone is done to evaluate the presence or absence of any pathological or physiological problem. The condition of oral hygiene maintained in the patient mouth is also an important factor to observe. The specific observation indices used in this study are detailed later in Section 6.6.1.

2. **Radiological Imaging:** Observation of the area specifically, both before and after any of the surgical procedures, is essential in order to quantify the bone quality. As discussed in Section 6.3.1, this has been done using OPG and IOPA x-rays in the present study. Occasionally, CT scans have also been used for more detailed investigations of the specific implantation site(s).

3. **Study Cast:** The impression of both the jaws are taken by the clinician for the preparation of multiple study casts. Diagnostic splints, fitted with dentures relevant to the implant to be inserted in the edentulous region, are then placed over the study cast as shown in Fig. 6.6(a). These are then called surgical splints and are used by the clinician to determine the orientation of the surgical drill bits to be placed, following which the dental implantation is done. The surgical splint is also used in the articulator to see the occlusal relationship of the final implanted jaw. These tasks form an integral part of the treatment plan.

4. **Ridge Mapping:** This procedure is utilized to determine the implant diameter and length. For this, a long axis is drawn by the clinician on a longitudinal cut section of one of the study casts in the crestal to apical direction. A reamer is gently inserted under local anaesthesia at various positions in the labial and lingual gingival soft tissue of the patient surrounding the edentulous region. The depth of insertion of the reamer at these positions is marked on the cut section of the study cast as shown in Fig. 6.6(b), thus marking the thickness of the soft gingival tissue. The remaining portion maps the hard tissue, or ridge, portion.

Surgical Procedure

As stated earlier, two-stage surgical procedure was used in all cases of implantations using HAP or bioactive glass coated implant. The primary surgery have been done after disinfection and sol application. The first incision was either a crestal incision or, as is more usual, it is given a little away from the crest to obtain a periosteal flap. This flap naturally covers the implant and has to be raised to see the bone. The surgical splint was used to get the proportion, position and alignment of the socket to be drilled. The drilled socket was prepared subsequently with drills and the implant was placed with the help of hand driven wrench. A low speed, high torque (850-1250 rpm, 20-50 µcm) drilling system with normal saline as cooling system, or physiodispenser, was used. After insertion of implant, the soft tissue was sutured with absorbable vicryl suture materials. As mentioned earlier, in this two-stage procedure, there is complete coverage of the implant with the soft tissue, or periosteal flap, post insertion of the implant. Thus, it requires a second surgical procedure to expose the implant preparatory to the final loading with the acrylic crown.

Armamentarium

The armamentarium used for the total dental implantation procedures is listed here- after

1. Mouth mirror, Dental explorer
2. University of North Carolina probe(UNC-15)
3. Endodontic files Number 15 with rubber stopper.
4. Cast with surgical stent.
5. Local anesthetic solution(2%Lignocaine hydrochloride & adrenaline 1:200000)
6. Disposable gloves.
7. Disposable mouth masks &head caps.
8. Disposable syringe -10cc.
9. Povidine iodine solution -5%.
10. Chlorhexidine mouth wash(0.2%)
11. Normal saline-500ml.
12. Routine surgical set.
13. Physio dispenser with 20:1 reduction gear hand piece.
14. Implant surgical kits.
15. Vicryl suture 5-0.

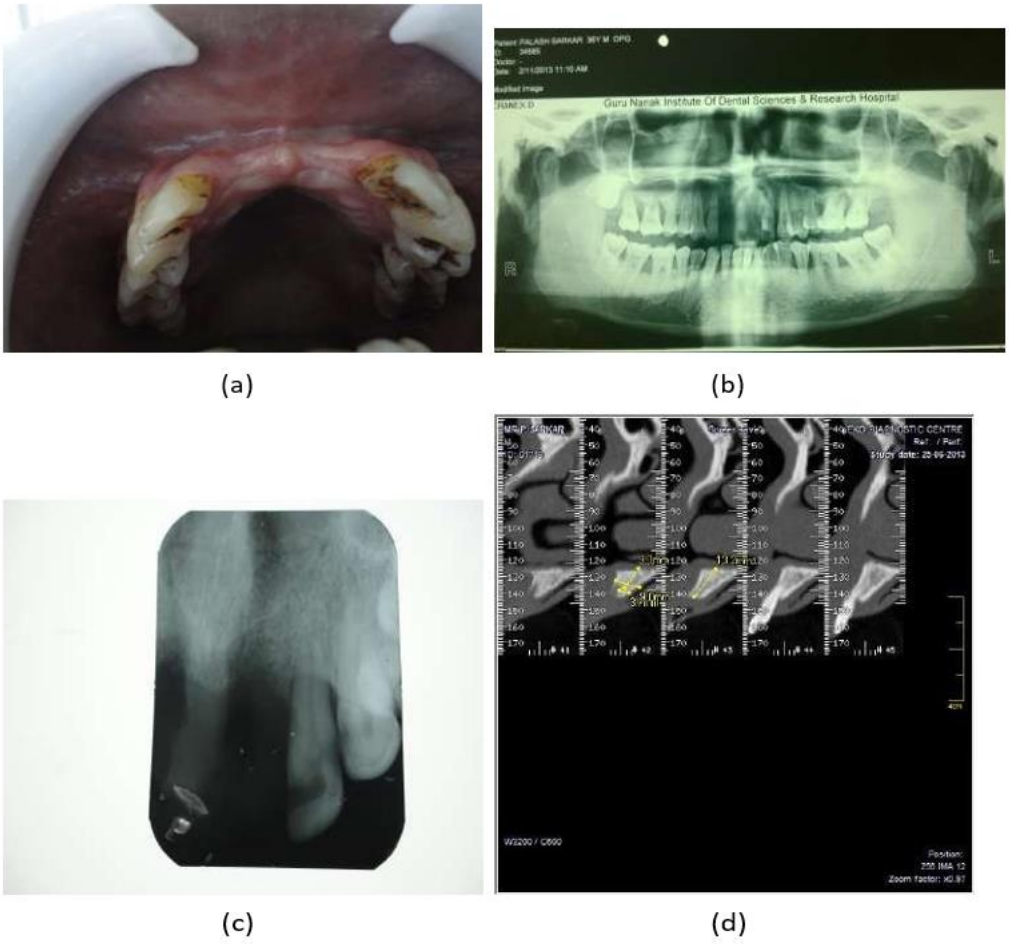

Figure 6.5: Pre-operative observations of human subject (a) Edentulous region (b) OPG x-ray (c) IOPA x-ray (d) CT scan

Post-operative Procedures

Post-surgical instructions were given. Patients were recalled after immediate man- agement for 1 week. Recall visits were at 1, 2- and 3-month intervals. After 3 months, the patients were given local anaesthesia. The flap was raised to see the implant.

Post clinical evaluations were done based on x-rays taken of the implanted site and clinical observation of the same. After 3 months, the implant was exposed and the healing screw, as detailed in Section 3.3.3, was inserted to get proper soft tissue opening. Then, the abutment screw, detailed in Section 3.3.4, was given for prosthetic purpose. The lab procedures were done to place the crown over the

abutment screw. The follow-up assessment was kept on to observe any changes in the implant-bone interface and also to monitor the oral health condition.

Case Study

(a) (b)

Figure 6.6: Pre-operative measurements of human subject (a) Acrylic denture for diagnostic and surgical stent (b) Ridge mapping.

In order to illustrate the procedures adopted for the dental implantation, a par- ticular case study is being presented here prior to the overall observations based on multiple instances of dental implantations.

Pre-operative evaluation of the edentulous site of implant insertion is performed in order to determine the presence of important anatomical structures and also whether any pathological lesion is present or not. Radio-imaging of the particular edentulous region is done as shown in Fig. 6.5(a). Thereafter, the overall view of the mandible and maxilla is observed using the OPG as shown in Fig. 6.5(b). This is used to determine the suitability of the site to receive a dental implant. The IOPA x-ray, as shown in Fig. 6.5(c), shows the availability of the bone at the specific edentulous area in the upper anterior region. Fig. 6.5(d) shows the view of the CT scan which is used to observe the bone quality and also to ensure the availability of bone in the pre-determined position at the desired site.

Another pre-operative task involves the preparation of the dental models, or study casts, made of dental plaster. For this, an impression of the edentulous region is taken. The impression is used to articulate the study cast in order to determine the bite of the patient in edentulous situation. Thereafter, a wax

rim is placed over the study cast to mount the acrylic teeth and observe the functional and aesthetic situ- ation. This assembly is then acrylized as shown in Fig. 6.6(a) to make pre-operative dentures for the patient. The acrylic denture is of even more importance from the surgical point of view since it is used as a diagnostic and surgical splint during inser- tion of the dental implant. Fig. 6.6(b) shows the method of ridge mapping, which is used for obtaining the measurement of the dental implant using the study cast.

Fig. 6.7 shows the surgical technique used for dental implantation in the human subject. As shown in Fig. 6.7(a), an aseptic procedure has been adopted for drilling the bone using a physiodispenser. Thereafter, as shown in Fig. 6.7(b), the implant is inserted into the drilled site using a finger wrench. Using this procedure, two(2) dental implants have been inserted as evident in Fig. 6.7(c).

Dental implantation requires a long term post-operative evaluation process. The patient comes for frequent recall visits during which the dental surgeon evaluates the area clinically. This includes the monitoring of the oral hygiene and also performing a bleeding on probing test using the implant probe with a graded plastic tip, as shown.

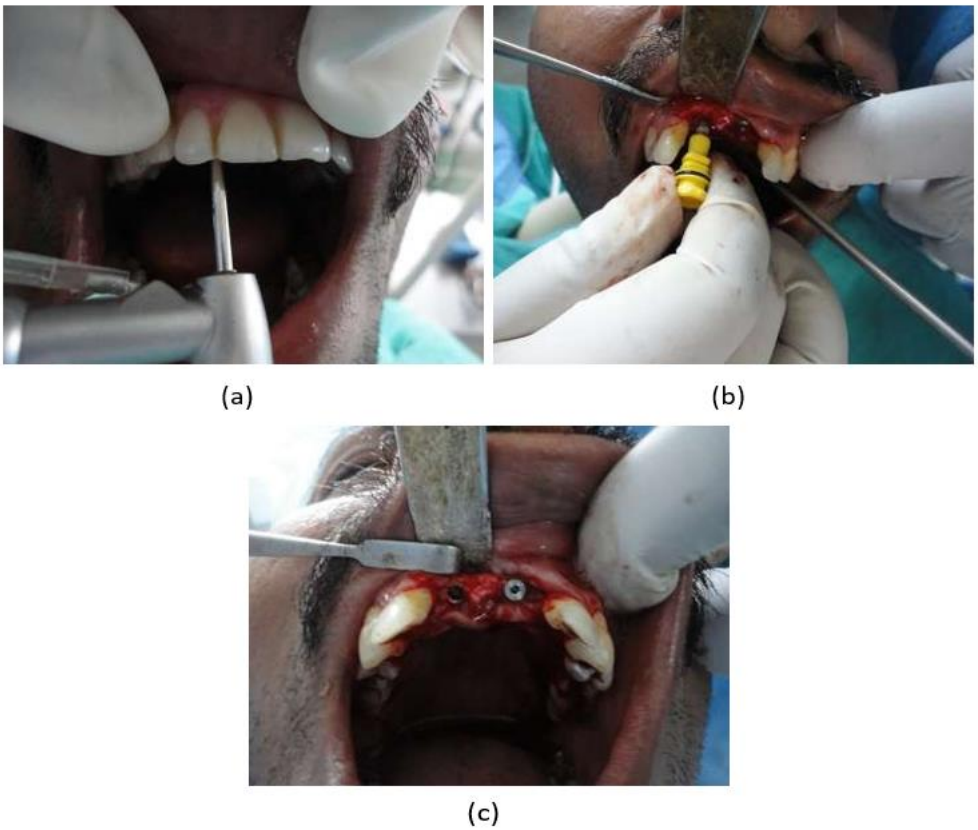

Figure 6.7: Dental Implantation in human subject (a) Surgical drilling (b) Implant insertion (c) Implant in situ in Fig. 6.8(a). The post-operative IOPA x-rays taken after 3 months of the surgery are shown in

Fig. 6.8(b). It is inferred that the implants are well placed in situ and ready for the placement of the superstructure. Fig. 6.8(c) shows the photograph of the patient's mouth, after the placement of the crowns on the implants.

Evaluation of Patients with Dental Implants

20 HAP coated dental implants were inserted in the jaws of 16 patients, while 20 bioactive glass coated implants were used in 19 patients. Primary stability was

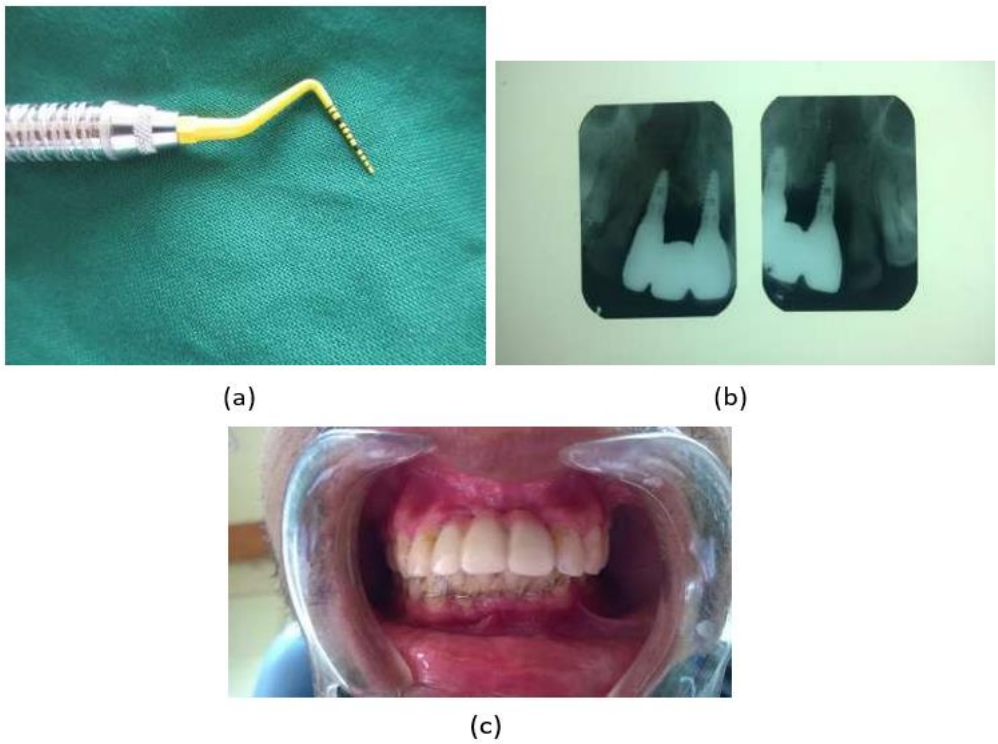

Figure 6.8: Post-operative evaluation of human subject (a) Implant probe (b) Post- operative radiographs (c) Prosthesis in situ achieved in all cases.

Thereafter, since the dental implantations used here are based on the two stage surgical technique, so clinical and radio-imaging techniques have been used for the post-operative evaluation. These observations have been made by the clinician for the period of 3 months at intervals of 0, 1 and 3 months respectively. A few indices were monitored for 6 and 12 months also. The patients were given superstructure or the crown finally at the end of 3 months in most of the cases.

Clinical Observations

The present study focusses on monitoring the bleeding on probing, oral hygiene, the diagnosis of mobility of dental implant in-situ, the measurement of clinical at- tachment level and also monitoring the tenderness on percussion. The evaluation procedures are detailed hereafter. The clinical evaluation of the patients have been done in terms of bleeding on probing, oral hygiene, mobility of the implants, clinical attachment level and tenderness on percussion. The results are plotted in Fig. 6.9 and tabulated in Tables 6.5 and 6.4.

1. Bleeding on probing: Gingival bleeding has to be monitored in case of dental implantations since it is directly related to the oral hygiene condition of the individual. This has been observed in-situ using a plastic probe by keeping it at the level of gingival margin. The results are maintained in terms of a score ranging from 0 to 3, where the scores are indicative of the following:
0 - no bleeding,
1 - bleeding on probing (gingival inflammation), 2 - bleeding on light probing,
3 - bleeding on slightest provocation.

No bleeding on probing was observed in any of the cases, although slight gin- gival inflammation, which is normally to be expected, is observed in the 1st month for HAP 4.0mm and both varieties of bioactive glass implants as shown in Fig. 6.9(a) and stated in Table 6.5. Thus, it can be inferred that inflam- mation at gingival margin is initially present within acceptable limits in some cases. However, no clinical bleeding is seen after 3 months of implant insertion in all cases, which indicates that the patients have been motivated to maintain a healthy oral hygiene.

2. Oral Hygiene: Oral hygiene is an important criteria for the proper assimila- tion of the implant in the jaw. However, tenderness and anxiety may sometimes create problems in maintaining the oral hygiene. The oral hygiene is stated in %, where 0% indicates worst oral hygiene while 100% indicates the best.

The figures for oral hygiene in all cases is shown in Fig. 6.9(b) and stated in Table 6.4. In concurrence with the results from bleeding on probing, it is found that the oral hygiene levels are best and are maintained at the same levels in case of HAP 3.5mm. This is so for the HAP 4.0mm implants also, although the bleeding on probing results showed initial inflammations in these cases. However,

contrary to the observations from bleeding on probing, both the bioactive glass coated implants show a drop in oral hygiene maintenance, which might be due to some remnant irritation or inflammation that prevents the patient from cleaning the implanted area properly.

Implant Type	Oral Hygiene (%)		Clinical Attachment Level (mm)			
	1st mth Mean(SD)	3rd mth Mean(SD)	1st mth Mean(SD)	3rd mth Mean(SD)	6th mth Mean(SD)	12th mth Mean(SD)
HAP 3.5mm	90(4.5)	90(4.5)	2(0.1)	2(0.1)	3(0.15)	2(0.1)
HAP 4.0mm	90(4.5)	90(4.5)	2(0.1)	2(0.1)	4(0.2)	2(0.1)
Bioactive glass 3.5mm	90(4.5)	80(4.0)	3(0.15)	2(0.1)	3(0.15)	4(0.2)
Bioactive glass 4.0mm	90(4.5)	76(3.75)	2(0.1)	3(0.15)	3.5(0.18)	5(0.25)

Table 6.4: Post-operative Assessment: Oral Hygiene & Clinical Attachment Level of Patient

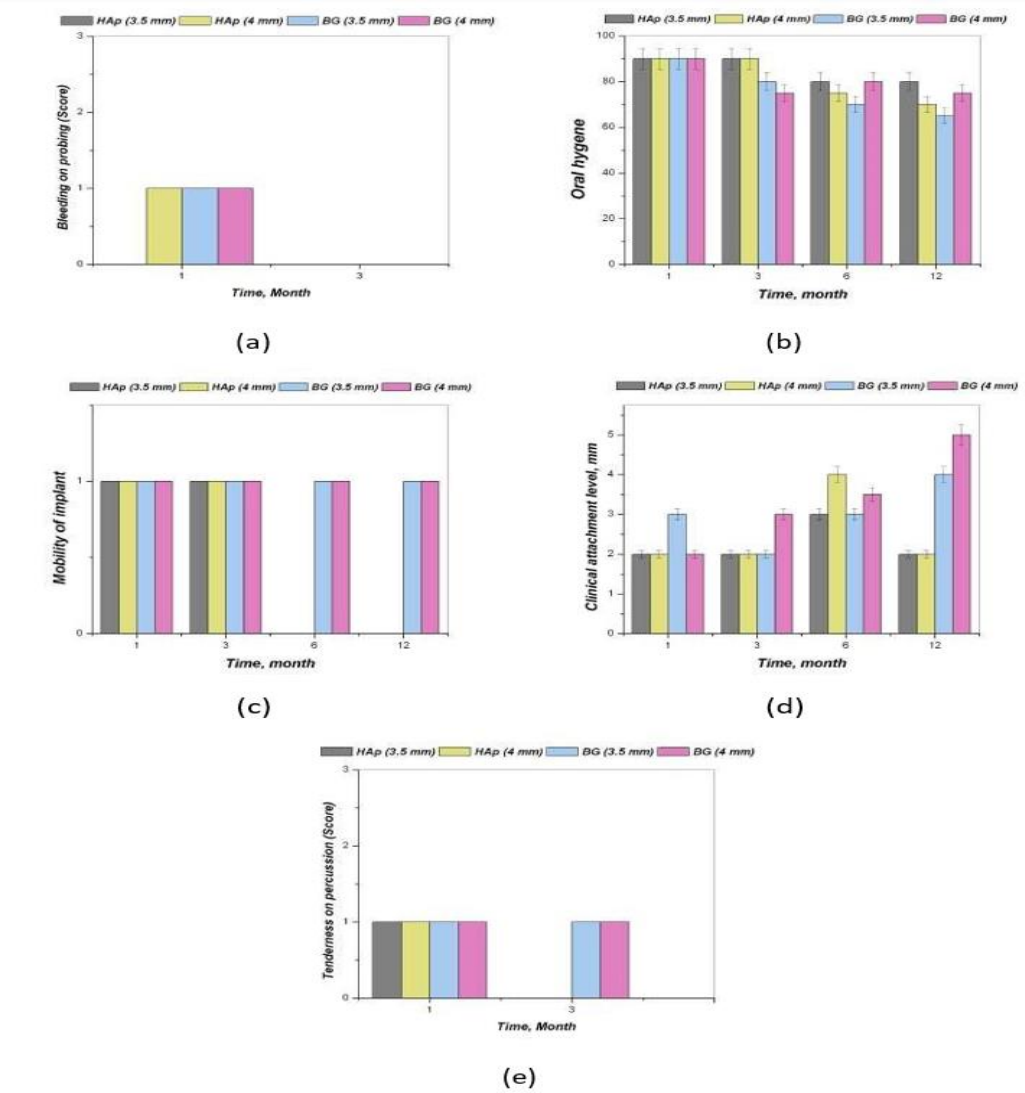

Figure 6.9: Post-operative clinical observations in human subjects (a) Bleeding on Probing (b) Oral hygiene (Gingival Index) (c) Mobility (d) Clinical attachment level (e) Tenderness on Percussion.

3. Mobility: The mobility of the dental implant needs to be monitored post- operatively in each recall visit. This has been examined with a hard probe and a score ranging from 0 to 3 has been used for recording the results. The scores are indicative of the following:
0 - no mobility,
1 - slight horizontal mobility within 1mm,
2 - slight horizontal and/or vertical mobility within 2mm, 3 - both horizontal and vertical mobility more than 2mm.

The score values for implant mobility, as stated in Table 6.5 and shown in Fig. 6.9(c), are found to be 1 in all cases. It is to be noted that slight horizontal mo- bility, ranging less than 1mm, is within the physiological limit and viscoleastic property. This is to be expected in most cases and it is very rare to have no mobility at all. Thus, the mobility is within acceptable range in all cases.

4. Clinical Attachment Level: Although clinical attachment level is usually not monitored in case of two-stage implants, yet, in the present study, this has been monitored till 12months after the implant insertion. This has been measured in mm.

The clinical attachment level is shown in Fig. 6.9(d) and stated in Table 6.4. It is observed to be satisfactory in all cases, since the value does not go below a value of 2mm in any case.

A detailed analysis of the results show that in the case of the HAP coated implants, it is observed that the value typically increases at 6 months but thereafter, there is a loss in CAL indicating loss of connective tissue in situ. It can however be inferred that since the CAL does not drop below the immediate post-surgical values, hence there is no cause for concern. This phenomena is not observed in case of the bioactive glass coated implants. Instead, in these cases, the CAL improves steadily from 3 months onwards. This phenomena and its implications, particularly in view of the contra-indications obtained for these implants from the oral hygiene results, needs to be further investigated.

5. Tenderness on Percussion: In case of dental implantations, tenderness of the implanted site on percussion with a moderately hard object has also been assessed till 3 months post-operatively. In this case, a score ranging from 0 to 3 has been used for recording the results based on the patient's subjective rating of the pain level. These indicate the following:

0 - no tenderness,

1 - slight tenderness on percussion,

2 - moderate tenderness on percussion,

3 - extreme tenderness on percussion.

As shown in Fig. 6.9(e) and stated in Table 6.5, slight tenderness was present in all cases at 1 month and was present in case of the bioactive glass coated implants at 3 months also. This supports the inference from the results on oral hygiene. As may be expected, tenderness was not observed at 3 months in case of the HAP coated implants, thus supporting all other results analysed. It must also be noted that the overall tenderness did not exceed 1, which is within pathological limits, in any case. Hence, all the implants have acceptable levels of tenderness on percussion.

Implant Type	Bleeding on Probing		Implant Mobility		Tenderness	
	1st mth	3rd mth	1st mth	3rd mth	1st mth	3rd mth
HAP 3.5mm	0	0	1	1	1	0
HAP 4.0mm	1	0	1	1	1	0
Bioactive glass 3.5mm	1	0	1	1	1	1
Bioactive glass 4.0mm	1	0	1	1	1	1

Table 6.5: Post-operative Assessment Scores of Patients

The clinical observations show that all the coated implants were accepted in the human jaw physiologically. However, a comparison of the different varieties clearly indicate that the HAP coated implants are better accepted within the human jaw and cause less discomfort or pain as compared to the bioactive glass coated implants. This results in better maintenance of the oral hygiene in case of the HAP coated implants. Thus, in human trials also, the HAP coated dental implants have been found to be the most favorable, from both the clinical and the patients subjective observations.

Figure 6.10: Pre-op and Post-op Bone quality

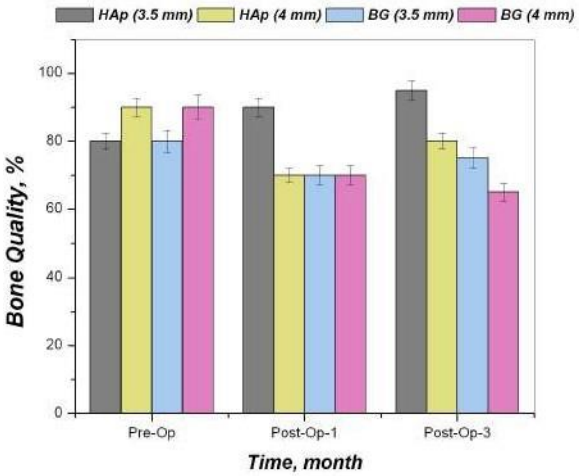

Radiographic Analysis

Implant Type	Bone Quality (%)		
	pre-op Mean(SD)	1st mth Mean(SD)	3rd mth Mean(SD)
HAP 3.5mm	80(2.4)	90(2.7)	95(2.8)
HAP 4.0mm	90(2.7)	70(2.1)	80(2.4)
Bioactive glass 3.5mm	80(3.2)	70(2.8)	75(3.0)
Bioactive glass 4.0mm	90(3.6)	70(2.8)	65(2.6)

Table 6.6: Post-operative Assessment of Bone Quality and Volume

As mentioned earlier, radio-imaging techniques have been used to determine the post-operative bone quality and/or quantity, after insertion of the dental implant in the human jaw. In the present study, the post operative panoramic views or OPG has been used with the IOPA x-rays of small region of the

implanted area. Radiographs showing the marginal bone level in recall patients are compared with their immediate. PROPOSED EVALUATION OF PATIENT SATISFACTION 163 post implant insertion radiographs. The similarity in density, geometry and contrast of the two radiographs are used to evaluate the implant-bone relationship.

The radiological images obtained prior to and after the implant insertion have also been used in the present study for a quantification of the bone quality in %. These have been shown in Fig. 6.10 and stated in Table 6.6. The bar diagram shows that the threaded variety of the HAP coated implants have been surrounded by maximum amount of bone in the 1,3,6 months. Surprisingly, the diameter of 4mm HAP showed little less value in the 1st month, then gradually the bone again increased from the 3rd month onwards. Diameter 3.5mm of HAP coated implant followed the same pattern. In case of the bioactive glass coated implants, the results after 1 month match those for the HAP coated implants. However, there is subsequent loss of bone over time, which may be due to the loss of the bioactive glass coating at the cervical portion of the implant.

Proposed Evaluation of Patient Satisfaction

The Ethical guidelines for biomedical research on human participants, published by ICMR and available at http://icmr.nic.in, suggests recording the patients' comments regarding comfort and satisfaction regarding the procedure. In this work, this has been further delineated and a detailed subjective evaluation of the satisfaction level of all patients with the implantation(s) has been noted. Score values have been assigned to quantify the patient satisfaction levels, ranging from a maximum of 15 till a minimum of 0. These are designed such that the lesser the score is, the more acceptable the implant is to the patient. More specifically, a score of 15-13 is worst, poor ranges from 12-10, satisfactory ranges 9-7, good is 6-4 while excellent is 3-0. The results for the patient satisfaction level after 3 months of implant insertion are shown in Fig. 6.11(a) and (b) for each individual patient receiving the HAP coated or bioactive glass coated dental implant(s) respectively.

It is observed that in case of HAP coated implants, the score reduces below 8 or 9 in all cases after 3 months while the corresponding figure for the bioactive glass coated implant is in general within 9-10, with the worst figure remaining at 10 in a particular case over the total duration. In both cases, the best scores are 2, while the number of scores within 3-6 are slightly more (9 out of 16 patients) in case of

the HAP coated dental implants as compared to that for bioactive glass coated implants (10 out of 19 patients). Thus, the subjective evaluation of patient satisfaction also establishes the acceptability of all varieties of implants, with the HAP coated implants showing slightly better acceptance.

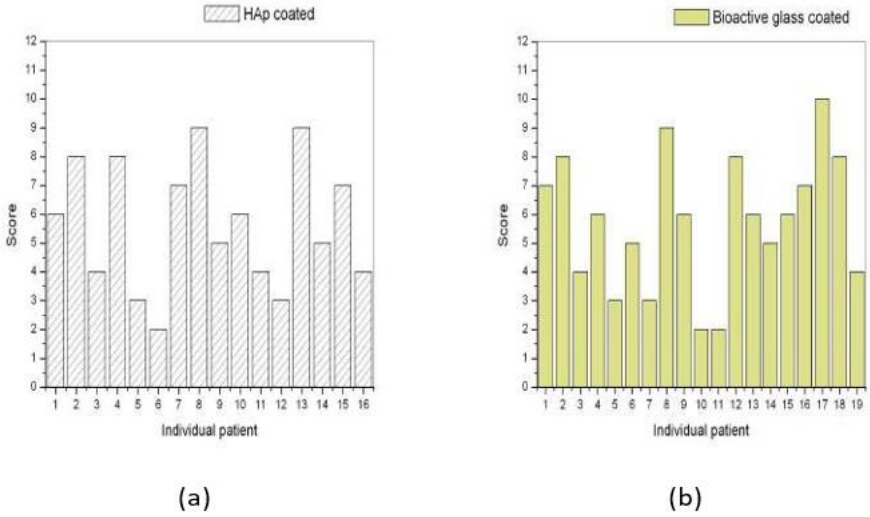

Figure 6.11: Satisfaction score in bar chart for (a) HAP coated threaded implant (c) bioactive glass coated threaded implant

Discussions

This chapter primarily deals with the use of the varieties of the newly proposed, bio- active coated, threaded dental implants for the functional rehabilitation in human subjects. In doing so, a two-fold study has been discussed in this Chapter. The first objective of the human trials was to evaluate the performance of the threaded dental implant systems, designed in this study and coated with the indigenously prepared HAP and bioactive glass coatings, in terms of their functional restorative capabilities and tissue regenerative abilities. The second objective was to evaluate the performance of the indigenously developed bioceramic HAP powder as hard tissue regenerative material, which is often a requirement prior to implantation in cases of insufficient bone in the area to be implanted.

A discussion of the criteria used by the clinician for the human subject selec- tion in the present study, followed by the procedures used to identify and meet the dental implantation site selection, including the specific requirements in terms of bone volume forms the background for the studies conducted on human subjects. Radiological studies provide an essential basis for pre-operative and post-operative assessments in both surgical procedures, that of hard tissue regeneration as well as dental implantation.

It has been established that in a developing country like India, the use of the low cost, yet effective, OPG x-rays and IOPA x-rays suffice for the purpose, while CT scans can be, and have been used only occasionally in the present study, whenever the need arises for a more detailed investigation.

As mentioned earlier, in cases where ridge augmentation was required, this has been done using the HAP filler. The multi-patient trials have established the capabil- ity of the HAP powder in recovering the bone loss in the edentulous region, as evident from the 92% gain of loss of attachment (LOA), the 64% reduction in the pocket depth and the associated, though marginal (26.1%), gain of clinical attachment level (CAL).

Pre-operative radiographs have been analyzed and clinical observations have been done prior to the dental implantation, primarily to assess the quality of the ridge at the implantation site of the non-excluded subjects. Diagnostic and surgical splints have then been used to select the proper implant dimensions, pre-determine the surgical procedure to be adopted, perform ridge mapping and also to assess apriori the occlusal relationship of the final implant fitted with the crown.

A total number of 40 coated threaded dental implants were used, 20 numbers of HAP coated implants in 16 patients and 20 numbers of bioactive glass coated implants in 19 patients. Depending on the particular implantation site, the dental implants used had one of the two diameters, 3.5mm or 4.0mm, while all other dimen- sions were identical. Several clinical and radiological indices have been monitored post-operatively for a period ranging till 3 months and/or 12 months in order to assess the performance of the various implants. The results for implant mobility and bleeding on probing show the equal acceptability of both the HAP and the bioactive glass coated implants. However, the results for CAL show an anomalous increase in case of the bioactive glass coated implants from 6 month onwards, which is associated with a fall in the oral hygiene. This can be ascribed to some remnant discomfort or some inflammation at the implantation site, as also evident from the retained tenderness on percussion in these cases. These factors as well as the associated low %age of bone volume in these cases, as compared to the HAP coated dental implants, indicate that the HAP coated dental implants are better accepted physiologically in the human subjects.

A new patient satisfaction score has been proposed in the present study to sepa- rately assess the subjective evaluation of the patients following the ICMR guidelines available online at

http://icmr.nic.in. In several cases, it was observed that the level of satisfaction also depends on the time and type of the placement of the super- structure over the implant prosthetic abutment. Based on the scores, it is observed that all 40 implantations done with both types of coated dental implants, HAP and bioactive glass, are acceptable to the patients. In no case do the scores degrade below the level satisfactory (score range of 9-7), except for 1 case of a bioactive glass coated implant, where it borders on poor with a score of 10. the level excellent (scores of 3 and 2) have also been achieved for both HAP and bioactive glass coated implants. Overall, it can be stated that the goal of satisfaction of the patients has been attained in both cases of the coated threaded implants proposed in this work. However, the HAP coated implants may be said to be slightly more acceptable to patients based on the average scores.

Thus, this study establishes the use of the indigenously prepared HAP filler as a tissue regenerative material. It further establishes the usability of the proposed threaded implant system with only 3 components and with either the HAP or the bioactive glass coating in human dental implantations and also establishes their func- tional and aesthetic rehabilitative capabilities.

CONCLUSION

As stated by Misch [129], the goal of present day dentistry is to rehabilitate the functional stomatognathic system, in particular the jaw bones, of a patient to a normal contour, function, comfort and aesthetics regardless of the atrophy, injury or disease of the functional system. The aim of this thesis is to design a simple yet effective dental implant and to investigate the use of certain specific indigenously developed bio-active materials, as coatings on the designed implant and as fillers for hard tissue regeneration in the region to be implanted. This is expected to lead to the development of a novel, complete coated dental implant system, which will provide a human acceptable option, both functional and aesthetic.

Nowadays, various types of alloplastic materials are being widely used to regener- ate the lost hard tissues or as bone filling materials for the purpose of conserving the natural dentition. In the present work, two particular variants of such synthetically prepared bio-active materials, namely a variant of the bio-ceramic hydroxyapatite, henceforth referred to as HAP, and another of bio-active glass, henceforth referred to as bioactive glass, prepared and characterized at the CSIR-Central Glass and Ce- ramic Research Institute (CSIR-CGCRI), Kolkata [97, 184, 39, 141], have been used for tissue regeneration and dental implantation procedures. The powder preparation process and some relevant powder characterizations of the indigenously prepared HAP and bioactive glass powders have been analyzed in Chapter 2 of the thesis to determine a) the ability of these bio-active powders to obtain physico-chemical attachment to the bone by means of their bioactivity; and b) the usability of these powders as coating material on metallic implant surfaces in terms of their bonding strength.

The presence of high peaks of Ca and P ions in the XRD patterns of both HAP and bioactive glass powders are indicative of the bioactive capability of these powders when in contact with the bone. This capability of the powders is further substanti- ated from the structural information received from SEM micrographs as well as the information about the presence of critical functional groups from the FTIR spec- trum, albeit in different ways. In case of the HAP powder, both the SEM and the FTIR results confirm the crystallinity of the powder even at temperatures as high as 1250◦C. This is known to improve the bioactivity of the HAP powder [74]. On the other hand, bioactive glass exhibits a non-crystalline glassy amorphous character, as evident in the SEM micrographs as well as the FTIR

spectrum. However, the confirmed presence of the hydroxyl group (-OH) in the FTIR spectrum of bioactive glass powder is indicative of its bioactivity [74].

For use of these powders as coatings on the metallic implant surfaces, it is nec- essary to ensure high bonding strength under high temperatures. The results of the DTA-TGA confirm that HAP powders calcined at 800◦C are suitable for use as implant coatings. The corresponding results for the bioactive glass powder indicate that the glass transition temperature is about 750◦C and there is no crystalline phase formation till 800◦C, hence these powders are also usable as coatings. Furthermore, as expected for both these types of bioceramic powders [170], there is no water ab- sorption, thus leading to better adherence capability of these powders when used as implant coatings within the bone.

These findings establish the usability of both these materials as osseo-regenerative fillers and/or coatings on a suitable dental implant.

A successful dental implantation requires an union between the implant and the surrounding hard tissues, often referred to as the implant-bone interface or the bone- implant contact (BIC) [135]. In Chapter 3, a novel design of the dental implant has been proposed, which is simple yet effective, in terms of the expected BIC, and is also human acceptable, both functionally and aesthetically. The proposed indigenous dental implant has only three essential components-the implant body, the healing screw and the abutment screw instead of the multiple components listed in literature [130] for a standard stage II implant. The combination of these three elements suffice to provide all required functionalities without causing patient discomfort or affecting the aesthetics. In particular, the healing screw is used in place of the first stage cover screw and/or the hygiene screw while the single abutment screw is used in place of the healing abutment and/or abutment screw. As is the usual practice, the material used for these dental implants is titanium (Ti) alloy.

An important factor for the improved BIC is the macro-design of the dental implant, specifically involving the designs of the shape of the implant, the thread form, the neck geometry and similar details. As in the case of certain popular implant designs, in this case also the implant body has ’V’ shaped parabolic threads on the essentially smooth, cylindrical, tapered implant surface in order to provide more physical attachment for the implant. But, a typical feature of the proposed design is the

increased angulation of 50◦. This is specifically provided to address the reduction in effective angulation in the coated form of the dental implant due to the coating of the implant threads.

In order to assess the feasibility of the use of the HAP and bioactive glass powders as coatings on the proposed dental implant, the available characterizations of stainless steel SS316L substrates coated with HAP powder and further heat treated at 600◦C [39]; and of Ti alloy surfaces coated with bioactive glass powder and further heat treated at 650◦C [184] have also been considered in this Chapter. It must be noted that the use of SS316L in case of HAP coatings, in place of Ti alloy, reduced the trial costs while retaining the utility of the experiments. This was not possible in case of bioactive glass since, in this case, the matching of the thermal coefficients of coating and substrate plays a major role in the adhesion of the coating to the substrate. It is also to be noted that the heat treatment temperatures in both cases were decided based on the DTA-TGA results obtained for the respective powders, as stated in Chapter 2.

As in the case of the HAP coated powders, the XRD of the HAP coated SS316L substrates affirm the crystallinity of the coating while the FTIR analysis indicates the presence of Ca-P compounds necessary for bioactivity. The coating surface mor- phology revealed from the SEM micrographs exhibit roughness and porosities in the coating of sizes less than 30µm, thus enhancing the resorption and subsequent physico-chemical contact. This fact is further validated from the bonding strength value of ∼ 13 MPa.

A similar study of the bioactive glass coated Ti surface reveals the retention of the essential amorphous nature of the glass with some additional peaks corresponding to quartz and Na2Ca2Si3O9 crystalline phases. Si-O and P-O groups could be identified from the FTIR spectra in this case also, as in case of the bioactive glass powder. Yet, borates and phosphates, which further aid the bioactivity, could not be definitely pin pointed. The SEM micrographs, however, are observed to be uniform with a desirable rough and relatively thick interface (∼ 4µm). The hardness and elastic modulus of the coating (6.52 GPa and 72 GPa) respectively are found to be superior compared to other bioactive glass coating compositions reported by other researchers [65].

Thus, overall, a novel macro-design of the dental implant has been proposed in Chapter 3. This implant design, along with any one of the two bio-active coatings, the bio-ceramic HAP or the glass based

bioactive glass, can be expected to provide the required surface roughness and increase the points of contact at the implant- bone interface. Furthermore, the biocompatible material is expected to enhance the bioactivity in the surrounding tissues favourably and provide faster healing and/or stronger BIC in the long run.

Prior to use of the newly developed implant system in humans, it is necessary to evaluate the performance of the uncoated implants as well as the implants coated with the bioactive materials in in-vivo applications. For this purpose, animal studies are an essential stop prior to clinical use in humans. However, in most cases, testing in any one particular animal species cannot ensure the fulfilment of all the requirements of the ideal model. In the scope of the present work, three stages of animal studies have been done for the benefit of human beings. The next two Chapters contain details of some systematic in-vivo animal studies performed in order to study and validate the expectations from the proposed implant design, both uncoated and coated. It must be stated that all in-vivo trials, whether on uncoated or coated implants, were done using Ti alloy implants. The use of the HAP powder as bio-active filler for tissue augmentation has also been investigated in one of the studies. In all cases, animal experiments were done following the guidelines by Indian National Science Academy, 2000, after constituting an Institutional Animal Ethics Committee (IAEC) following the guidelines specified by the Committee for the Purpose of Control and Supervision of Experiments of Animals (CPCSEA).

Chapter 4 contains details of two sets of studies that were done on rabbits to determine the osseous regeneration capability in relation to the in-vivo situation. These studies were performed in-vivo in the metaphyseal region of the hind leg of Australian chinchilla rabbits and hence, necessitated the use of a single stage Ti im- plant, which was similar to the proposed implant design, yet was smaller in size. The aim of the two sets of in-vivo studies was to investigate the relationships and interac- tions between the bone and the Ti-alloy implant, without or with bioactive coatings. In addition to evaluating the tissue regeneration capabilities of the different implant systems, these studies were expected to provide a qualitative and quantitative eval- uation of the interfacial bone response and interfacial biomechanical strength with time in the various cases. In all cases, the rabbits used were sacrificed at predeter- mined durations and SEM-EDAX, histopathological evaluations and push out tests were performed on the hard tissues.

The first set of studies was performed to ascertain the bioactivity of the smooth variant as well as the threaded form of the single stage implant, referred to as the Ti (smooth) and Ti (screw) implants respectively, while the bio-ceramic HAP powder was used as a positive control. The second set of rabbit studies was done with all 4 variants of coated implants, HAP or bioactive glass used as coatings on the Ti (smooth) and Ti (screw) implants. It must be stated at the outset that post- operative evaluations in both sets of studies established the absence of any kind of adverse responses with the Ti-alloy based implants inserted into the system, whether immunological or allergic or acute inflammatory. This establishes the bio-tolerance of all of these proposed implant varieties.

In the first set of studies, it is evident from the SEM photomicrographs that the Ti (screw) and the Ti (smooth) implants as well as the HAP granules were well placed within the mid-metaphyseal portion of the tibia of the rabbit in the holes made with drill-bits of same diameter. In due course of time, the growth of the fibrous tissue along the marginal part of the respective implants and filler is also observed. According to Maloney et al.(1990) [119], the placement of Ti (smooth) and Ti (screw) type of implants into the mid-metaphyseal region of the rabbits causes osteolysis. In the present study also, respective EDAX pictures in the interface show that post implant insertion, the quantity of Ca and P ions decrease from 1st to 2nd month for both types of implants, indicating the osteolysis process. However, there is a marked increase of Ca ions in the 3rd month in case of Ti (screw) implants indicating natural healing. It is further observed that the rate of woven bone to lamellated bone formation during this period is satisfactory and increases steadily in all cases, thus establishing the bioactivity of all these materials and in particular, of the Ti (screw) implants.

Supportive analysis is obtained from the study of the interfacial gaps in all these cases. It is observed that after 1 month of implant insertion, the interfacial gap is larger in case of the Ti (screw) implant than the Ti (smooth) implant. This can be ascribed to the initial predominance of bone osteolysis phenomena as a traumatic consequence of the torque applied during insertion of the Ti (screw) model. This is subsequently observed to be covered by the woven bone and the interfacial gap is found to be almost the same after 2 months for both the Ti (smooth) and the Ti (screw) implants. As the surfaces were not chemically treated, it is expected that the bone apposition in the close proximity of the implant should be the same and that is observed in these cases also.

A comparison of the interfacial gap (from SEM) and interfacial strengths (from push out tests) in these two cases show that while the interfacial strength is much more in case of the Ti (screw) implants, yet the average interfacial gaps are lesser in case of the Ti (smooth) implants. It can also be inferred from this that the regeneration of bone along the Ti (smooth) type of implants was faster than that of the Ti (screw) type while the stability or mechanical locking provided by the threaded macro-design of the Ti (screw) is more. In case of HAP filler, the interfacial gap between the bone and HAP granule was visible only after the 1st month. Thereafter, as the bone grew, the gap was uniquely absent indicating the acceptability of the HAP powder for tissue regeneration. Histopathology in all three cases proves the bio-tolerance of the HAP filler and Ti implants.

Thus, this first study establishes that these materials are acceptable for use in biological bodies in terms of tissue regeneration. Furthermore, all the studies estab- lish that a duration of 3 months can be treated as a substantial time period for hard tissue formation around the abutment.

Based on this finding, the second set of studies were conducted for 3 months, after which the animals were sacrificed. The SEM-EDAX as well as the histopathological observations clearly show that the effectiveness of the bio-active coatings, whether HAP or bioactive glass, are more in the case of Ti (screw) implant design, as com- pared to the Ti (smooth) implants. This can be interpreted as follows. In case of the coated Ti (smooth) implants, the mechanical locking feature of the thread is absent and this inhibits the development of intimate contact between the implant and the bone and hence, results in poor primary stability. The presence of threads in the implant macro-design retain the mechanical locking feature in spite of some surface smoothening due to the coating and hence, this enhances the BIC when coat- ings are used on the Ti (screw) implants. The inferences from the SEM-EDAX and histopathological observations are supported quantitatively by the push out results. It must be noted here that this impact of the mechanical locking feature validates the proposed design of the threads with the increased angulation of 50◦ in the dental implant.

The observations also establish that of the two coated Ti (screw) implant varieties, the HAP coated Ti (screw) implant is more effective than the bioactive glass coated Ti (screw) implant, specifically in terms of the increased BIC and interfacial strength. Thus, the HAP coated Ti (screw) implant is the most acceptable of all four varieties of implants. On the basis of the SEM-EDAX results for the HAP coated Ti (screw) implant, this can be ascribed to the roughness of the coating feature. Additionally,

it can be inferred from the SEM-EDAX of the sacrificed rabbits with implants that another factor for the acceptability of the HAP coated Ti (screw) implant is that the formation of bone in the specific environment matches that of the implant, while the bioactive glass coatings on the Ti implants exhibit rapid dissolution unmatched by the rate of (cancellous) bone formation in the rabbit tissue.

Combining the inferences from both sets of studies, it can thus be stated that the uncoated Ti (screw) implant design is more effective as compared to the uncoated Ti (smooth) implants in terms of the BIC as well as the tissue regeneration capability. This observation holds true for the respective coated forms of these implants also, whether HAP coated or bioactive glass coated and can be ascribed to the increased surface roughness of the implants due to the coatings. This finding is supported by the analysis of the interfacial strengths of these implant varieties also. These obser- vations primarily establish that the proposed threaded implant macro-design of the Ti (screw) implant, whether uncoated or coated, provides enhanced tissue regenera- tion as compared to any respective Ti (smooth) implant of similar dimensions. So, taking into account the differences in bony tissues of rabbits and humans, all further studies have been conducted using uncoated, HAP coated and bioactive glass coated threaded Ti implants.

This study also establishes the effectiveness of the use of the indigenously devel- oped HAP powder as a filler material, alongside its use as a coating on the proposed Ti (screw) implant. A possible interpretation for this may be that in spite of an ab- sence of chemical bonding between the HAP coating and the gingival mucosal tissue, the time of dissolution of this particular type of bioactive material matches that of the (cancellous) bone formation around the implant in rabbits.

Subsequent to the validation of the tissue regeneration capability of the newly developed implant systems, it is necessary to ensure the functional capability of the implants, prior to their use in humans. Since this is intricately linked to the proper match of the implant systems to the underlying bone structure, hence dogs are used in dental implant studies. This is primarily due the availability of both cortical and trabecular bones in the canine jaw, which mimics the case in humans.

In Chapter 5, details of in-vivo implantation studies performed in the anterior as- pect of dog mandibles and in edentulous portions of the canine jaw have been stated. Uncoated, HAP coated and bioactive glass coated varieties of the threaded Ti dental implants designed in the present work have been used

for the canine implantations. Mongrel dogs were used for the study and these were kept in natural habitats all through. The objective of this study was to interpret the bio-compatibility of the proposed dental implants in the canine jaw. This was done by determining the sta- bility of the implant using an indigenously developed resonance frequency analysis (RFA) based instrumentation system [26, 168]. For the study, the frequency at which the maximum resonance is recorded during an experiment using the instrumentation system has been considered as the RF value. All observations have been based on the change of the average RF measured in-vivo, referred to as the RF (sensor), from the daily reference RF measured externally prior to connecting the sensor to the implant, referred to as RF (open). The loading of the RF sensors by the implant placed within the bone changes the unloaded, alternatively referred as open, resonance frequencies of the sensors. This was recorded as the respective change in RF for the day, denoted as daily ΔRF. The functional restoration of implants are expected to cause changes in these ΔRF values over time, which were recorded simultaneously using two different sensors.

The positive and/or positively changing nature of ΔRF in the first two days of implantation in all cases indicate primary acceptability of the uncoated, HAP coated as well as bioactive glass coated threaded implants. The bone osteolysis, which forms an integral part of the implantation process [119], prior to functional restoration and tissue regeneration, is also indicated in each case by a subsequent fall in ΔRF.

The functional and para-functional loading of the bone in the implanted region also affect the ΔRF values. The dominance of these effects on the ΔRF values is most consistently observed in the HAP coated implants with both sensors showing similar natures of changes in ΔRF with time. This can be ascribed to a good match between the HAP coated implant macro-design and the quality of jaw bone. On the other hand, the changes in ΔRF measured for uncoated and bioactive glass coated implants using the 2 piezo sensors are not always consistent. This may be due to the fact that the absence of any bioactive coating or a mismatch of the bioactive glass coating dissolution rate with the bone formation rate in the particular implanted region in the canine model fails to dominate the RF response of the sensor(s). However, this inconsistency is not necessarily a contra-indication of the functional restorative ability of the particular implant. This is evident from the results for a single case pertaining to the use of an uncoated threaded implant, which provides a classical example of functional restoration

followed by successful tissue regeneration, with the implant being retained in the dog jaw bone for more than 49 days.

It is evident from all these observations that the proposed implant macro-design, without or with the proposed HAP or bioactive glass coatings, ensures in-vivo bio- compatibility and provides functional restoration of the implanted mammalian jaw. It is further noted that in case of the canine model also, the HAP coated threaded implant is the most acceptable since this macro-design provides the most consistent results in terms of functional restoration.

On the basis of these results obtained for the various animal studies, several in - vivo human implantations have been performed using the HAP and bioactive glass coated threaded Ti dental implants, which are discussed in Chapter 6. This chapter thus deals with the use of the varieties of the newly proposed, bio-active coated, threaded dental implants for the functional rehabilitation in human subjects. In doing so, a two-fold study has been discussed in this Chapter. The primary objective of the human trials was to evaluate the performance of the threaded dental implant systems, designed in this study and coated with the indigenously prepared HAP and bioactive glass coatings, in terms of their functional restorative capabilities and tissue regenerative abilities. The secondary objective was to evaluate the performance of the indigenously developed bioceramic HAP powder as hard tissue regenerative material, which is often a requirement prior to implantation, in cases of insufficient bone in the area to be implanted.

A discussion of the criteria used by the clinician for the human subject selec- tion in the present study, followed by the procedures used to identify and meet the dental implantation site selection, including the specific requirements in terms of bone volume forms the background for the studies conducted on human subjects. Radiological studies provide an essential basis for pre-operative and post-operative assessments in both surgical procedures, that of hard tissue regeneration as well as dental implantation. It has been established in this study that in a developing coun- try like India, the use of the low cost, yet effective, OPG x-rays and IOPA x-rays suffice for the purpose, while CT scans can be, and have been used only occasionally in the present study, whenever the need arises for a more detailed investigation.

Proceeding for the dental implantation, pre-operative radiographs have been an- alyzed and clinical observations have been done prior to the procedure, primarily to assess the quality of the ridge at the implantation site of the non-excluded sub- jects. In cases where ridge augmentation was required, this has been done using the HAP filler. Multi-patient trials have established the capability of the HAP powder in recovering the bone loss in the edentulous region. It is observed that there is 92% gain in the loss of attachment (LOA). This indicates the almost total recovery of bone level in the edentulous region in terms of the fixed point cemento enamel junc- tion (CEJ), which is determined in this case with respect to the neighouring teeth. This is further supported by the observation of satisfactory (64%) reduction in the pocket depth. The gain in the clinical attachment level (CAL) at 26.1% is not very acceptable in absolute terms. But, in terms of the use of HAP as a filler material, it can be inferred that it assists the formation of bone in the particular region of implant insertion. Thus, the overall inference from these studies validate the claim of hard tissue regeneration and/or soft tissue formation at the site of dental implant placement using the bioceramic HAP filler.

After ensuring that the bone quality requirement is met, the next step is that of preparing diagnostic and surgical splints. These have been used to select the proper implant dimensions, pre-determine the surgical procedure to be adopted, perform ridge mapping and also to assess apriori the occlusal relationship of the final implant fitted with the crown.

Using this procedure, a total number of 40 coated threaded dental implants were placed in human subjects, 20 numbers of HAP coated implants in 16 patients and 20 numbers of bioactive glass coated implants in 19 patients. Depending on the particular implantation site, the dental implants used had one of the two diameters, 3.5mm or 4.0mm, while all other dimensions were identical. Several clinical and radiological indices have been monitored post-operatively for a period ranging till 3 months and/or 12 months in order to assess the performance of the various implants. The results for implant mobility and bleeding on probing show the equal acceptability of both the HAP and the bioactive glass coated implants. However, the results for CAL show an anomalous increase in case of the bioactive glass coated implants from 6 month onwards, which is associated with a fall in the oral hygiene. This can be ascribed to some remnant discomfort or some inflammation at the implantation site, as also evident from the retained tenderness on percussion in these cases. These factors as well as the associated low percentage of bone volume in these cases, as compared to the HAP coated dental implants, indicate that the HAP coated dental implants are better accepted physiologically in the human subjects.

A new patient satisfaction score ranging from 0 to 15 has been proposed in the present study to separately assess the subjective evaluation of the patients following the ICMR guidelines available online at http://icmr.nic.in. The score 0 indicates excellent while a score of 15 is termed the worst. Based on the score results, it was observed in several cases that the level of satisfaction also depends on the time and type of the placement of the superstructure over the implant prosthetic abutment. However, in general, it is observed that all 40 implantations done with both types of coated dental implants, HAP and bioactive glass, are acceptable to the patients. In no case do the scores degrade below the level satisfactory (score range of 9-7), except for 1 case of a bioactive glass coated implant, where it borders on poor with a score of 10. The level excellent (scores of 3 and 2) have also been achieved for both HAP and bioactive glass coated implants. Overall, it can be stated that the goal of satisfaction of the patients has been attained in both cases of the coated threaded implants proposed in this work. However, the HAP coated implants may be said to be slightly more acceptable to patients based on the average scores.

Thus, this study establishes the bio-tolerance and BIC enhancing capability of the proposed threaded Ti dental implant system with only 3 components. Furthermore, it is established that both the indigenously prepared materials, HAP as well as bioactive glass, provide tissue regeneration in human dental implantations when used as a coating on the proposed dental implant and they also provide functional and aesthetic rehabilitation. In addition, this study establishes the use of the indigenously prepared HAP filler as a tissue regenerative material, which is also applicable in dental implantations in cases where preliminary ridge augmentation is a necessity. Overall, this study provides two options (HAP coated or bioactive glass coated) of a novel, indigenously developed, complete coated threaded Ti dental implant system. Furthermore, since this dental implant is simple in design, so it can be used to develop a commercial product which is available to the common man in developing or under-developed countries at an affordable price.

Scope for Future Work

In order to develop a commercially viable, yet affordable design of the complete, coated threaded dental implant, it is necessary to conduct more extensive multi- central human trials over a suitably large period of time. All evaluation results as mentioned in this work, including the proposed patient

satisfaction scores, obtained from these trials need to be analyzed in detail to appreciate the need for any changes in implant design, coating material or coating procedure.

A future objective could be the development of a totally indigenous implantation system which involves additionally the design and development of an indigenous surgical armamentarium, including the drill bits. In order to do this, extensive animal and human trials are needed before a commercial product can be launched in terms of a total indigenously developed dental implantation system. Scope also exists for the development of an implant system in which all the three components proposed in this work, along with the crown, are made of the same bio-compatible material.

In order to study the functional aspects of dental implants, ex-vivo studies in goat mandibles are gaining more importance in recent times, particularly since the goat mandibular structure is observed to be similar in form to the human mandible [152]. Ex-vivo RFA studies could be performed in goat mandibles using the developed coated implants under varied loading in order to gain better understanding of the implantation dynamics. Cytocompatibility analysis can also be done using ex-vivo procedures on stem cells to determine the various growth factors.

In this context, it may be noted that the rights to the commercial production of the HAP and bioactive glass powders synthesized at CSIR-CGCRI, Kolkata have been proprietarily acquired by one Indian company dealing with bioceramics. They have also acquired the rights of production of a few other hydroxyapatite and bioac- tive glass based composites, namely bi-phasic calcium phosphate (BCP), β-tri cal- cium phosphate (β-TCP) and a hydroxyapatite-bioactive glass composite referred to as HABG. These materials have been shown to exhibit better adhesion strength and bioactivity as compared to the stand alone HAP or bioactive glass powders [34, 94, 39, 83]. Consequently, the work done in this thesis could be extended to investigate the effect of these materials used as coatings on the implant proposed in this work.

Based on the positive findings establishing the bio-compatibility and the bio- activity of the indigenously developed HAP and bioactive glass powders, as reported in this work, it is worthwhile to investigate the use of these materials as coatings and/or fillers in other human implantation or tissue regeneration applications, not necessarily dental. Some work in this aspect has already been pursued in terms of ocular implants [96, 141, 95]. It must be noted however, that the use of the bioactive glass

powders as tissue regenerative material needs to be established in animal studies since that has not been done in this work. In the context of other implantation applications, it may also be worthwhile to look into design alterations of the implant in a manner similar to that proposed in this work. In particular, the implant geometry alterations may be of relevance in those applications too since the mechanical locking feature of the threaded design and its impact in subsequent bone growth in the implanted region, which have been established in this study, affect those applications also.

Bibliography

[1] American Society for Testing, Materials: Metallic, Inorganic Coatings, Metal Powders, Metal Powder Products, volume 02.05, chapter B212-09, (ASTM Standard) Standard test method for apparent density of free-flowing metal powders using the Hall flowmeter funnel. ASTM International, West Con- shohocken, PA, 1999.

[2] American Society for Testing, Materials: Metallic, Inorganic Coatings, Metal Powders, Metal Powder Products, volume 02.05, chapter C633-01, (ASTM Standard) Standard test method for adhesion or cohesion strength of thermal spray coatings. ASTM International, West Conshohocken, PA, 2001.

[3] M. Aaboe, E.M. Pinholt, and E. Hjorting-Hansen. Unicortical critical size defect of rabbit tibia is larger than 8 mm. J Craniofac Surg, 5(3):201–203, 1994.

[4] E.A. Abou Neel, D.M. Pickup, S.P. Valappil, R.J. Newport, and J.C. Knowles. Bioactive functional materials: a perspective on phosphate-based glasses. J Mater Chem, 19:690–701, 2009.

[5] Heba Abuhussein, Giorgio Pagni, Alberto Rebaudi, and Hom-Lay Wang. The effect of thread pattern upon implant osseointegration. Clinical oral implants research, 21(2):129–136, 2010.

[6] R. Adell, U.I. Lekholm, B. Rockler, and P.I. Branemark. A 15-year study of osseointegrated implants in the treatment of the edentulous jaw. International Journal of Oral Surgery, 10(6):387–416, 1981.

[7] S. Agathopoulos, D.U. Tulyaganov, J.M.G. Ventura, S. Kannan, M.A. Karakas- sides, and J.M.F. Ferreira. Formation of hydroxyapatite onto glasses of the CaO − MgO − SiO2 system with B2O3, Na2O, CaF2 and P2O5 additives. Biomaterials, 27(9):1832–1840, 2006.

[8] J.S. Al-Sanabani, A.A. Madfa, and F.A. Al-Sanabani. Review article: Appli- cation of calcium phosphate materials in dentistry. International Journal of Biomaterials, pages 1–12, 2013.

[9] T. Albrektsson, P.I. Branemark, H.A. Hansson, and J. Lindstrom. Osseoin- tegrated titanium implants. requirements for ensuring a long-lasting, direct bone-toimplant anchorage in man. Acta orthopaedica Scandinavica, 52:155– 170, 1981.

[10] C.R. Ananth and N. Chandra. Numerical modeling of fiber push-out test in metallic and intermetallic matrix composites-mechanics of the failure process. Journal of Composite Materials, 29(11):1488–1514, 1995.

[11] T. L. Arinzeh, T. Tran, J. Mcalary, and G. Daculsi. A comparative study of biphasic calcium phosphate ceramics for human mesenchymal stem-cell- induced bone formation. Biomaterials, 26(17):3631–3638, 2005.

[12] P. Ausiello, P. Francios, M. Martorelli, and D.C. Watts. Effects of thread features in osseo-integrated titanium implants using a statistics-based finite element method. Dental Materials, 28:919–927, 2012.

[13] Baillie, S. and Nzihou, A. The kinetics of surface area reduction during isother- mal sintering of hydroxyapatite adsorbent. Chemical Engineering Journal , 98(1-2):141–152, 2004.

[14] L. Barbier and E. Schepers. Adaptive bone remodeling around oral implants under axial and nonaxial loading conditions in the dog mandible. Int J Oral Maxillofac Implants, 12:215?223, 1997.

[15] F. Barrere, C. M. Van Der Valk, and R. A. J. Dalmeijer. Osteogenecity of octacalcium phosphate coatings applied on porous metal implants. Journal of Biomedical Materials Research A, 66(4):779–788, 2003.

[16] R. B.Heimann. Classic and Advanced Ceramics from Fundamentals to Appli- cation. 2010.

[17] R.S. Boggan, J.T. Strong, C.E. Misch, and M.W. Bidez. Influence of hex geometry and prosthetic table width on static and fatigue strength of dental implants. Journal of Prosthetic Dentistry, 82:436–440, 1999.

[18] M. Bohner. Physical and chemical aspects of calcium phosphates used in spinal surgery. European Spine Journal, 10(2):S114–S121, 2001.

[19] P.I. Branemark. Osseointegrated implants in the treatment of the edentulous jaw. Experience from a 10-year period, Scandinavian Journal of Plastic Recon- structive Surgery, 11(Suppl. 16):1–132, 1977.

[20] M. Brizuela, L.A. Garcia, J.L. Viviente, I. Braceras, and J.L. Onate. Tribo- logical study of lubricious dlc biocompatible coatings. Journal of Materials Science: Materials in Medicine, 13(12):1129–1133, 2002.

[21] J.B. Brunski. In vivo bone response to biomechanical loading at the bone/dental-implant interface. Advances in Dental Research, 13:99–119, 1999.

[22] Joel D Bumgardner, Gregg J Boring, Robert C Cooper Jr, Cheng Gao, Sumal Givaruangsawat, Jerome A Gilbert, Craig M Misch, and David E Steflik. Pre- liminary evaluation of a new dental implant design in canine models. Implant dentistry, 9(3):252, 2000.

[23] L. Carlsson, T. Rostlund, B. Albrektsson, and T. Albrektsson. Implant fixation improved by close fit. cylindrical implant-bone interface studied in rabbits. Acta Orthop Scand, 59:272–275, 1988.

[24] Abhijit Chakraborty. A Study on Calcium Hydroxyapatite as Bone Graft and Implant Coating. Master's thesis, Calcutta University, 1998.

[25] E. Chang, W. J. Chang, B. C. Wang, and C. Y. Yang. Plasma spraying of zirconia-reinforced hydroxyapatite composite coatings on titanium. part i phase, microstructure and bonding strength. Journal of Materials Science: Materials in Medicine, 8(4):193–200, 1997.

[26] Ipsita Chatterjee.Study of Dental Implant Stability using Resonance Fre- quency Analysis (RFA). Master's thesis, Jadavpur University, May 2006.

[27] Chen, C.C. and Ding, S.J. Effect of heat treatment on characteristics of plasma sprayed hydroxyapatite coatings. Materials Transactions, 47(3):935–940, 2006.

[28] L. Chia-Chin, L. Shang-Chih, K. Ming-Jen, W. Shu-Wei, and F. Ping-Yuen. Ef- fects of implant threads on the contact area and stress distribution of marginal bone. Journal of Dental Sciences, 5(3):156–165, 2010.

[29] Choi, D. and Marra, K.G. and Kumta, P.N. Chemical synthesis of hydroxyapatite/poly(-caprolactone) composites. Materials Research Bulletin, 39(3):417–432, 2004.

[30] S. Christian, M. Doris, and S. Alexis. The fluorohydroxyapatite (fha) frios algipore is a suitable biomaterial for the reconstruction of severely atrophic human maxillae. Clinical Oral Implants Research, 14(6):743–749, 2003.

[31] S.H. Chung, S.J. Heo, J.Y. Koak, S.K. Kim, J.B. Lee, and J.S. Han. Effects of implant geometry and surface treatment on osseointegration after functional loading: a dog study. Journal of Oral Rehabilitation, 35:229–236, 2008.

[32] D.L. Cochran, D. Buser, C.M. ten Bruggenkate, D. Weingart, T.M. Taylor, J.P. Bernard, F. Peters, and J.P. Simpson. The use of reduced healing times on iti implants with a sandblasted and acid-etched (sla) surface: early results from clinical trials on iti sla implants. Clinical oral implants research, 13:144–153, 2002.

[33] K. de Groot, J. G. C. Wolke, and J. A. Jansen. State of the art: hydroxyapatite coatings for dental implants. Journal of Oral Implantology, 20:232–234, 1994.

[34] T. Debnath, A. Chakraborty, and T.K. Pal. A clinical comparative study with HABG and HAp. Journal of Indian Society of Periodontology, 2014.

[35] S.R. Desai, M.S. Desai, G. Katti, and I. Karthikeyan. Evaluation of design parameters of eight dental implant designs: A two-dimensional finite element analysis. Nigerian Journal of Clinical Practice, 15(2):176–181, 2012.

[36] A. Dey, A.K. Mukhopadhyay, S. Gangadharan, M.K. Sinha, and D. Basu. Characterization of microplasma sprayed hydroxyapatite coating. Journal of Thermal Spray Technology, 18(4):578–592, 2009.

[37] A. Dey, A.K. Mukhopadhyay, S. Gangadharan, M.K. Sinha, and D. Basu. Development of hydroxyapatite coating by microplasma spraying. Materials and Manufacturing Processes , 24(12):1321–1330, 2009.

[38] A. Dey, A.K. Mukhopadhyay, S. Gangadharan, M.K. Sinha, D. Basu, and N.R. Bandyopadhyay. Nanoindentation study of microplasma sprayed hydroxyap- atite coating. Ceramics International, 35(6):2295–2304, 2009.

[39] A. Dey, S.K. Nandi, B. Kundu, C. Kumar, P. Mukherjee, S. Roy, A.K. Mukhopadhyay, M.K. Sinha, and D. Basu. Evaluation of hydroxyapatite and β-tri calcium phosphate microplasma spray coated pin intra-medullary for bone repair in a rabbit model. Ceramics International, 37(4):1377–1391, 2011.

[40] W.J.A. Dhert, C.P.A.T. Klein, and J.A. Jansen. A histological and histomor- phometrical investigation of fluorapatite, magnesiumwhitlockite, and hydrox- ylapatite plasma-sprayed coatings in goats. Journal of Biomedical Materials Research Part A, 27(1):127–138, 1993.

[41] W.J.A. Dhert, P. Thomsen, A.K. Blomgren, M. Esposito, L.E. Ericson, and
A.J. Verbout. Integration of press-fit implants in cortical bone: A study on interface kinetics. Journal of Biomedical Materials Research, 41(4):574–83, 1998.

[42] I.W. Donald. Preparation, properties and chemistry of glass-and glass-ceramic- to-metal seals and coatings. Journal of Materials Science: Materials in Medicine, 28(11):2841–2886, 1993.

[43] D.P. Dowling, P.V. Kola, K. Donnelly, T.C. Kelly, K. Brumitt, and L. Lloyd. Evaluation of diamond-like carbon-coated orthopaedic implants. Diamond and Related Materials, 6:390–393, 1997.

[44] Brown W. E. and L. C. Chow. Combinations of sparingly soluble calcium phosphates in slurries and pastes. US Patent no. 4, 518, 430, 1986.

[45] F.D. Jones ed. Machine Shop Training Course. Industrial Press, 1964.

[46] Elthuri Sunil, Abhijit Chakraborty, Ratna Ghosh and Bhaswati Goswami. De- sign of transducers for resonance frequency measurement to assess the dental implant stability in vitro. In Proceedings of the 33rd annual Conference of the IEEE Industrial Electronics Society (IECON), pages 2158–2162, Taipei, Taiwan, November, 5-8 2007.

[47] M. Epple, K. Ganesan, and Heumann R. Application of calcium phosphate nanoparticles in biomedicine. Journal of Materials Chemistry, 20(1):18–23, 2010.

[48] M. P. Ferraz and C. M. Monteiro, F. J.and Manuel. Hydroxyapatite nanopar- ticles: a review of preparation methodologies. Journal of Applied Biomaterials and Biomechanics, 2(2):74–80, 2004.

[49] Fowler, B.O. Infrared studies of apatites. II. Preparation of normal and isotopi- cally substituted calcium, strontium, and barium hydroxyapatites and spectra- structure-composition correlations. Inorganic Chemistry, 13(1):207–214, 1974.

[50] Fowler, B.O. and Moreno, E.C. and Brown, W.E. Infra-red spectra of hy- droxyapatite, octacalcium phosphate and pyrolysed octacalcium phosphate. Archives of Oral Biology, 11(5):477–492, 1966.

[51] J.W. Frame, P.G. Rout, and R.M. Browne. Ridge augmentation using solid and porous hydroxylapatite particles with and without autogenous bone or plaster. J Oral Maxillofac Surg, 45:771–778, 1987.

[52] S. J. Froum, D. P. Tarnow, S. S. Wallace, M. D. Rohrer, and S. C. Cho. Sinus floor elevation using anorganic bovine bone matrix (osteograf/n) with and without autogenous bone: a clinical, histologic, radiographic, and histo- morphometric analysis-part 2 of an ongoing prospective study. International Journal of Periodontics and Restorative Dentistry, 18(6):529–543, 1998.

[53] P.A. Fugazzotto. Success and failure rates of osseointegrated implants in func- tion in regenerated bone for 72 to 133 months. International Journal of Oral & Maxillofacial Implants, 20:77–83, 2005.

[54] R. J. Furlong and J. F. Osborn. Fixation of hip prostheses by hydroxyapatite ceramic coatings. Journal of Bone and Joint Surgery B, 73(5):741–745, 1991.

[55] P. Gabbott. Principles and Applications of Thermal Analysis, chapter A prac- tical introduction to differential scanning calorimetry, pages 41,88. Blackwell Publishing Limited, Iowa, 2008.

[56] D. D. Gammage, A. E. Bowman, R. M. Meffert, R. J. Cassingham, and W. A. Davenport. Histologic and scanning electron micrographic comparison of the osseous interface in loaded imz and integral implants. The International Jour- nal of Periodontics& Restorative Dentistry, 10(2):124–135, 1990.

[57] R. G. T. Geesink. Osteoconductive coatings for total joint arthroplasty. Clinical Orthopaedics and Related Research, 395:53–65, 2002.

[58] R.G.T. Geesink and N.H.M. Hoefnagels. Six-year results of hydroxyapatite- coated total hip replacement. Journal of Bone and Joint Surgery, American Edition, 77-B(Suppl III):534–547, 1995.

[59] M. Geetha, A.K. Singh, R. Asokamani, and A.K. Gogia. Ti based biomaterials, the ultimate choice for orthopaedic implants - a review. Progress in Materials Science, 54:397–425, 2009.

[60] J.P. Geng, Q.S. Ma, W. Xu, K.B. Tan, and G.R. Liu. Finite element analysis of four threadform configurations in a stepped screw implant. Journal of Oral Rehabilitation, 31:233–239, 2004.

[61] J.P. Geng and X.X. Ma. A differential mathematical model to evaluate side?surface of an archimede implant. Shanghai Shengwu Gongcheng Yixue, 50:19, 1995.

[62] J.P. Geng, D.W. Xu, K.B. Tan, and G.R. Liu. Finite element analysis of an osseointegrated stepped screw dental implant. Journal of Oral Implantology, 30:223–233, 2004.

[63] V. Gilsanz, T.F. Roe, D.T. Gibbens, E.E. Schulz, M.E. Carlson, O. Gonzalez, and M.I. Boechat. Effect of sex steroids on peak bone density of growing rabbits. Am J Physiol, 255:E416–E421, 1988.

[64] J.M. Gomez-Vega, E. Saiz, and A.P. Tomsia. Glass-based coatings for titanium implant alloys. Journal of Biomedical Materials Research , 46(4):549–559, 1999.

[65] J.M. Gomez-Vega, E. Saiz, A.P. Tomsia, G.W. Marshall, and S.J. Marshall. Bioactive glass coatings with hydroxyapatite and bioglass particles on ti-based implants. 1. processing. Biomaterials, 21(2):105–111, 2000.

[66] C.J. Goodacre, G. Bernal, K. Rungcharassaeng, and J.Y. Kan. Clinical compli- cations with implants and implant prostheses. Journal of Prosthetic Dentistry, 90:121–132, 2003.

[67] M. Gottlander and T. Albrektsson. Histomorphometric studies of hydroxylapatite-coated and uncoated cp titanium threaded implants in bone. The International Journal of Oral & Maxillofacial Implants, 6(4):399–404, 1991.

[68] S. Gronthos, J. Brahim, and W. Li. Stem cell properties of human dental pulp stem cells. Journal of Dental Research, 81(8):531–535, 2002.

[69] A.C. Guyton and J. E. Hall. Textbook of Medical Physiology. Elsevier Saunders, Pennysylvania, 2006.

[70] R. Haas, N. Mensdorff-Pouilly, G. Mailath, and G. Watzek. Branemark single tooth implants: a preliminary report of 76 implants. Journal of Prosthetic Dentistry, 73:274–279, 1995.

[71] T. Han, F.A. Jr. Carranza, and E.B. Kenney. Calcium phosphate ceramics in dentistry: A review of the literature. J West Soc Periodontol: Periodontal Abstr, 32:88–108, 1984.

[72] S. Hansson and M. Werke. The implant thread as a retention element in cortical bone: The effect of thread size and thread profile: a finite element study. Journal of Biomechanics, 36:1247–1258, 2003.

[73] D.G. Hazzard, R.T. Bronson, G.E. McClearn, and R. Strong. Selection of an appropriate animal model to study aging processes with special emphasis on the use of rat strains. J Gerontol, 47:B63–B64, 1992.

[74] L. L. Hench. Bioceramics: From concept to clinic. Journal of the American Ceramic Society, 74(7):1487–1510, 1991.

[75] L.L. Hench. The story of bioglass. Journal of Materials Science: Materials in Medicine, 17(11):967–978, 2006.

[76] L.L. Hench and O.H. Andersson. An Introduction of Bioceramics, chapter Bioactive glass coatings, pages 239–259. World Scientific, Singapore, 1993.

[77] L.L. Hench and J.M. Polak. Third-generation biomedical materials. Science, 295:1014–1017, 2002.

[78] L.L. Hench, R.J. Splinter, W.C. Allen, and T.K. Greenlee. Bonding mecha- nisms at the interface of ceramic prosthetic materials. Journal of Biomedical Materials Research, 5(6):117–141, 1971.

[79] J.S. Hermann, D. Buser, R.K. Schenk, F.L. Higginbottom, and D.L. Cochran. Biologic width around titanium implants. a physiologically formed and stable dimension over time. Clinical Oral Implants Research, 11(1):1–11, 2000.

[80] J.O. Hollinger, J. Brekke, E. Gruskin, and D. Lee. Role of bone substitutes. Clin Orthop, 324:55–65, 1996.

[81] J. A. Hubbell. Biomaterials in tissue engineering. Nature Biotechnology, 13(6):565–576, 1995.

[82] S.F. Hulbert, F.W. Cooke, J.J. Klawitter, R. B. Leonard, B.W. Sauer, D.D. Moyle, and H. B. Skinner. Attachment of prostheses to the musculo-skeletal system by tissue ingrowth and mechanical interlocking. Journal of Biomedical Materials Research Part A, 7(3):1–23, 1973.

[83] A. Jana, A. Chakraborty, and T.K. Pal. Regeneration of periodontal tissue with β-TCP in perio-endo liason-A case report. Indian Dental Association- West Bengal State Branch, 30(1):25–29, 2014.

[84] M. Jarcho. Calcium phosphate ceramics as hard tissue prosthetics. Clinical Orthopaedics & Related Research, 157:259–278, June 1981.

[85] M. Jarcho. Biomaterial aspects of calcium phosphates. properties and applica- tions. Dental Clinics of North America, 30(1):25–47, 1986.

[86] M.W. Johnson, S.M. Sullivan, M. Rohrer, and M. Collier. Regeneration of peri-implant infrabony defects using perioglas: a pilot study in rabbits. Int J Oral Maxillofac Implants, 12(6):835–839, 1997.

[87] J.R. Jones. Review of bioactive glass: From hench to hybrids. Acta Biomate-rialia, 9:4457–4486, 2013.

[88] S.B. Jung, D.E. Day, T. Day, W. Stoecker, and P. Taylor. Treatment of non- healing diabetic venous stasis ulcers with bioactive glass nanofibers. Wound Repair Regen, 19:A30, 2011.

[89] H. Kido and S. Saha. Effect of ha coating on the long term survival of dental implants: a review of the literature. Journal of Long Term Effects of Medical Implants, 6(2):119–133, 1996.

[90] L.T. Kircos. Preprosthetic imaging in prospective. University of Chicago Press, Chicago, U.S.A., 1990.

[91] H.P. Klug and L.E. Alexander. X-Ray Diffraction Procedures: for Polycrys- talline and Amorphous Materials. Wiley-VCH, New Jersey, 2nd edition, 1974.

[92] T. Kokubo. Bioactive glass ceramics: Properties and applications. Biomateri- als, 12(2):155–163, 1991.

[93] L. Kong, B.L. Liu, K.J. Hu, D.H. Li, Y.L. Song, P. Ma, and J. Yang. Optimized thread pitch design and stress analysis of the cylinder screwed dental implant. Hua Xi Kou Qiang Yi Xue Za Zhi, 24:509–515, 2006.

[94] B. Kundu, A. Lemos, C. Soundrapandian, P.S. Sen, S. Datta, J.M.F. Fer- reira, and Basu D. Development of porous hap and β-tcp scaffolds by starch consolidation with foaming method and drug-chitosan bilayered scaffold based drug delivery system. Journal of Materials Science: Materials in Medicine, 21(11):2955–2969, 2010.

[95] B. Kundu, D. Sanyal, and D. Basu. Physiological and elastic properties of highly porous hydroxyapatite potential for integrated eye implants: Effects of sirc and l-929 cell lines. Ceramics International, 39(3):2651–2664, 2012.

[96] B. Kundu, M.K. Sinha, S. Mitra, and D. Basu. Synthetic hydroxyapatite- based integrated orbital implants - a human pilot trial. Indian Journal of Ophthalmology, 53(4):235–241, 2005.

[97] Biswanath Kundu. Synthetic hydroxyapatite based integrated ocular implants for efficient rehabilitation of human patients: An in vitro and in vivo experi- mentation. PhD thesis, Jadavpur University, Kolkata, India, 2014.

[98] S. H. Kwon, Y. K. Jun, S. H. Hong, I. S. Lee, H. E. Kim, and Y. Y. Won. Calcium phosphate bioceramics with various porosities and dissolution rates. Journal of the American Ceramic Society, 85(12):3129–3131, 2002.

[99] E. Landi, A. Tampieri, G. Celotti, and S. Sprio. Densification behaviour and mechanisms of synthetic hydroxyapatites. Journal of the European Ceramic Society, 20(14-15):2377–2387, 2000.

[100] N.P. Lang and G. Salvi. Clinical Periodontology and Implant Dentistry. 5th edition, chapter Implants in restorative dentistry, pages 1138–1145. Denmark: Blackwell Munksgaard, 2008.

[101] R.Z. LeGeros. Calcium phosphate materials in restorative dentistry: A review. Advances in Dental Research, 2(1):164–180, 1988.

[102] R.Z. LeGeros. Monographs in Oral Science, volume 15, chapter Calcium phos- phates in oral biology and medicine, page 32. Karger, New York, 1991.

[103] R.Z. LeGeros. Properties of osteoconductive biomaterials: calcium phosphates. Clinical Orthopaedics and Related Research, 395:81–98, 2002.

[104]LeGeros, R.Z. and Contiguglia, S.R. and Alfrey, A.C. Pathological calcifica- tions associated with uremia: two types of calcium phosphate deposits. Calci- fied Tissue Research , 13(3):173–185, 1973.

[105] U. Lekholm and G.A. Zarb. Tissue Integrated Prostheses: Osseointegration in Clinical Dentistry, chapter Patient selection and preparation, pages 199–209. Quintessence Publishing Co., Inc, 1985.

[106] J. Lemons. Biomaterials in Implant Dentistry Contemporary Implant Den- tistry. St Louis:Mosby, 1993.

[107] Long-Hao Li, Young-min Kong, Hae-Woon Kim, Young-Woon Kim, Hyoun-Ee Kim, and Seong-Joo Heo. Improved biological performance of ti implants due to surface modification by micro-arc oxidation. Biomaterials, 25(14):2867–2875, 2004.

[108] E.S. Liang Jr, P.G.and Ferguson Jr and E.S. Hodge. Tissue reaction in rabbit muscle exposed to metallic implants. Journal of Biomedical Materials Research Part A, 1(1):135–149, 1967.

[109] L. I. Linkow. Bone transplants using the symphysis, the iliac crest and synthetic bone materials. The Journal of oral implantology, 11(2):211–247, 1983.

[110] L. I. Linkow and R. Chercheve Theories and Techniques of oral implantology. St. Louis, Mosby, 1970.

[111] T. L. Livingston, S. Gordon, and M. Archambault. Mesenchymal stem cells combined with biphasic calcium phosphate ceramics promote bone regener ation. Journal of Materials Science: Materials in Medicine, 14(3):211–218, 2003.

[112] M. Long and H.J. Rack. Titanium alloys in total joint replacement. a materials science perspective. Biomaterials, 19(18):1621–1639, 1998.

[113] S. Lopez-Esteban, E. Saiz, S. Fujino, T. Oku, K. Suganuma, and A.P. Tom- sia. Bioactive glass coatings for orthopedic metallic implants. Journal of the European Ceramic Society , 23(15):2921–2930, 2003.

[114] P. Ma, H.C. Liu, D.H. Li, S. Lin, Z. Shi, and Q.J. Peng. Influence of helix angle and density on primary stability of immediately loaded dental implants: three-dimensional finite element analysis. Journal of Stomatology, 42:618–621, 2007.

[115] D.E. Mac Donald, F. Betts, S.B. Doty, and A.L. Boskey. A methodological study for the analysis of apatite-coated dental implants retrieved from humans. Annals of Periodontology, 5(1):175–184, 2000.

[116] D.E. Mac Donald, F. Betts, M. Stranick, S. Doty, and A.L. Boskey. Physico- chemical study of plasma-sprayed hydroxyapatite-coated implants in humans. Journal of Biomedical Materials Research Part A, 54(4):480–490, 2001.

[117] T.E. Madden and J.G. Caton. Animal models for periodontal disease. Methods Enzymol, 235:106–119, 1994.

[118] G. Mailath, B. Stoiber, G. Watzek, and M. Matejka. Bone resorption at the entry of osseointegrated implants - a biomechanical phenomenon. finite element study. Zeitschrift fur Stomatologie, 86:207–216, 1989.

[119] W.J. Maloney, M. Jasty, A. Rosenberg, and W. H. Harris. Bone lysis in well- fixed cemented femoral components. The Journal of Bone and Joint Surgery, 72(6):966–970, 1990.

[120] M. Mapara, B. S. Thomas, and K. M. Bhat. Rabbit as an animal model for experimental research. Dental Research Journal, 9(1):111–118, 2012.

[121] L. Martini, M. Fini, G. Giavaresi, and R. Giardino. Sheep model in orthopedic research: a literature review. Comp Med, 51:292–299, 2001.

[122] B.S. McAllister and K. Haghighat. Bone augmentation techniques. J Peri- odontol, 78:377–396, 2007.

[123] R.M. Meffert, J.R. Thomas, K.M. Hamilton, and C.N. Brownstein. Hydroxy- lapatite as an alloplastic graft in the treatment of human periodontal osseous defects. Journal of Periodontology, 56(2):63–73, 1985.

[124] H.J. Meijer, F.J. Starmans, W.H. Steen, and F. Bosman. A three-dimensional, finite-element analysis of bone around dental implants in an edentulous human mandible. Archives of Oral Biology, 38:491–496, 1993.

[125] N. Meredith. A review of nondestructive test methods and their application to measure the stability and osseointegration of bone anchored endosseous implants. Critical Review of Biomedical Engineering, 26:275–291, 1998.

[126] N. Meredith, D. Alleyne, and P. Cawley. Quantitative determination of the stability of the implant-tissue interface using resonance frequency analysis. Clinical Oral Implants Research, 7(3):261–267, 1996.

[127] N. Meredith, F. Shagaldi, L. Alleyne, D.and Sennerby, and P. Cawley. The application of resonance frequency measurements to study the stability of ti- tanium implants during healing in the rabbit tibia. Clinical Oral Implants Research, 8(3):234–243, 1997.

[128] D. S. Metsger, T. D. Driskell, and J. R. Paulsrud. Tricalcium phosphate ceramic-a resorbable bone implant: review and current status. The Journal of the American Dental Association, 105(6):1035–1038, 1982.

[129] C.E. Misch. Contemporary Implant Dentistry - 3rd Edition, chapter Rationale for dental implants, pages 1–25. Mosby, St. Louies, 2008.

[130] C.E. Misch. Contemporary Implant Dentistry - 3rd Edition, chapter Generic root form component terminology, pages 26–37. Mosby, St. Louies, 2008.

[131] C.E. Misch. Contemporary Implant Dentistry - 3rd Edition, chapter Available Bone and Dental Implant Treatment Plans. Mosby, St. Louies, 2008.

[132] C.E. Misch. Contemporary Implant Dentistry - 3rd Edition, chapter Implant Body Size: A Biomechanical and Esthetic Rationale. Mosby, St. Louies, 2008.

[133] C.E. Misch, M.W. Bidez, and M. Sharawy. A bioengineered implant for a predetermined bone cellular response to loading forces. a literature review and case report. Journal of Periodontology, 72:1276–1286, 2001.

[134] C.E. Misch and K.W. Judy. Classification of partially edentulous arches for implant dentistry. The International Journal of Oral Implantology: Implantol- ogist, 4(2):7–12, 1987.

[135] C.E. Misch, J. Todd Strong, and Martha Warren Bidez. Contemporary Implant Dentistry - 3rd Edition, chapter Scientific Rationale for Dental Implant Design, pages 200–229. Mosby, St. Louies, 2008.

[136] S.Moldovan. Dental implants: A comprehensive review. http://www.dentalcare.com/media/en-US/education/ce420/ce420.pdf, 2013.

[137] Mostafa, N.Y. Characterization, thermal stability and sintering of hydroxyap- atite powders prepared by different routes. Materials Chemistry and Physics , 94(2-3):333–341, 2005.

[138] M. Motoyoshi, S. Yano, T. Tsuruoka, and N. Shimizu. Biomechanical effect of abutment on stability of orthodontic mini-implant. a finite element analysis. Clinical Oral Implants Research, 16:480–485, 2005.

[139] E. Munting, M. Verhelpen, F. Li, and A. Vincent. Handbook of Bioactive Ceramics, Vol.2, chapter Contribution of hydroxyapatite coatings to implant fixation. CRC Press, Boca Raton, Fla, USA, 1990.

[140] S. Nag, R. Banerjee, and H.L. Fraser. Microstructural evolution and strength- ening mechanisms in tinbzrta, timozrfe and ti15mo biocompatible alloys. Mater Sci Eng C, 25(3):357–362, 2005.

[141] S.K. Nandi, B. Kundu, P. Mukherjee, T.K. Mandal, S. Datta, D.K. De, and
D. Basu. In vitro and in vivo release of cefuroxime axetil from bioactive glass as an implantable delivery system in experimental osteomyelitis. Ceramics International, 35(8):3207–3216, 2009.

[142] U. Nayar and S. Iyer. Implant Site DevelopmentPart I. International Journal of Clinical Implant Dentistry, 1(2):41–44, 2009.

[143] J.G. Neyt, J.A. Buckwalter, and N.C. Carroll. Use of animal models in mus- culoskeletal research. Iowa Orthop J, 18:118–123, 1998.

[144] M. Niinomi. Recent metallic materials for biomedical applications. Met Mater Trans, 32A:477–486, 2001.

[145] M. Niinomi, D. Kuroda, K. Fukunaga, M. Morinaga, Y. Kato, T. Yashiro, and
A. Suzuki. Corrosion wear fracture of new β type biomedical titanium alloys.
Mater Sci Eng, A263:193199, 1999.

[146] D. Norhidayu, I. Sopyan, and S. Ramesh. Development of zinc doped hydrox- yapatite for bone implant applications. ICCBT, 24:257–270, 2008.

[147] K. Okamoto, T. Matsuura, R. Hosokawa, and Y. Akagawa. Rgd peptides regulate the specific adhesion scheme of osteoblasts to hydroxyapatite but not to titanium. Journal of Dental Research, 77(3):481–487, 1998.

[148] Y. Okazaki and E. Gotoh. Comparison of metal release from various metallic biomaterials in vitro. Biomaterials, 26(1):11–21, 2005.

[149] Colgate Oral and Dental Health Resource Center. What are dental implants types of dental implants. http://www.colgate.com/app/CP/US/EN/OC/Information/Articles/Oral- and-Dental-Health-at-Any-Age/Seniors/Dentures-and-Dental- Implants/article/What-are-Dental-Implants.cvsp, 2015.

[150] J.F. Osborn and H. Newesely. The material science of calcium phosphate ceramics. Biomaterials, 1(2):108–111, 1980.

[151] Ota, Y. and Iwashita, T. and Kasuga, T. and Abe,Y. Novel preparation method of hydroxyapatite fibers. Journal of the American Ceramic Society , 81(6):1665–1668, 1998.

[152] T.K. Pal, A. Chakraborty, and S. Banerjee. A micro-anatomical comparison of goat jaw cancellous bone with human mandible: Histomorphometric study for implant dentistry. Journal of the International Clinical Dental Research Organization, 6(1):4–7, 2014.

[153] J.B. Park and J.D. Bronzino. Biomaterials: principles and applications. Boca Rator, FL: CRC Press, 2003.

[154] Jong-Chul Park, Jung-Woo Lee, Soung-Min Kim, and Jong-Ho Lee. Implant stability measuring devices and randomized clinical trial for is q value change pattern measured from two different directions by magnetic rfa, implant dentistry a rapidly evolving practice. http://www.intechopen.com/books/implant-dentistry-a-rapidly-evolving- practice/implant-stability-measuring-devices-and-randomized-clinical-trial- for-isq-value-change-pattern-measu, 2011. InTech.

[155] A. Pazo, E. Saiz, and A.P. Tomsia. Silicate glass coatings on ti-based implants.
Acta Materialia, 46(7):2551–2558, 1998.

[156] AI Pearce, RG Richards, S Milz, E Schneider, SG Pearce, et al. Animal models for implant biomaterial research in bone: a review. European Cells Materials, 13(1):1–10, 2007.

[157] C.R. Perry. Bone repair techniques, bone graft, and bone graft substitutes. Clin Orthop, 252:71–86, 1999.

[158] Soben Peter. Essentials of Preventive and Community Dentistry. Arya Medi Publishing House, India, 5th edition edition, 2013.

[159] J. F. Piecuch. Augmentation of the atrophic edentulous ridge with porous re- plamineform hydroxyapatite (interpore-200). Dental clinics of North America, 30(2):291–305, 1986.

[160] P.J. Prendergast and R. Huiskes. Microdamage and osteocyte-lacuna strain in bone: a microstructural finite element analysis. Journal of Biomechanical Engineering, 118:240–246, 1996.

[161] P.I. Branemark R. Adell, U. Lekholm. Osseointegration in Clinical Dentistry,, chapter Tissue Integrated Prostheses. Quintessence Publishing Co., Inc, 1985.

[162] S. Ramakrishna, J. Mayer, E. Wintermantel, and W. Leong Kam. Biomedical applications of polymer-composite materials:a review. Composites Science and Technology, 61:1189–1224, 2001.

[163] D. Richard, N. Dumelie, and H. Benhayoune. Behavior of human osteoblast- like cells in contact with electrodeposited calcium phosphate coatings. Journal of Biomedical Materials Research B, 79(1):108–115, 2006.

[164] M.R. Rieger, W.K. Adams, and G.L. Kinzel. A finite element survey of eleven endosseous implants. J Prosthet Dent, 63:457?465, 1990.

[165] L. Roderic.The biomedical engineering handbook, chapter Composite bioma- terials, pages 309–314. Boca Raton, FL: CRC Press, 1995.

[166] E. Rompen, D. DaSilva, A.K. Lundgren, J. Gottlow, and L. Sennerby. Stability measurements of a double-threaded titanium implant design with turned or oxidised surface. Applied Osseointegration Research, 1:1820, 2000.

[167] D.M. Roy and S.K. Linnehan. Hydroxyapatite formed from coral skeletal car- bonate by hydrothermal exchange. Nature, 247:220–222, 1974.

[168] Sanghamitra Ghosal, Paramita Banerjee, Bhaswati Goswami and Ratna Ghosh. Determination of stability of dental implant from impedance studies us- ing resonance frequency analysis. In Proceedings of Second International Con- ference on Emerging Applications of Information Technology,(EAIT), pages 71–74, Kolkata, India, 2011.

[169] Santamarina, J.C. and Klein, K.A. and Wang, Y.H. and Prencke, E. Spe- cific surface: determination and relevance. Canadian Geotechnical Journal, 39(1):233–241, 2002.

[170] Santosa, C. and Clarke, R.L. and Braden, M. and Guitian, F. and Davy, K.W.M. Water absorption characteristics of dental composites incorporating hydroxyapatite filler. Biomaterials, 23:1897–1904, 2002.

[171] B.W. Sauer, A.M. Weinstein, J.J. Klawitter, S.F. Hulbert, R.B. Leonard, and J.G. Bagwell. The role of porous polymeric materials in prosthesis attachment. Journal of Biomedical Materials Research Part A, 8(3):145–153, 1974.

[172] C. Schmidt, A.A. Ignatius, and L.E. Claes. Proliferation and differentiation parameters of human osteoblasts on titanium and steel surfaces. J Biomed Mater Res, 54:209–215, 2001

[173] J.M. Schmitt, D.C. Buck, S.P. Joh, S.E. Lynch, and J.O. Hollinger. Comparison of porous bone mineral and biologically active glass in critical sized defects. J Periodontol, 68(11):1043–1053, 1997.

[174] J.M. Schmitt, K. Hwang, and S.R. Winn. Bone morphogenetic proteins: An update on basic biology and clinical relevance. J Orthop Res, 17:269–278, 1999.

[175] J. Schrooten and J.A. Helsen. Adhesion of bioactive glass coating to Ti6Al4V oral implant. Biomaterials, 21(14):1461–1469, 2000.

[176] F. Schwarz, K. Bieling, T. Latz, E. Nuesry, and J. Becker. Healing of intrabony peri-implantitis defects following application of a nanocrystalline hydroxyap- atite (ostim?) or a bovine-derived xenograft (bio-oss) in combination with a collagen membrane (bio-gide). a case series. Journal of Clinical Periodontology, 33(7):491–499, 2006.

[177] K.A. Selvig. Discussion: animal models in reconstructive therapy. J Periodon- tol, 65(12):1169–1172, 1994.

[178] L. Sennerby and N. Meredith. Implant stability measurements using resonance frequency analysis: biological and biomechanical aspects and clinical implica- tions. Periodontology, 47:5156, 2000.

[179] A. Sethi and T. Kaus. Maxillary ridge expansion with simultaneous implant placement: 5-year results of an ongoing clinical study. Int J Oral Maxillofac Implants, 15:491–499, 2000.

[180] J.A. Shibli, S. Grassi, L.C. de Figueiredo, M. Feres, Jr. Marcantonio, E.,
G. Iezzi, and Piattelli. Influence of implant surface topography on early osseoin- tegration: ahistological study in human jaws. Journal of biomedical materials research. Part B, Applied biomaterials, 80:377–385, 2007.

[181] L.B. Shulman, T.D. Driskell, and M.S. Block. Implants in Dentistry, chapter Dental implants: A historical perspective, pages 33–44. Saunders, Philadelphia, 1997.

[182] K. Soballe, E.S. Hanse, H. Brockstedt-Rasmussen, and C. Bunger. Hydroxya- patite coating converts fibrous tissue to bone around loaded implants. Journal of Bone and Joint Surgery, American Edition, 75-B(2):270–278, 1993.

[183] W.A. Soskolne, S. Cohen, L. Sennerby, A. Wennerberg, and L. Shapira. The effect oftitanium surface roughness on the adhesion of monocytes and their secretion of tnf-alpha and pge2. Clinical oral implants research, 13:86–89, 2002.

[184] C. Soundrapandian. Prolonged release biocompatible skeletal drug delivery system - Development and optimization. PhD thesis, Jadavpur University, Kolkata, India, 2011.

[185] Sridhar, T.M. and Kamachi Mudali, U. and Subbaiyan, M. Sintering atmo- sphere and temperature effects on hydroxyapatite coated type 316L stainless steel. Corrosion Science, 45(10):2337–2359, 2003.

[186] V. Stanic, N. Nicoli Aldini, M. Fini, G. Giavaresi, R. Giardino, A. Krajewski, A. Ravaglioli, M. Mazzocchi, B. Dubini, and M.G. Ponzi Bossi. Osteointegra- tion of bioactive glass-coated zirconia in healthy bone: An in vivo evaluation. Biomaterials, 23(18):3833–3841, 2002.

[187] H.R. Stanley, M.B. Hall, A.E. Clark, C.J. King, L.L. Hench, and J.J. Berte. Using 45s5 bioglass cones as endosseous ridge maintenance implants to prevent alveolar ridge resorption: a 5-year evaluation. Int J Oral Maxillofac Implants, 12:95–105, 1997.

[188] D.V. Steenberghe, M. Marechal, and M. Quirynen. Clinical Periodontology 10th Edition, chapter Biological aspects of oral implants, pages 1072–1086. Saunders, St. Louies, 2006.

[189] J. Steigenga, K. Al-Shammari, C. Misch, F.H. Jr Nociti, and H.L. Wang. Ef- fects of implant thread geometry on percentage of osseointegration and re- sistance to reverse torque in the tibia of rabbits. Journal of Periodontology, 75:1233–1241, 2004.

[190] J.T. Steigenga, K.F. al Shammari, F.H. Nociti, C.E. Misch, and H.L. Wang. Dental implant design and its relationship to long-term implant success. Im- plant Dentistry, 12:306–317, 2003.

[191] X. Struillou, H. Boutigny, A. Soueidan, and P. Layrolle. Experimental animal models in periodontology: A review. The Open Dentistry Journal, 4:37–47, 2010.

[192] K. Takaoka, E. Segawa, K. Noguchi, H. Kishimoto, and M. Urade. Maxillary subperiosteal implantitis that caused severe bone resorption of the maxilla with perforation of the maxillary sinus and sinusitis: A case report. Open Journal of Stomatology, 3:226–229, 2013.

[193] D.P. Tarnow, R.N. Eskow, and J. Zamzok. Aesthetics and implant dentistry. Periodontology 2000, 11:85–94, 1996.

[194] O.H. Tatum. The Omni Implant System. In Albama Implant Congress, Birm- ingham, Alabama, 1988.

[195] S.H. Teoh. Fatigue of biomaterials: a review. International Journal of Fatigue, 22(10):825–837, 2000.

[196] T.V. Thamaraiselvi and S. Rajeswari. Biological evaluation of bioceramic ma- terials: a review. Trends in Biomaterials and Artificial Organs, 18(1):9–17, 2004.

[197] K. A. Thomas, J. F. Kay, S. D. Cook, and M. Jarcho. The effect of surface macrotexture and hydroxylapatite coating on the mechanical strengths and his tologic profiles of titanium implant materials. Journal of Biomedical Materials Research, 21(12):1395–1414, 1987.

[198] P. Torricelli, E. Verne, C.V. Brovarone, P. Appendino, F. Rustichelli, A. Kra- jewski, A. Ravaglioli, G. Pierini, M. Fini, and G. Giavaresi. Biological glass coating on ceramic materials: In

vitro evaluation using primary osteoblast cul- tures from healthy and osteopenic rat bone. Biomaterials, 22(18):2535–2543, 2001.

[199] Y. C. Tsui, C. Doyle, and T.W. Clyne. Plasma sprayed hydroxyapatite coatings on titanium substrates. part 1: mechanical properties and residual stress levels. Biomaterials, 19(22):2015–2029, 1998. [200]A. Uchida, N. Araki, Y. Shinto, H. Yoshikawa, E. Kurisaki, and K. Ono. The use of calcium hydroxyapatite ceramic in bone tumour surgery. Journal of Bone and Joint Surgery B, 72(2):298–302, 1990.

[201] M. Valen and W.M. Locante. Laminoss immediate?load implants: I. introduc- ing osteocompression in dentistry. J Oral Implantol, 26:177?84, 2000.

[202] M. Viceconti, R. Muccini, M. Bernakiewicz, M. Baleani, and L. Cristofolini. Large-sliding contact elements accurately predict levels of boneimplant micro- motion relevant to osseointegration. Journal of Biomechanics, 33(12):1611– 1618, 2000.

[203] B.C. Wang, T.M. Lee, E. Chang, and C.Y. Yang. The shear strength and the failure mode of plasma-sprayed hydroxyapatite coating to bone: The effect of coating thickness. Journal of Biomedical Materials Research, 27(10):1315– 1327, 1993.

[204] C.J. Wang, A.L. Yettram, M.S. Yao, and P. Procter. Finite element analysis of a gamma nail within a fractured femur. Medical Engineering and Physics, 20(9):677–683, 1998.

[205] K. Wang. The use of titanium for medical applications in the usa. Mater Sci Eng, A Struct Mater: Prop Microstruct Process, 213:134–137, 1996.

[206] K.L. Wapner. Implications of metallic corrosion in total knee arthroplasty. Clin Orthop Relat Res, 271:12–20, 1991.

[207] P. Weber, S. Utzschneider, P. Sadoghi, M.F. Pietschmann, A. Ficklscherer, and V. Jansson. Navigation in minimally invasive unicompartmental knee arthro- plasty has no advantage in comparison to a conventional minimally invasive implantation. Archives of Orthopaedic and Trauma Surgery, 132(2):281–288, 2012.

[208] M. Weinlaender, E. B. Kenney, V. Lekovic, J. Beumer 3rd., P. K. Moy, and
S. Lewis. Histomorphometry of bone apposition around three types of en- dosseous dental implants. The International Journal of Oral & Maxillofacial Implants, 7(4):491–496, 1992.

[209] A.M. Weinstein, J.J. Klawitter, S.C. Anand, and R. Schuessler. Stress analysis of porous rooted dental implants. J Dent Res, 55:772?777, 1976.

[210] Weng, W. and Baptista, J.L. Sol-gel derived porous hydroxyapatite coatings.
Journal of Materials Science, 9(3):159–163, 1998.

[211] A. Wennerberg and T. Albrektsson. Effects of titanium surface topography on bone integration: A systematic review. Clinical Oral Implants Research, 20(S4):172–184, 2009.

[212] D.F. Williams. On the mechanisms of biocompatibility. Biomaterials, 29(20):2941–2953, 2008.

[213] D.L. Wise, D.J. Trantolo, Kai-Uwe Lewandrowski, J.D. Gresser, and M. Cat- taneo. Biomaterials Engineering and Devices: Volume 2 Orthopedic, Dental, and Bone Graft Applications: Human Applications. Berlin: Humana Press, 2000.

[214] G.L. Yang, F.M. He, X.F. Yang, X.X. Wang, and S.F. Zhao. Bone responses to titanium implants surface-roughened by sandblasted and double etched treat- ments in a rabbit model. Oral Surgery, Oral Medicine, Oral Pathology, Oral Radiology and Endodontics, 106:516–524, 2008.

[215] Y.C. Yang and E. Chang. Influence of residual stress on bonding strength and fracture of plasma-sprayed hydroxyapatite coatings on Ti-6Al-4V substrate. Biomaterials, 22(13):1827–1836, 2001.

[216] Y.C. Yang and E. Chang. The bonding of plasma-sprayed hydroxyapatite coatings to titanium: effect of processing, porosity and residual stress. Thin Solid Films, 444(1-2):260–275, 2003.

[217] Yoshimura, M. and Suda, H. and Okamoto, K. and Ioku, K. Hydrothermal synthesis of biocompatible whiskers. Journal of Materials Science, 29(13):3399– 3402, 1994.

[218] Zhou, J. and Zhang, X. and Chen, J. and Zeng, S. and de Groot, K. High temperature characteristics of synthetic hydroxyapatite. Journal of Materials Science: Materials in Medicine, 4(1):83–85, 1993.

[219] O. Zinger, K. Anselme, A. Denzer, P. Habersetzer, M. Wieland, J. Jeanfils, P. Hardouin, and D. Landolt. Time-dependent morphology and adhesion of osteoblastic cells on titanium model surfaces featuring scale-resolved topogra- phy. Biomaterials, 25(14):2695–2711, 2004.